DESIGN OF A POWERED ABOVE KNEE PROSTHESIS USING PNEUMATIC ARTIFICIAL MUSCLES

by

GARRETT C. WAYCASTER

A THESIS

Submitted in partial fulfillment of the requirements
for the degree of Master of Science
in the Department of Mechanical Engineering
in the Graduate School of
The University of Alabama

TUSCALOOSA, ALABAMA

2010

ABSTRACT

This paper describes the mechanical design for both a one and two degree of freedom above-knee (AK) prosthesis actuated by pneumatic artificial muscles. Powered prosthetics aim to improve the quality of life of the 50% of AK amputees who never regain the ability to walk. Pneumatic artificial muscle (PAM) provides great potential in prosthetics, since this type of actuator features a high power density and similar characteristics to human muscles. Currently, commercially available AK prosthetics are largely passive devices, and no research has been conducted on PAM actuators in AK prosthetics. In this thesis, the design requirements of an above knee prosthesis using PAM are discussed and a prototype one degree of freedom prosthesis with a PAM actuated knee joint is constructed. This prototype is then tested, and based on the results a new actuator is developed. This new actuator uses a flexible tendon and an elliptical pulley to improve torque, adding more functionality and increasing the maximum mass of a user by 25 kilograms. This actuator is also tested and compared to the initial prototype design. Finally, this new actuator is incorporated into the design of a two degree of freedom prosthesis with an actuated ankle as well as the knee joint.

DEDICATION

To my wife, Lauren

Thank you for your love, support, and guidance

LIST OF ACRONYMS AND SYMBOLS

a_{dia}	Ellipse Semi-major Diameter
b_{dia}	Ellipse Semi-minor Diameter
F	Force
L_0	Slider Crank Actuator Fixed Point x Coordinate
L_1	Slider Crank Actuator Fixed Point y Coordinate
m	Line Slope
r	Pulley Radius
r_0	Radial Coordinate of Pulley Center
r_{eff}	Effective Radius
T_{act}	Actual Torque Output
T_{req}	Required Torque Output
x_0	Pulley Muscle Fixed Point Relative x-axis Position
y_0	Pulley Muscle Fixed Point Relative y-axis Position

Greek Letters

$\Delta\gamma$	Change in Knee Rotation Angle
γ	Knee Rotation Angle
θ	Angular Coordinate of Pulley Radius
θ_0	Angular Coordinate of Pulley Center
φ	Ellipse Rotation

Acronyms

AK	Above Knee
DOF	Degree of Freedom
PAM	Pneumatic Artificial Muscle
TBM	Total Body Mass

ACKNOWLEDGMENTS

I would especially like to thank Dr. Xiangrong Shen for providing me with the opportunity to work on this project, and for his help and support along the way. I would also like to thank Dr. Beth Todd, Dr. Keith Williams, and Dr. Mark Richardson for their assistance as part of my thesis committee. I would like to thank the Graduate Council and the Mechanical Engineering department for their financial support during my graduate study. Additionally I would like to thank the Graduate Student Association for their financial support for my research work. Finally, I would like to thank my fellow students, Daniel Christ, Alston Pike, and Marco Wu, for their discussion, hard work, and encouragement in association with this project.

CONTENTS

LIST OF TABLES

LIST OF FIGURES

CHAPTER 1: INTRODUCTION

1.1 Motivation

A 2005 study estimates that 1.6 million Americans currently live with the loss of a limb, and of these 623,000 are classified as major amputations of a lower limb. Additionally, projections predict that the number of people in the US with limb loss could double by 2050 (Ziegler-Graham, 2008). Incident rates from 1988-1996 show that over 30,000 hospital discharges each year involve an above knee amputation. Of these incidents, nearly 95% are attributed to vascular disease, such as diabetes. Trauma related incidents account for 4% of AK amputations, with cancer-related and congenital above knee amputations together accounting for less than 1% (Dillingham, 2002). One important measure of amputee mobility is energy cost of ambulation, which is typically given as $\frac{mL\ O_2}{kg*m}$, which represents the amount of oxygen consumption required per kilogram body mass to walk one meter per second. Above knee amputees show an increase in the energy cost of ambulation over healthy individuals of 33% for unilateral traumatic amputees, 86% for unilateral vascular amputees, and 120% for bilateral AK amputees (Waters, 1999). This increased energy expenditure prevents between 50% and 62% of above knee amputees from regaining full ambulatory function (Tang, 2008), particularly in the large population of older, vascular amputees.

Even when an amputee is able to regain ambulation, there are certain tasks that passive prosthetics are simply incapable of performing, such as stair climbing. This is because passive prosthetics are only capable of dissipating energy and cannot generate positive power at the knee

joint. Powered prosthetics seek to reduce or eliminate many of the problems amputees face with ambulation. By providing positive power, the prosthesis eliminates the need for the user to generate rotation of the prosthesis with their hip. Powered prosthetics may provide support as well as propulsion at all joint angles, including climbing and descending stairs and slopes, which requires a significant amount of power from the knee joint.

One of the key difficulties in creating a powered prosthesis is the selection of an appropriate actuator. Electric motors, hydraulic systems, and traditional pneumatic cylinders have each been used as a potential method for creating a powered AK prosthesis, but each has its own limitations. A novel actuator, pneumatic artificial muscles, has also been identified as a potential prosthetic actuator.

1.2 Objective

The objective of this research is to determine the viability of pneumatic artificial muscles as an above knee prosthetic actuator. A successful prosthesis must be able to produce an appropriate torque curve and range of motion to allow for a user to carry out basic ambulatory tasks. Additionally, a prosthesis must maintain similar physical properties, such as size and mass, to a biological leg. Actuation methods will be evaluated and tested, and a functional prosthesis will be designed.

1.3 Organization of the Thesis

This thesis is divided into seven chapters. Chapter 2 gives an overview of previous literature written about transfemoral prostheses and powered prosthetics. Chapter 3 details the design requirements of a powered transfemoral prosthesis. Chapter 4 details the design and

testing of a 1 DOF design. Chapter 5 details the development and testing of a novel actuator configuration. The conceptual design of a 2 DOF prosthesis, featuring both an articulated knee and ankle, is described in Chapter 6. Chapter 7 provides a conclusion to the thesis with recommendations for future work.

CHAPTER 2: BACKGROUND AND LITERATURE REVIEW

2.1 Current Commercial Prosthetics

Several different types of above knee prosthetics are commercially available today, and range from simple mechanical joints to advanced computer controlled hydraulic joints. Each variety of prosthesis has its own inherent strengths and weaknesses based on the activity level and fitness of the user. This section will describe several types of commercial prosthetics and their working method. Tang et al (2008) provide a complete overview of prosthetic technology.

The most basic of traditional prosthetics is a mechanical joint. These types of prosthetics use a simple one degree of freedom joint, which makes them relatively inexpensive and very reliable, since they have fewer components. In some cases, these prosthetics utilize an adjustable frictional pad, which can help adjust swing speed of the prosthetic. An elastic or spring loaded mechanism may be added to help ensure full extension is achieved. The main drawback of these methods is that the spring and friction adjustment only functions for one gait speed, limiting patient mobility. Therefore, these prosthetics are generally only utilized if a patient has limited access to modern healthcare and prosthetic maintenance. Even with more advanced actuators, some users may utilize a locking knee mechanism during walking. While this results in an unusual gait pattern, it generally results in a lower heart rate and in some cases a reduced energy cost of ambulation as compared to open knee gait.

One other mechanical device used specifically in bilateral amputees is a foreshortened prosthesis, often referred to as "stubbies." These are prosthetic feet that attach directly at the stump, allowing bilateral amputees a greater level of mobility and decreased energy cost. These prosthetics are commonly used during initial rehabilitation, and some patients may choose to continue use of these after rehabilitation because of their simplicity.

An advancement from simple mechanical prosthetics is the advent of pneumatically or hydraulically damped joints. These use either a compressed air or hydraulic fluid filled cylinder with a moveable plunger in the middle. This provides a non-linear force during the gait cycle, allowing for users to successfully maintain a larger range of walking speeds than with a friction joint. Pneumatic dampers are easier to maintain and less affected by ambient conditions; however, they can function irregularly at higher walking speeds. Hydraulic dampers function better at high speeds and are well suited for more athletic amputees.

New innovations in AK prosthetics involve a hydraulic joint that is controlled with the use of a microprocessor, the most commercially successful of which are the OttoBock C-Leg® (OttoBock, 2010), the Ossur RHEO Knee® (Ossur, 2010), and the Freedom Innovations Plié® MPC Knee (Freedom Innovations, 2010). This allows for variable damping throughout the swing phase and the ability to lock the knee joint in any position. A potentiometer is utilized to determine the joint angle, and based on several preprogrammed walking modes, a stepper motor automatically adjusts the size of an orifice in a hydraulic cylinder. This allows for dynamically variable damping which can be adjusted to account for different users and a wide variety of activities.

Figure 2.1 OttoBock C-Leg®

Currently only one commercially available product goes beyond the passive prosthesis to provide positive power at the knee joint, the Ossur PowerKnee™. The PowerKnee™ uses an electric motor to provide positive power at the joint, assisting users during all phases of gait and allowing for tasks such as stair climbing and standing from a seated position. It is controlled using a foot orthosis under the prosthetic foot to detect pressure on the leg, and an accelerometer attached to the ankle of a sound leg. This allows for a technique known as echo control to be utilized to control the knee. However, the PowerKnee™ has some complications that decrease its use. Since it utilizes echo control from a user's sound leg, bilateral amputees are not able to

use the PowerKnee™. The prosthesis weighs about 4.5 kg, roughly 3 times the mass of comparable passive prosthetics like the C-Leg®. The battery pack of the PowerKnee™ only provides for about 4 hours of continuous operation, making it ineffective for users who seek high mobility. Finally, the PowerKnee™ costs about $120,000, five to six times more than the C-Leg®. Since the PowerKnee™ is a fairly new device, most health insurance providers will not cover the purchase of a PowerKnee™, which makes it infeasible for many amputees.

Figure 2.2 Ossur PowerKnee™

2.2 Current Prosthetics Research

Several efforts have been made to develop a powered prosthesis that can viably replace passive prosthetics and improve quality of life for AK amputees. Multiple actuation methods have been utilized, including electric motors, hydraulics, and pneumatics.

Hata and Hori (2002a, 2002b) utilized direct actuation of the knee joint by an AC servo motor. They then developed a complex model to simulate human walking gait, as well as proposing a variable stiffness mechanism to minimize the torque requirements when the leg is in a static position. The design is capable of providing roughly 100 N-m of torque and a rotational velocity of 6.5 rad/sec. This design poses some limitations, since the selected motor alone has a mass of nearly 2 kg and would require a DC/AC inverter to make the design portable.

Martinez-Villalpando and Herr (2009) use a pair of series elastic actuators in an agonist-antagonist configuration. That is to say, the two actuators together control the motion of the knee joint, and the forces of the actuators can be varied to modify the stiffness of the joint. These series elastic actuators, as developed by Robinson et al (1999), consist of a motor-lead screw combination connected to a linear spring. As the motor turns the lead screw, the entire system shifts, stretching or compressing the springs and applying a force to the joint. While this configuration does allow for control of the compliance of the joint, the actuator is still fairly heavy (1.13 kg) and has a small output force (750N), meaning that it will require a large moment arm to produce adequate torque as required by the knee joint.

Fite et al (2007) have developed a powered prosthesis using a DC electric motor. Rather than actuating the joint directly, the motor turns a ball screw in a slider-crank configuration. This allows for the motor to generate a large joint torque without the use of heavy gearboxes.

The 150 W DC motor and ball screw combination is able to provide an intermittent output force of 1880 N. The authors report that this actuator and geometry are capable of providing torque for walking and stair climbing for users up to 85 kg. The prosthesis has a mass of approximately 3 kg, but must be tethered to a workstation to provide power and control. The DC motor allows for the direct use of battery power, however in order to provide a suitable operating time, a large quantity of batteries is required, which can make the system difficult to use.

Sup et al (2008) apply pneumatic cylinders as a prosthetic actuator to develop a powered prosthesis with actuated knee and ankle joints. These actuators are placed in a slider-crank configuration, as with Fite et al. This design is capable of reproducing the torque curve for a 75 kg user and, since pneumatic actuators are used, the joint compliance can be controlled by adjusting pressure in the cylinder. The authors propose use of chemo-fluidic actuation, using a monopropellant and catalyst to produce pressurized gas. This allows for the use of liquid fuel, which is much more energy dense and easier to transport than a pressurized gas.

Sup et al (2009) go on to produce another powered prosthesis where the pneumatic cylinders of the first design are replaced with a motor-ball screw actuator, as in Fite et al. Additionally, a compression spring is incorporated into the design of the ankle actuator, similar to Martinez-Villalpando and Herr. This spring allows for additional force to be generated at toe-off of the foot which is the time when most of the propulsive force of walking is required. This new design has a mass of 4.2 kg and is capable of supporting an 85 kg user over a distance of 9 km.

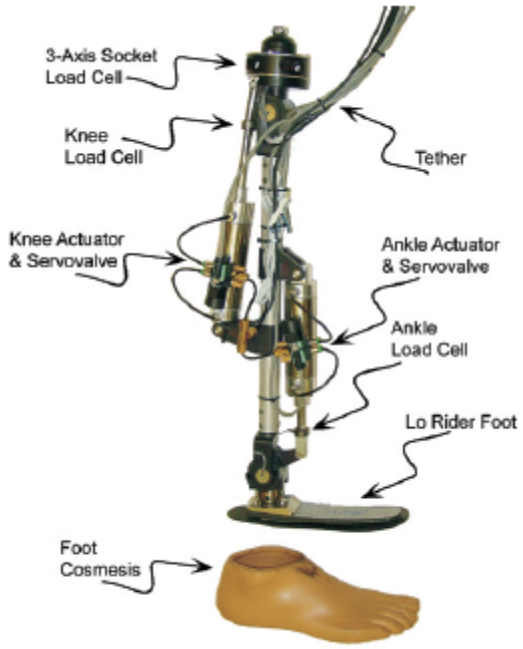

Figure 2.3 Pneumatic 2 DOF AK prosthesis from Sup et al

Lambrecht and Kazerooni (2009) have developed a semi-active hydraulic prosthesis. The prosthesis is semi-active because it functions during large portions of the gait cycle the same way commercial products like the C-Leg® and Rheo Knee® operate, by adjusting the joint damping to improve swing control. Additionally, a hydraulic pump can provide power to assist with knee flexion and extension to ensure a normal gait cycle is maintained, as well as providing short term power for activities such as stair climbing or standing. The prosthesis has a mass of less than 4 kg, and using a combination of active and passive modes is capable of 3000 steps per day. However, this prosthesis is designed mainly to assist a user with a powered swing and stance, not to contribute a large amount of positive work during walking.

2.3 Pneumatic Artificial Muscles

Pneumatic artificial muscles are pneumatic actuators that, when pressurized, expand radially and contract axially, exerting an axial force. Pneumatic muscles are sorted into several types depending on the construction such as braided, pleated, netted, and embedded muscles. The most common type is the braided pneumatic muscle, as shown in Figure 2.4 (Dearden, 2002), which consists of an inner membrane and an outer woven fiber mesh. The fiber mesh, relative to the membrane, can be considered as inextensible, and is wrapped around the membrane at an angle. For this reason, when the inner membrane is pressurized, the radius expands, forcing the total length of the muscle to shorten and the fibers maintain a constant length. McKibben muscles are the most commonly used and researched muscles, and are distinguished from other types of braided muscle by having both the membrane and fiber mesh fixed to an adaptor at both ends. J.L. McKibben invented this type of muscle in the 1950's as an orthotic actuator (Daerden, 2002). McKibben type muscles are commercially available from several companies, such as FESTO and Shadow, in a variety of diameters and lengths.

Since the pressurized membrane changes shape as the muscle shortens, the static force output of the muscle is a function of both the current pressure and percent hysteresis, or shortening. Under quasi-static conditions, the output force can be expressed as

$$F = -P\frac{dV}{dl} \tag{2.1}$$

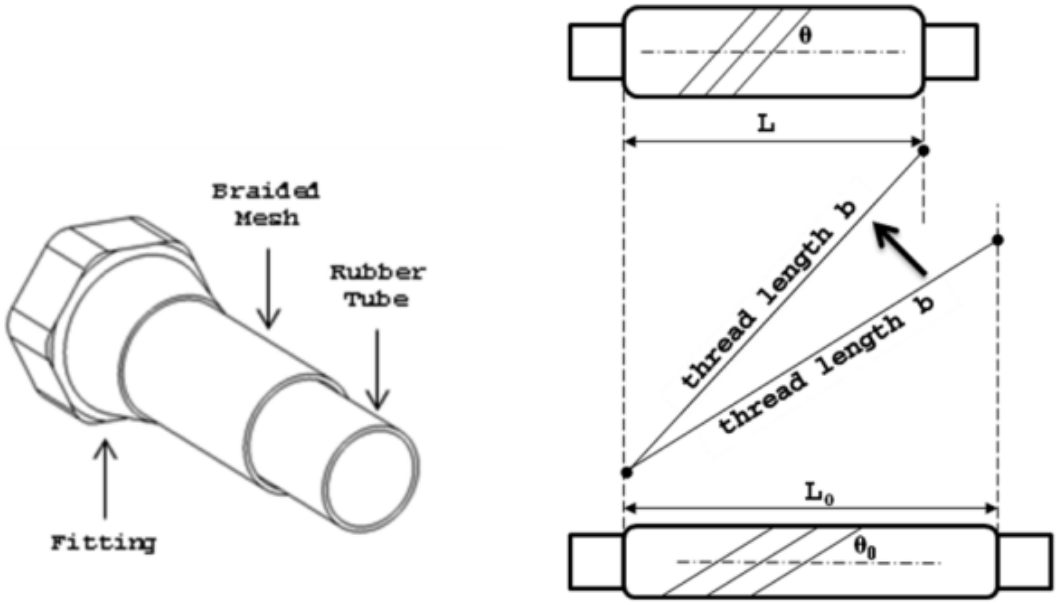

Figure 2.4 Structure of braided pneumatic artificial muscles

The isobaric force profile for commercially available Festo PAM is given in Figure 2.5. This non-linear relationship can make PAM difficult to model and control. Due to the nature of the PAM, they function as only single acting actuators. That is to say, they can only apply a contractive force in the axial direction, they are unable to apply or carry extensive or radial loads. Additionally, the stroke length, or hysteresis, of PAM is smaller than a similar sized pneumatic cylinder. Commercial PAM are capable of contraction of between 25% and 40% of their nominal length and up to 6 kN of axial force. However, PAM actuators have reported to have a power density of between 1.5 kW/kg (Caldwell, 1993) and 10 kW/kg (Hannaford, 1990). This is an order of magnitude higher than reported values of 0.4 kW/kg for pneumatic cylinders and 0.1 kW/kg for electric motors (Isermann, 1993). This power density comparison does not account for the energy density of a power source, which has long been a limiting factor of pneumatics, since compressors and pressurized tanks are quite heavy. However, new chemo-fluidic actuation

methods could potentially provide a source power more energy dense than current battery technology.

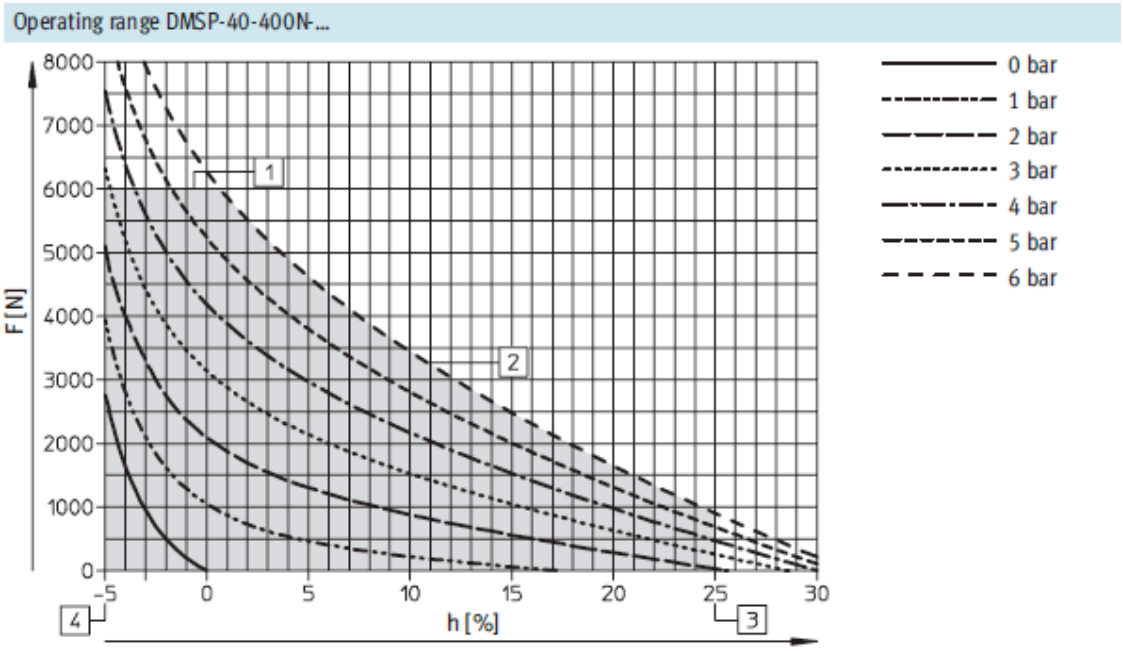

Figure 2.5 Isobaric hysteresis-force curves for FESTO PAM

To the best of the author's knowledge, attempts to implement PAM as an above knee prosthesis actuator have not been made. Research has been conducted on PAM in below knee applications, as well as bio-robotics.

Versluys et al (2008) utilize three pleated pneumatic muscles in an antagonistic slider-crank configuration. Two muscles located on the posterior of the leg control ankle plantarflexion, while one anterior muscle is used for dorsiflexion. This allows for a range of motion of 35 degrees and a peak torque of 200 N-m.

Hosoda et al (2006) demonstrate a bipedal robot powered solely by PAM. The robot is capable of walking, running, and jumping and uses antagonistic muscle pairs to power both the

knee and ankle joint. There are two important distinctions to make between robotics and prosthetics. Firstly, the mass of a robot can be designed to be much lighter than a human user, and as such the torque required for human locomotion is much higher. Secondly, muscles can be configured to match a healthy human leg; e.g. two muscles in the thigh, proximal to the knee joint, control the knee joint. Obviously, this is not possible with a prosthetic application, and all actuators must be placed in only the area of limb loss.

CHAPTER 3: DESIGN REQUIREMENTS OF A TRANSFEMORAL PROSTHESIS

3.1 Introduction to Gait and Prosthetics Design

One gait cycle is defined as the time from heel strike to heel strike of the same leg. Gait can be broken into two main phases, swing and stance. As the name indicates, swing phase is the period in which the leg is off the ground, while stance phase is the period in which the leg maintains contact. Figure 3.1 demonstrates a standard gait pattern.

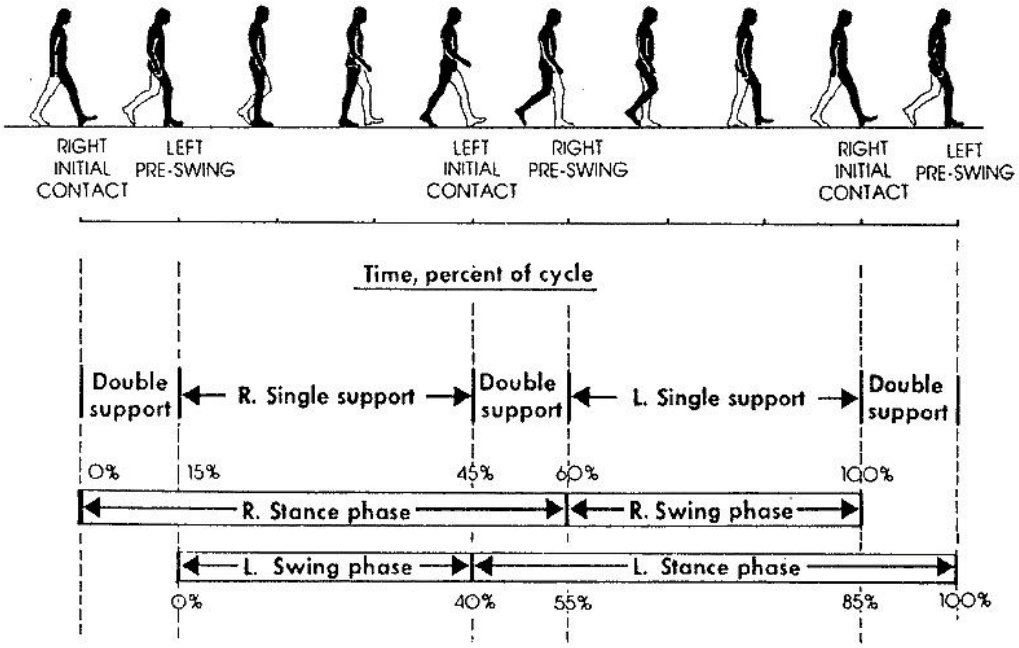

Figure 3.1 Normal gait cycle (Enderle, 2005)

During regular walking, human legs serve four major functions: balance, position, support, and power (Enderle, 2005). Traditional passive prosthetics can only fully account for two of these functions, balance and support. Position of the prosthesis must be controlled by the

user, and new microprocessor controlled prosthetics can help make this easier. The major shortcoming of passive prosthetics is the inability to generate positive power at the joints. This means that normal healthy gate is impossible, since this power must come from the sound leg or be transferred to the hip joint, increasing the energy cost of walking.

3.2 Torque Requirements of a Prosthesis

The key difference between the powered prosthesis and a traditional passive prosthesis is the ability to generate positive power at the knee joint, so it is critically important that the torque provided by the prosthesis is comparable to biological norms. Winter (1991) and Riener (2002) have each conducted studies on level walking and stair climbing, respectively. Both studies provide joint angle and normalized joint torque for the entire gait cycle at the knee and ankle joints. The data from both studies is combined to determine the required range of motion, as well as the maximum torque required in both flexion and extension directions at each joint angle. Figure 3.2 and Figure 3.3 show the required torque curves for the knee and ankle joint, respectively.

3.3 Anthropometric Requirements of a Prosthesis

A successful prosthesis will be able to reproduce the mass and inertial characteristics of a normal human leg. Ideally, the prosthesis should be able to accommodate any user between a 5^{th} percentile female and a 95^{th} percentile male. Table 3.1 shows relevant parameters for both a 5% female and 95% male (McDowell 2008). Based on normalized data presented by Winter (2005), leg length, as defined from the ground to the axis of knee rotation, is 28.5% of total height. Therefore, a 5% female (1507 mm / 5 ft) should have a leg length of roughly 432 mm (17 in). A 95% male (1887 mm / 6 ft. 3 in.) should have a leg length of approximately 533 mm (21 in).

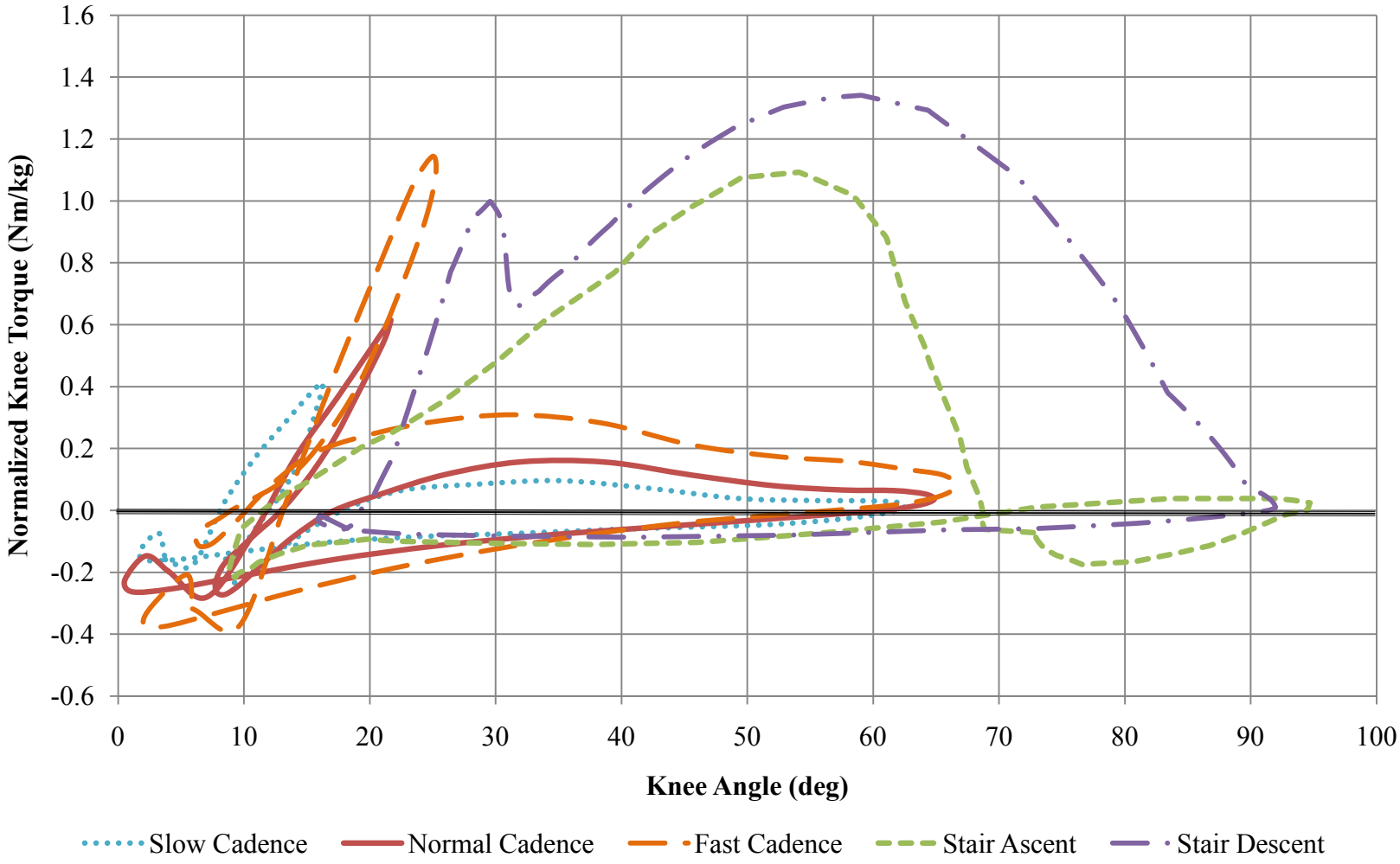

Figure 3.2 Normalized knee torque for various standard modes of ambulation

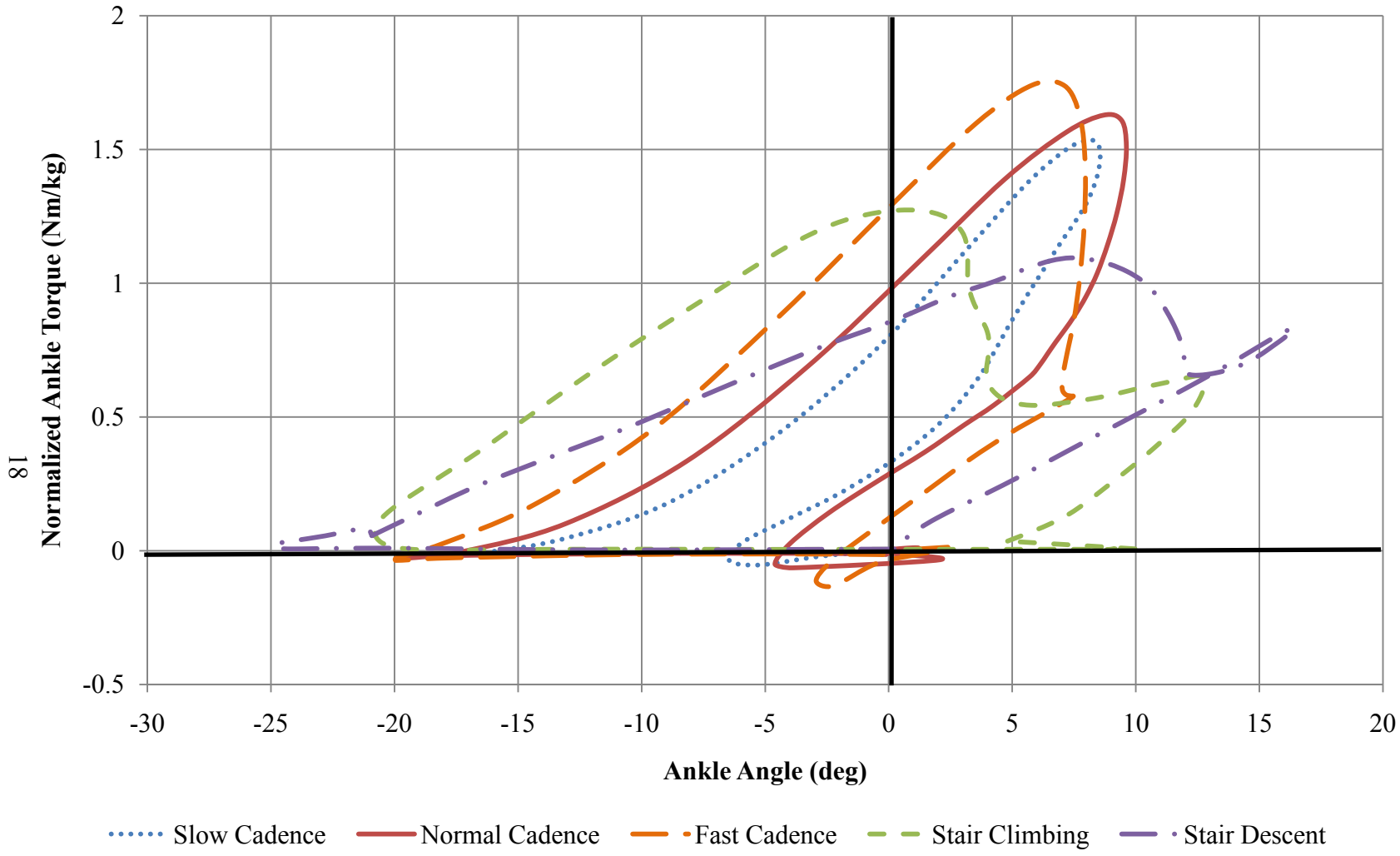

Figure 3.3 Normalized ankle torque for various standard modes of ambulation

Table 3.1 Anthropometric Data for 5% Female and 95% Male

	5% Female	**95% Male**
Total Body Mass	50 kg	125 kg
Height	1507 mm	1887 mm
Leg Length	432 mm	533 mm
Leg Mass	3.3 kg	7.6 kg
Below Knee Inertia	0.205 $kg\ m^2$	0.794 $kg\ m^2$

In order to maintain proper balance during walking, the mass of the prosthesis should be approximately the same as a sound leg, which is roughly 6.1% TBM. This means the mass of the prosthesis should be between 3 and 7.6 kilograms (6.6 – 16.75 pounds) for a 5% female (50 kg TBM) and 95% male (125 kg TBM), respectively. The inertia of the prosthesis about the hip joint should be comparable to anthropometric norms to avoid undue torque required at the hip. The normal radius of gyration for the foot and leg is 60.6% of the segment length from the proximal end of the leg. Therefore, the inertial properties of the leg should be between .205 kg-m^2 and .794 kg-m^2 to remain in the normal range from a 5% female to a 95% male (Winter, 2005).

Additionally, a prosthesis must reasonably retain the anthropometric form of a sound leg. Otherwise it will require special accommodations to be made throughout an amputee's lifestyle. Figure 3.4 demonstrates the anthropometric envelope of a 50% male leg with key dimensions annotated (Bodyworks, 2009). From this anthropometry it is assumed that a prosthesis should

attempt to maintain a cross section of roughly 125mm x 125mm (5”x5”) so as to reasonably resemble the size of a natural leg.

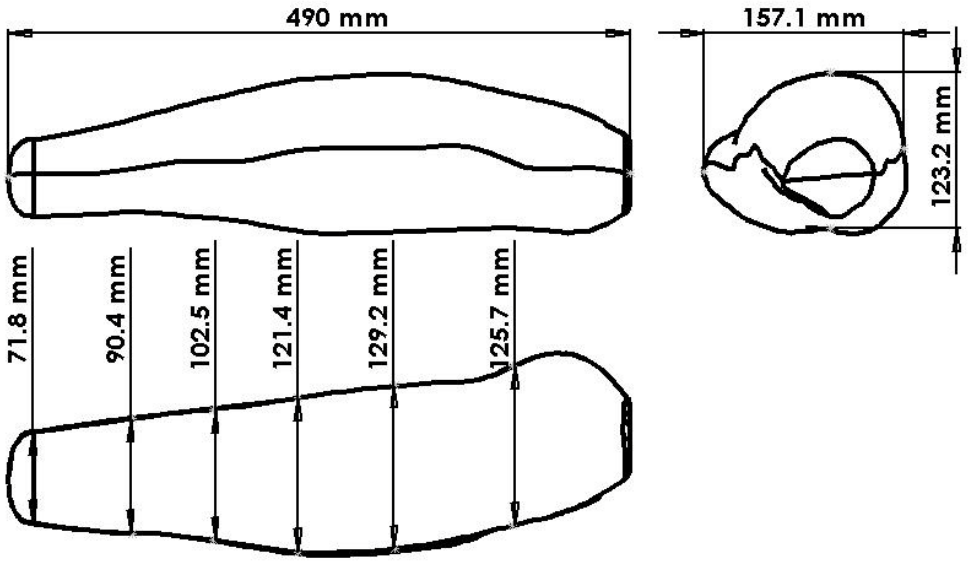

Figure 3.4 Annotated 50% male lower leg anthropometry

CHAPTER 4: DESIGN AND TESTING OF A ONE DOF PROSTHESIS

4.1 Conceptual Design

In order to begin the design of the prosthesis, the general form of the structure must be determined. Traditional leg prostheses generally utilize a single, cylindrical support with a single actuator fixed on the posterior side of the leg. However, PAM are single acting actuators, and thus two muscles must be used antagonistically to provide a full range of motion. As stated previously, when PAM are actuated their diameter increases as they shorten. Based on the muscles required to provide adequate torque and range of motion, the diameter of each muscle will reach approximately 75 mm (3 in.). In order to accommodate both muscles in the smallest envelope possible, two separate supporting bars are utilized as opposed to a single cylindrical support. As shown in Figure 4.1, this allows the PAM actuated leg to fit within the anthropomorphic envelope of a 50% male.

It is of course critically important that the prosthesis be able to withstand the internal forces of the actuators as well as external dynamic loads as applied by the user. Each PAM will be capable of generating a 6 kN force, and the leg will be designed to support the weight of a 95% male user. 6061 T6 aluminum alloy, which provides a yield strength of 275 MPa, will be used for the structural elements of the prosthesis based on its mass to strength ratio as well as its relatively low cost. Using these constraints, an Abaqus model is constructed. The Abaqus simulation shows a maximum stress of 165 MPa, which provides a minimum factor of safety

against yield of 1.67 and a maximum deflection of 0.025 mm. The graphical results of the simulation are shown in Figure 4.2.

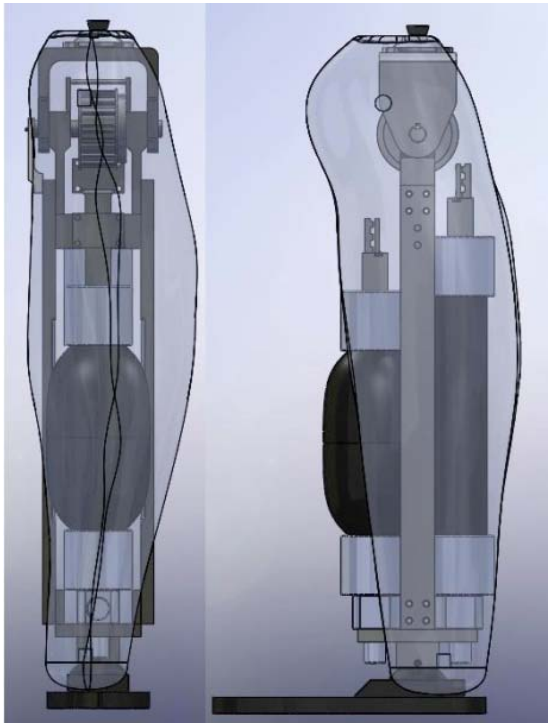

Figure 4.1 Front and side views of the 1 DOF prosthesis compared to a 50% male

Using this structure, the entire assembled prosthesis weighs approximately 3.2 kg, which is comparable to the healthy limb mass of a 5% female. Additionally, the inertia of the prosthesis is .107 kg-m^2, roughly half the inertia of a 5% female leg. This should allow a user to easily transition to walking with the prosthesis without any undue loads on the hip or thigh.

As stated previously, the PAM actuators must provide a user with adequate torque and range of motion to be able to reproduce an ideal, healthy walking gate. Two commercially

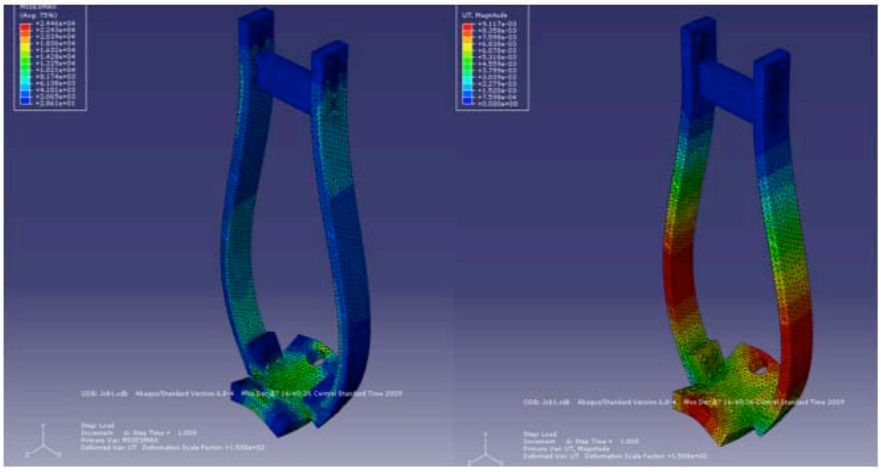

Figure 4.2 Abaqus results of maximum von Mises stress and deflection

available PAMs (FESTO DMSP-40-180N-RM-CM) were selected to actuate the knee joint antagonistically. Each PAM will be affixed to a solid plate near the foot and will contract from the proximal end. A Kevlar reinforced neoprene timing belt was affixed to the ends of both PAM and used to actuate a timing belt pulley attached to the upper half of the knee joint. The length of the muscle must be such that the prosthesis could be adjusted to fit within the anthropomorphic envelope of a 5% female, which is approximately 430 mm. For the commercial FESTO PAM, the maximum stroke is 25% of the nominal length.

The radius of the timing belt pulley (25 mm) and the required PAM stroke (40 mm) were then determined such that the prosthesis would meet all standard locomotive requirements for a 50% male. A graph of the available extensive and flexive torque for the prosthesis, as well as the torque required to allow for slow cadence, normal cadence, and stair climbing, is shown in Figure 4.3. Fast cadence walking and stair descent required too much torque and were not able to be accounted for.

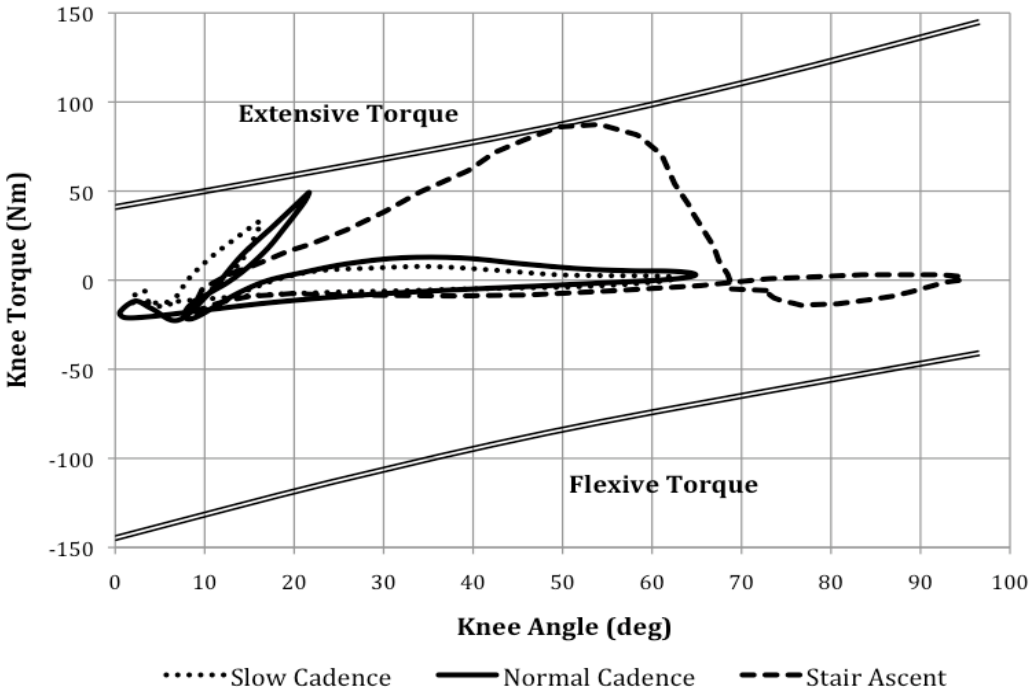

Figure 4.3 Available and required knee torque for a 50% male

The instrumentation of the prosthesis consists of two three-position pneumatic valves, two pressure sensors, a ground-force sensor, and a rotary potentiometer. The valves and pressure sensors are not incorporated directly into the design as they can be placed nearby with the source of compressed air. The potentiometer is affixed to the rotating shaft of the knee with a small plastic attachment created with a rapid prototyper. These sensors allow for calculation of joint angle and muscle force, thereby allowing torque calculations to be made. The ground force sensor consists of two force resistors which allow differentiation between stance and swing phases.

Figure 4.4 Instrumented prosthetic foot with force resistors

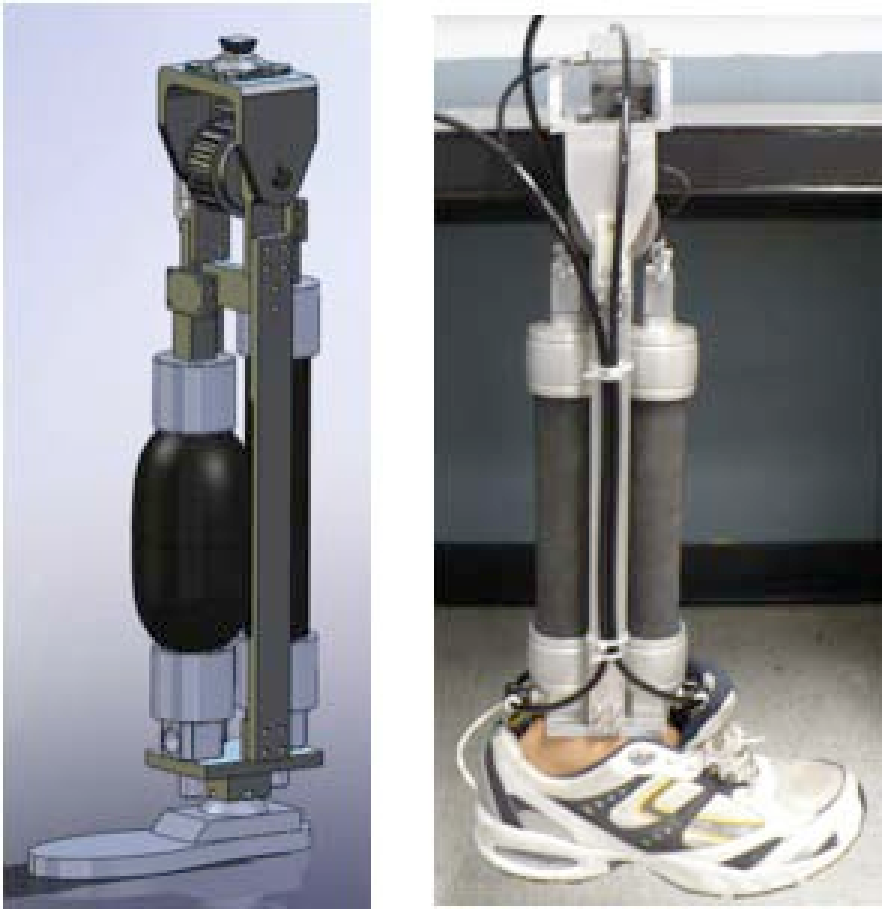

Figure 4.5 Computer model and completed prototype 1 DOF PAM prosthesis

4.2 Control

Sup et al. proposed an impedance based control approach, in which an artificial impedance is simulated on the joints of the prosthesis to provide a natural user-prosthesis interface for safe interaction (2008). Experimental results demonstrated a natural walking gait similar to the standard gait of healthy subjects. Considering the effectiveness of the impedance-based control approach by Sup et al., the method adopted for the control of the proposed leg prosthesis is similar in concept, but incorporates two important modifications. First, a two-state structure is adopted, which simplifies the instrumentation for the sensing and computation for the determination of the gait stage. Second, instead of a purely closed-loop simulation of the impedance, the proposed controller also incorporates the modulation of open-loop (i.e. physically existing) impedance through the modulation of the average pressure in the actuators. The combination of open-loop and closed-loop impedance modulation provides a closer facsimile to the human motor control process.

A standard gait cycle can be divided into two main modes or states: stance and swing. The stance mode starts with the heel strike, and from an impedance point of view, the knee joint maintains a high stiffness to provide stable support to the body, and prevent buckling. Also, a certain level of damping is required to provide shock absorption. As such, in the desired impedance behavior, as defined by the following equation, the values of K and B must be maintained at a high level.

$$\tau = K(\theta - \theta_e) + B\dot{\theta} \tag{4.1}$$

The swing mode, on the contrary, requires a much lower level of impedance. The low impedance facilitates the free swing motion without excessive efforts from the joints. As such, the stiffness can be set as zero, with a small damping value to improve the control over the swing motion. The timing of this mode switch will be dictated by the activation of the ground force sensor.

4.3 Testing

The first test performed simply checks that the actual range of motion matches the design criteria. This is done by fully flexing and extending the prosthesis and measuring the change in angle using the radial potentiometer. The range of motion of the prosthesis is found to be 91.8 degrees. Also, the prosthesis control method is tested. The normalized stride data is provided as an input to demonstrate the prosthesis's ability to accurately (within two standard deviations) follow the curve. The values of K and B from equation 4.1 are tuned for swing phase performance for this test. The results can be seen in Figure 4.6.

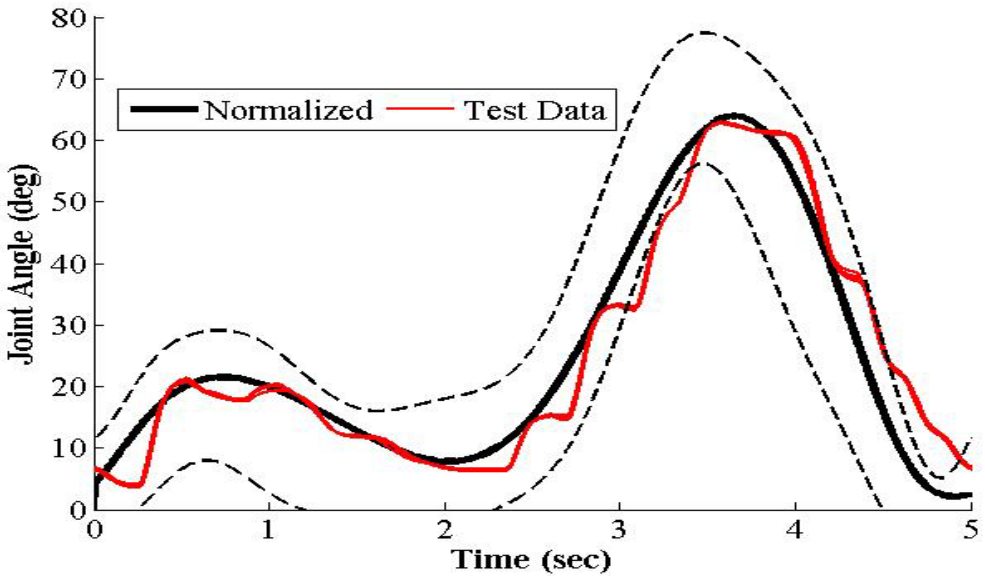

Figure 4.6 Control of the 1 DOF prosthesis

CHAPTER 5: NOVEL ACTUATOR DESIGN

5.1 Justification for New Actuator Design

One of the key shortfalls of the one degree of freedom, antagonistic design is its inability to match the full desired torque curve. Though the constant radius and antagonistic actuators make fabrication easier, the inability to reproduce the desired torque prevents the prosthesis from performing certain tasks. The speed of the PAM actuation is also a limiting factor of the design, and a new actuator could improve overall prosthesis speed. An actuator which utilizes a non-constant radius has the potential to improve both torque capacity and maximum speed. New actuator designs are analyzed to see if an improved, feasible option exists.

5.2 Comparison of Feasible Options for Actuation

In addition to the constant radius pulley, three new actuator designs are proposed and considered. They are three bar, variable radius pulley, and elliptical pulley. Each of these designs was analyzed to determine the optimal actuator for torque, speed, mass, and manufacturability requirements.

It is noted that in both knee flexion and ankle dorsiflexion directions, the required torque is significantly less than for knee extension and ankle plantarflexion. Therefore, rather than using two antagonistic PAM for each joint, a PAM-spring combination can be utilized, since the spring is only required to produce a relatively small torque. Two spring options are considered, a torsional spring and a linear spring. The spring must be selected and designed before the

actuator can be determined, since the spring torque will be constantly acting against the torque of the PAM.

Consideration was first given to the linear spring. The linear spring can be configured in a manner similar to the slider-crank actuator described in the subsequent section, allowing a non-linear spring torque and angle relationship. This way, it is possible to more closely reproduce the required torque and minimize the effect of the spring on the PAM actuator. For these reasons, a linear spring is selected for the initial tester design.

However, since the linear spring is used in a slider crank configuration, it must be relatively long and required a fixed point on the structure of the prosthesis. This means a linear spring takes up more space than a torsional spring and makes the prosthesis more difficult to have adjustable length. It is therefore determined that a torsional spring will be mounted on the shaft of the joint to provide return torque. While this does not provide the optimal output torque, it makes the design and manufacture much easier.

The slider-crank design was the first new actuator considered, as this has been widely used in other powered prosthetics that use pneumatic cylinders or even electric motors. The slider crank configuration uses a 3 sided, triangular design in which one side of the triangle is the actuator. The second side is the rigid support structure. The motion of the actuator causes the final side to rotate about a fixed point, providing a change in angle, γ. Therefore as the actuator contracts, the effective radius varies, allowing modification of the output torque. This actuator has 4 variables, referred to as L_0, L_1, θ_r, and r, as shown in Figure 5.1.

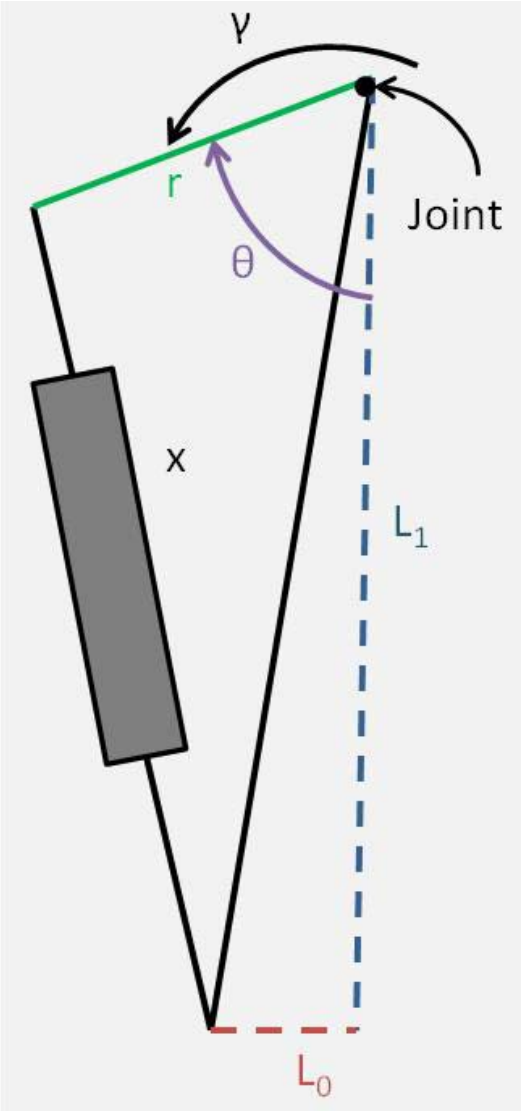

Figure 5.1 Slider-crank configuration

Next, consideration was given to a variable radius pulley design. This design would employ a flexible tendon wrapped around a pulley. This pulley would be designed so that it would provide a larger radius during high torque requirements and a smaller radius when more speed is desired. However, this actuator greatly increases the complexity of the design process and increases the difficulty of fabrication. The curvature of the pulley must be constrained to manufacturable, smooth curves. Additionally, to fully define the radius, either a large number of

variables or a rough approximation of the curve must be utilized, making the optimization very complex.

The final design consideration is a variation on the variable radius pulley, constraining the curve to an elliptical shape. This elliptical pulley greatly simplifies the design optimization and fabrication, reducing optimization variables to 5. These 5 variables are major and minor semi-diameter, rotation, and the coordinates of the ellipse center with relation to the center of rotation. Figure 5.2 provides a graphical representation of what each variable represents. The ellipse still provides improved torque output without greatly increasing the difficulty of fabrication or implementation.

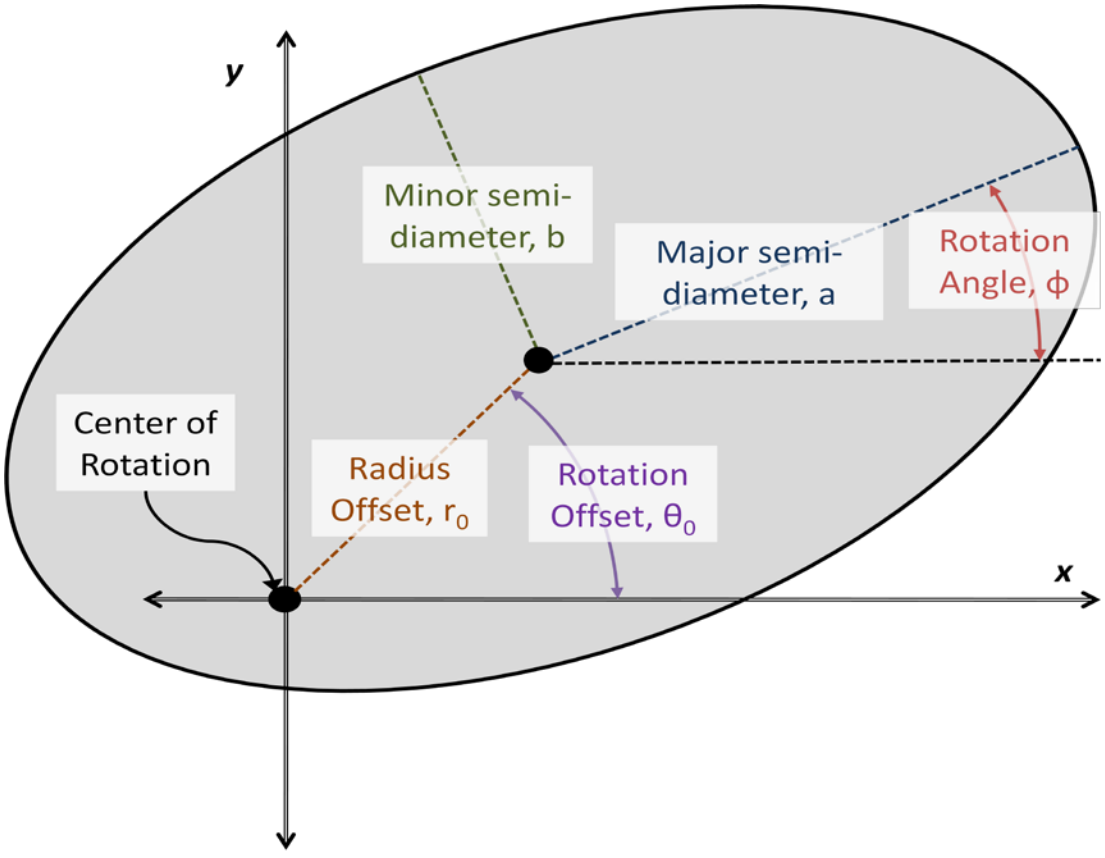

Figure 5.2 Definitions of important ellipse variables

5.3 Optimization Theory and Practice

In order to optimize the design of the actuator, it is critical to understand the mathematical theory of optimization. The most common optimization method is convex optimization. This method analyzes the gradient of an objective function in terms of any number of defining variables. A new point is then selected and the gradients again analyzed until a minimum is found. When an error function is used as the objective function, this process serves to find a point with the minimum error between an actual and desired function.

The issue with this approach is, as the name indicates, it only finds the minimum of a convex function. An irregular function, which may have multiple local minima, requires additional steps to ensure a global minima is found. Most of these methods involve examining a large grid of starting points all across the range of acceptable values for each variable.

Since the level of computation for optimization is quite high, particularly as the number of variables to optimize increases, it is helpful to utilize one of several readily available optimization software algorithms. Matlab offers such functionality as part of their optimization toolbox and global optimization toolbox. For the optimization of the actuator, the Matlab optimization solver "fmincon" is selected. This optimization solver is commonly used for most optimization problems, as it is suited to constrained, nonlinear, multivariable problems. Within the "fmincon" solver, the "interior-point" algorithm is selected, as it is a robust optimizer that is well suited to large-scale problems.

The solver "fmincon" serves as the method of local optimization, but as stated previously, additional steps must be taken to find a global solution. Two global optimization methods from the Matlab Global Optimization Toolbox are used, GlobalSearch and MultiStart.

MultiStart generates a user specified number of random, uniformly distributed points across the constraints of the system. Each one of these points is used as a starting point for the local solver "fmincon," and the solution of each run is compared and the minimum of all solutions is taken as the global minimum. The GlobalSearch solver works by generating a set of random starting points, similar to MultiStart, but then assigns a penalty value to each point based on the objective function and constraints. The point with the lowest penalty function is used as the start point for the "fmincon" local solver and once a minima is found, the region around that minima is flagged as being associated with the minima. The size of this region is based on the distance the local solver traveled from the starting point to the minima. At this point, GlobalSearch will continue to generate random starting points, however now each point is evaluated individually. If a start point is located within a region associated with an existing minima, it is not evaluated. Additionally, start points whose penalty value is above a given threshold will not be run. This process continues until the penalty threshold reaches a value such that no more points can be evaluated, and each of the located minima is compared to determine the global solution (Ugray, 2008).

Since each of these solvers is dependent on an input start point, as well as an array of randomly generated points, it is prudent to conduct multiple iterations using the GlobalSearch and MultiStart solvers. Once both solvers return the same minimum with the same input, it can be assumed that this is a global minimum.

The first step in optimizing the actuator design is the definition of an objective function. The required torque is created from the combined torque curves for normal and fast cadence walking, stair climbing, and stair descent for a 100 kg user. We define the error as the integral of

the difference between the actual and desired torque curves. Additionally, if the available torque is less than required, a penalty multiplier is applied to ensure that the solution is able to provide adequate torque for most or all of the joint rotation.

$$error = \int \begin{Bmatrix} T_{act}(\gamma) - T_{req}(\gamma) & if\ T_{act} > T_{req} \\ Pen * \left(T_{req}(\gamma) - T_{act}(\gamma)\right) & if\ T_{act} < T_{req} \end{Bmatrix} d\gamma \tag{5.1}$$

For most of the optimization procedures, the actual torque is defined as

$$T_{act}(\gamma) = F(\gamma) * r_{eff}(\gamma) \tag{5.2}$$

The FESTO pneumatic artificial muscles come with a manufacturer specified force profile, which is provided in Figure 5.3. A polynomial curve fit of the data provides the following equation

$$F = 2.8571 * (\%\square)^2 - 271.14 * (\%\square) + 5992.9 \tag{5.3}$$

In the case of the linear spring, the force is given as

$$F(\gamma) = K\Delta x + P \tag{5.4}$$

However, for the torsional spring, the torque is defined as

$$T_{act}(\gamma) = K\gamma + P \tag{5.5}$$

It is important to note that the optimization of the spring side of the actuator must be performed before the optimization of the muscle side. This is due to the fact that the spring torque will act constantly on the joint, and the muscle torque will have to overcome the spring torque to actuate the leg. A new desired torque can then be found that is the sum of the anthropometric required torque described in chapter 3 and the spring torque.

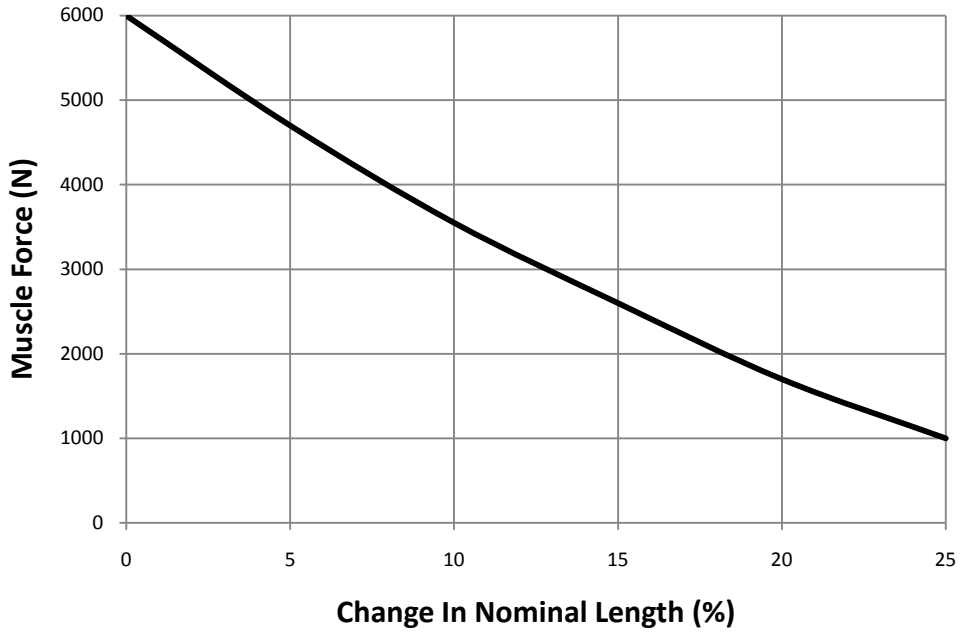

Figure 5.3 Maximum force profile for selected FESTO PAM

Each of the variables to be optimized is constrained to maintain geometric and manufacturing considerations and stay within the anthropometric envelope of the leg. Specifically, the fixed position of the actuator is dictated entirely by the overall available length and cross-section of the leg, and as such no optimization is performed on these variables. Additionally, the PAM actuators are constrained to ensure the maximum stroke value is not exceeded. Mathematical definitions of the effective radius and percent hysteresis for each actuator, as well as the specific optimization processes, can be found in the following sections.

5.4 Constant Radius Pulley Optimization

The optimization process for the constant radius pulley is fairly simple, since the design consists of only one variable: pulley radius. This means the percent hysteresis can be represented as

$$\%\square(\gamma) = r\Delta\gamma \tag{5.6}$$

This allows the available torque to be expressed in terms of radius and angle,

$$T_{act}(\gamma) = r(2.8571 * (r\Delta\gamma)^2 - 271.14 * (r\Delta\gamma) + 5992.9) \tag{5.7}$$

5.5 Slider Crank Actuator Optimization

The optimization of the slider crank actuator applies both to the PAM slider crank and the linear spring. The determination of the effective radius is based completely on the geometry of the actuator placement. Recall from Figure 5.1 that the slider crank geometry is defined by the terms L_0, L_1, θ, and r as well as the known actuator length, x. We can relate these four variables and the joint angle with the law of cosines as

$$x(\gamma) = \sqrt{r^2 + {L_0}^2 + {L_1}^2 - 2\cos(\theta - \gamma)\, r\sqrt{{L_0}^2 + {L_1}^2}} \tag{5.8}$$

The effective radius can then be determined by solving for the remaining angles and using trigonometry

$$r_{eff}(\gamma) = \sqrt{{L_0}^2 + {L_1}^2}\sin\left(\cos^{-1}\left(\frac{{L_1}^2 + {L_0}^2 + r^2 - x(\gamma)^2}{2r\sqrt{{L_0}^2 + {L_1}^2}}\right)\right) \tag{5.9}$$

Lastly, it is necessary to determine the percent hysteresis as a function of angle so that the force profiles of both a spring or PAM are known. The percent hysteresis can be shown as

$$\%\square(\gamma) = \frac{x(\max(\gamma)) - x(\gamma)}{L_{nom}} \tag{5.10}$$

5.6 Elliptical Actuator Optimization

Using the standard polar equation for an ellipse, the radius can be calculated as

$$P(\theta) = r_0((b^2 - a^2)\cos(\theta + \theta_0 - 2\varphi) + (a^2 + b^2)\cos(\theta - \theta_0))$$

$$R(\theta) = (b^2 - a^2)\cos(2\theta - 2\varphi) + a^2 + b^2$$

$$Q(\theta) = \sqrt{2}ab\sqrt{R(\theta) - 2r_0^2\sin^2(\theta - \theta_0)} \tag{5.11}$$

$$r(\theta) = \frac{P(\theta) + Q(\theta)}{R(\theta)}$$

For a given actuator configuration geometry, it is possible to determine the actual effective radius by finding a line tangent to the curve of the pulley that passes through the point representing the fixed end of the muscle. The perpendicular distance from this line to the center of the pulley is the effective radius. Given the coordinates of fixed point of the actuator relative

to the center of rotation as (x_0, y_0), the angle coordinate where the tangent line meets the pulley for a given joint rotation can be represented as

$$\theta_{eff}(\gamma) = \max_{0 \le \theta \le 180} (r(\theta)\cos(\theta - \gamma) - x_0) * (-y_0) - (r(\theta)\sin(\theta - \gamma) - y_0) * (-x_0) \tag{5.12}$$

In practice, it is much simpler to perform an exhaustive search of each point on the ellipse to find the tangent point. Knowing θ_{eff}, it is possible to determine the equation of a line tangent to the curve which also passes through the fixed point of the actuator. This equation of this line is

$$y = \frac{\left(r(\theta_{eff}(\gamma))\sin(\theta_{eff}(\gamma)) - y_0\right)}{\left(r(\theta_{eff}(\gamma))\cos(\theta_{eff}(\gamma)) - x_0\right)}(x - x_0) + y_0 \tag{5.13}$$

For simplicity, we define

$$m = \frac{\left(r(\theta_{eff}(\gamma))\sin(\theta_{eff}(\gamma)) - y_0\right)}{\left(r(\theta_{eff}(\gamma))\cos(\theta_{eff}(\gamma)) - x_0\right)} \tag{5.14}$$

The effective radius is then the perpendicular distance from this line to the rotation center of the pulley. This is given by the cross-product of the two vectors representing the line of action of the actuator and the line from the actuator fixed point to the rotational center, but can be represented more simply as

$$r_{eff}(\gamma) = \frac{abs(x_0\, m - y_0)}{\sqrt{m^2 + 1}} \tag{5.15}$$

Finally, it is necessary to determine the percent hysteresis as a function of theta

$$s = \int_{\gamma_1}^{\gamma_2} \sqrt{{r_{eff}}^2 + \left(\frac{dr_{eff}}{d\gamma}\right)^2}\, d\gamma \tag{5.16}$$

However, this integral does not have a closed form solution except under special circumstances, nor is there an explicit definition of the derivative of the effective radius. Therefore, an

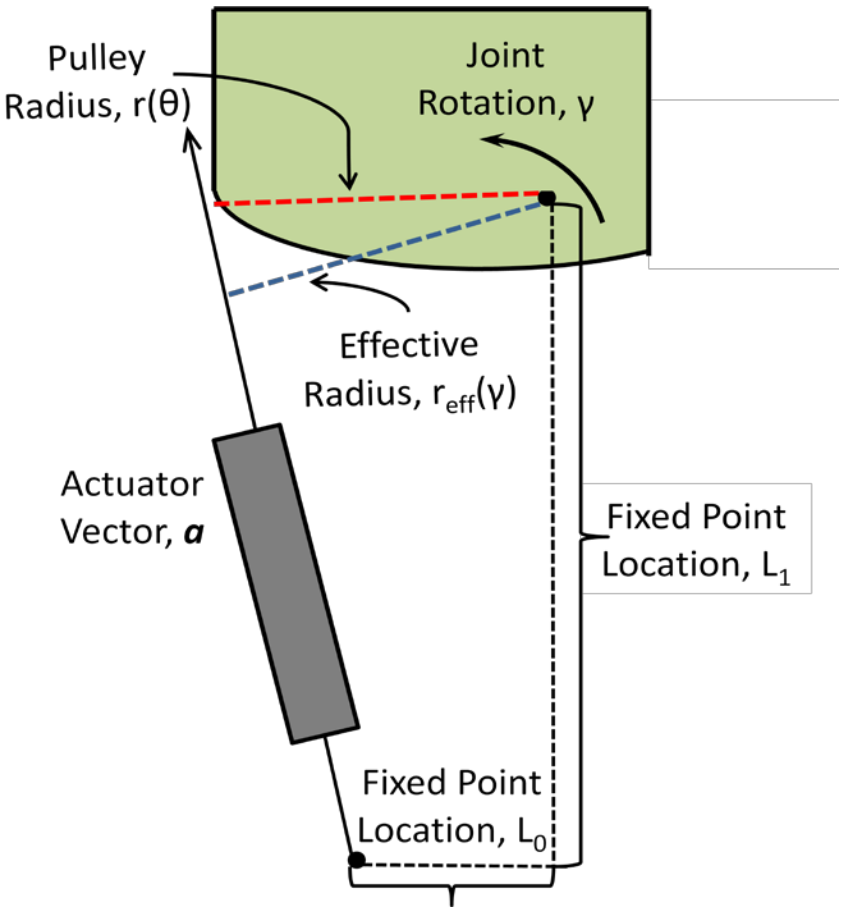

Figure 5.4 Elliptical pulley configuration

approximation is useful. For small changes in angle, it can be assumed that the arc length can be approximated as linear. This greatly reduces the complexity of the calculations, improving computation speed during optimization.

$$\%\square(\gamma) = \frac{\sum_{i=2}^{\gamma}\sqrt{r(i)^2 + r(i-\Delta\gamma)^2 - 2r(i)r(i-\Delta\gamma)\cos(i-i-\Delta\gamma)}}{L_{nom}} \tag{5.17}$$

Combining the above equations, it is possible to represent the actual torque in terms of γ for a given radius.

$$T_{act}(\gamma) = \frac{abs(x_0\, m - y_0)}{\sqrt{m^2+1}} * 2.8571 * \left(\frac{\sum_{i=2}^{\gamma}\sqrt{r(i)^2+r(i-\Delta\gamma)^2-2r(i)r(i-\Delta\gamma)\cos(i-i-\Delta\gamma)}}{L_{nom}}\right)^2 - 271.14 * \left(\frac{\sum_{i=2}^{\gamma}\sqrt{r(i)^2+r(i-\Delta\gamma)^2-2r(i)r(i-\Delta\gamma)\cos(i-i-\Delta\gamma)}}{L_{nom}}\right) + 5992.9 \tag{5.18}$$

5.7 Comparison of Actuation Methods

In order to compare each actuator design, optimization is performed for all three actuator configurations for the same FESTO DMSP-40-203N-RM-CM PAM at the knee joint and a shorter FESTO DMSP-40-152N-RM-CM PAM. The torque curves used to optimize each actuator are for a 100 kg user. After completing optimization, it can be seen that the elliptical pulley offers the best recreation of the biological torque curve for the knee, while the slider-crank actuator provides better results for the ankle joint.

Table 5.1 Optimized Torsion Spring Parameters

Variable Name	Knee	Ankle
Spring Constant, K	0.28 N-m/deg	0.339 N-m/deg
Pre-Tension Torque, P	43 N-m	7.55 N-m
Total optimized error, f	1269.2 N-m-deg	585.4 N-m-deg

Table 5.2 Optimized Linear Spring Parameters

Variable Name	Knee	Ankle
Spring Constant, K	3.81 N/mm	0.916 N/mm
Spring Nominal Length, L	136.5 mm	138.8 mm
Spring fixed point x location, x_0	31.75 mm	89.26 mm
Spring fixed point y location, y_0	187.3 mm	226.5 mm
Spring attachment length, r	42.44 mm	123.2 mm
Initial rotation, θ_r	145 deg	130 deg
Total optimized error, f	940.3 N-m-deg	407.1 N-m-deg

Table 5.3 Optimized Constant Radius Pulley Parameters

Variable Name	Knee	Ankle
Pulley radius, r	27 mm	39.8 mm
Total optimized error, f	40129 N-m-deg	2335.5 N-m-deg

Table 5.4 Optimized Slider Crank Parameters

Variable Name	Knee	Ankle
Muscle attach x direction, L_0	50.8 mm	69.85 mm
Muscle attach y direction, L_1	271 mm	282.6 mm
Attachment point length, r	38.3 mm	47.6 mm
Initial rotation, θ_r	170 deg	100.42 deg
Total optimized error, f	23989 N-m-deg	2255.4 N-m-deg

Table 5.5 Optimized Elliptical Pulley Parameters

Variable Name	Knee	Ankle
Major semi-diameter, a_{dia}	31.85 mm	66.7 mm
Minor semi-diameter, b_{dia}	9.1 mm	88.2 mm
Ellipse Rotation, φ	2.03 deg	90 deg
Ellipse center offset radius, r_0	10.8 mm	42 mm
Ellipse center offset angle, θ_0	7.5 deg	180 deg
Total optimized error, f	3141.7 N-m-deg	11726 N-m-deg

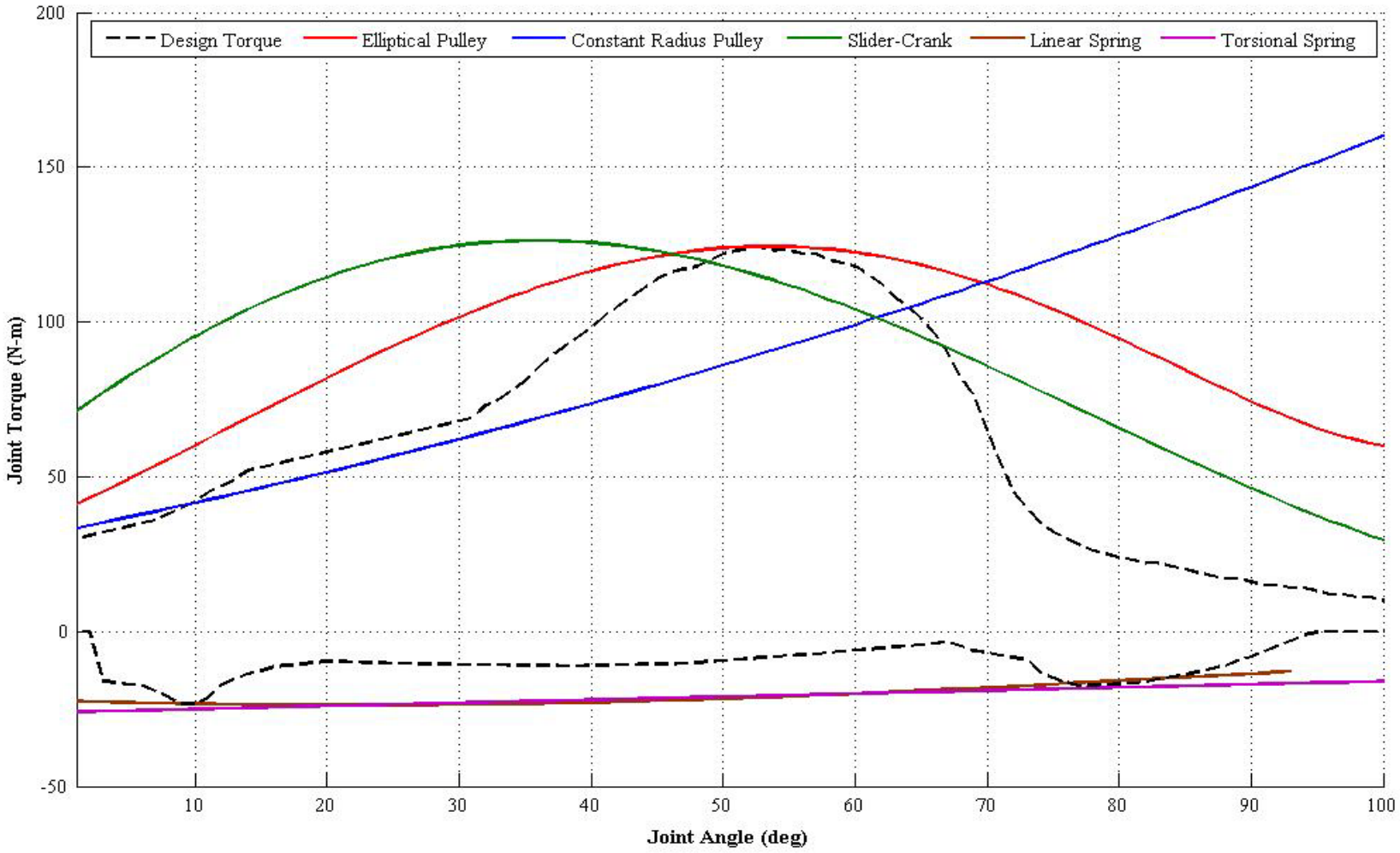

Figure 5.5 Optimized knee torque curves

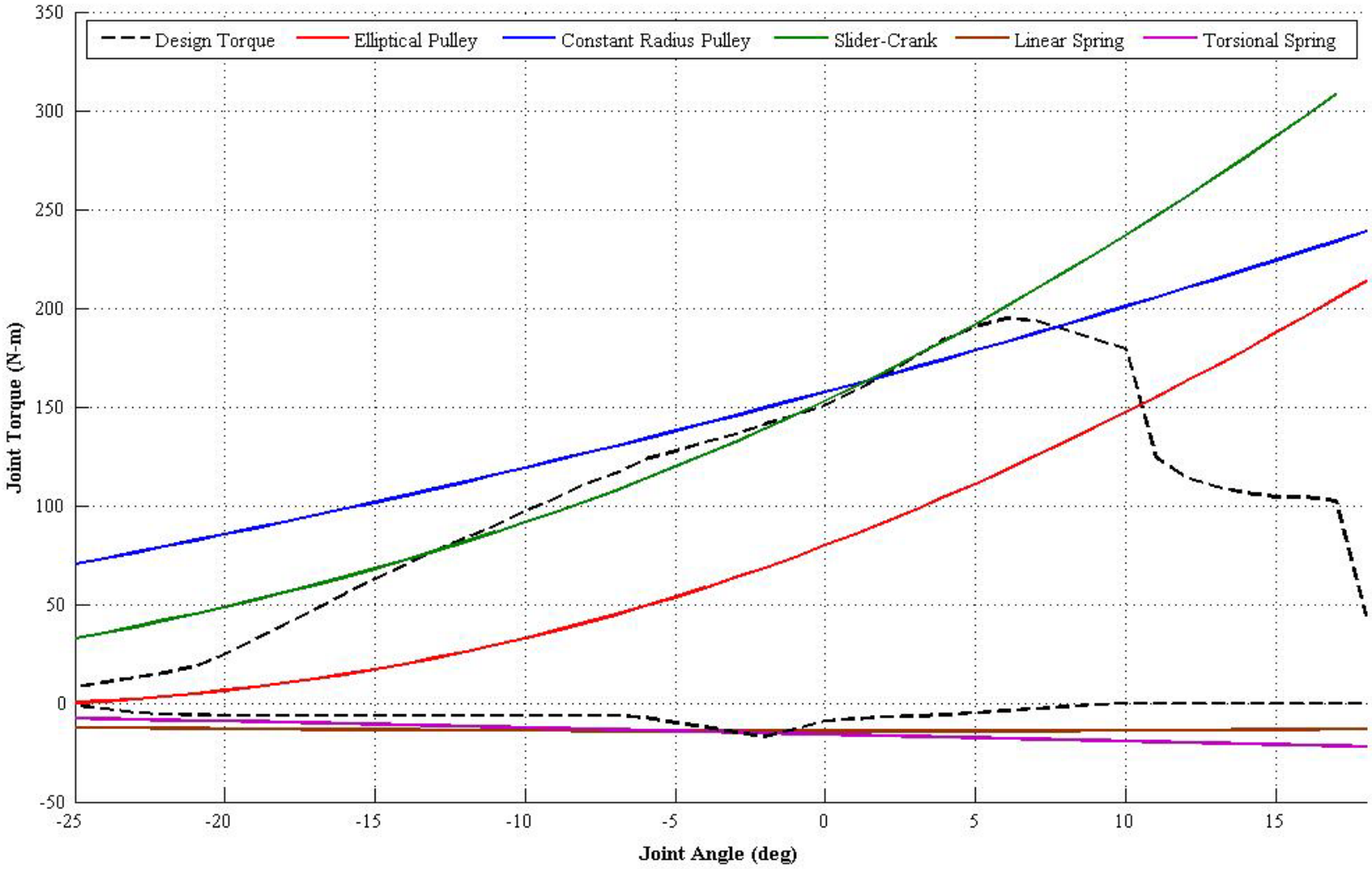

Figure 5.6 Optimized ankle torque curves

5.8 Construction and Testing

In order to test the effectiveness of this new actuator configuration, a tester is constructed. This will allow the spring-muscle-pulley combination to be evaluated without constructing a working prosthesis. The tester is simply constructed of two aluminum bars that are actuated about a shaft. A tube is attached at the bottom of the tester to allow for the addition of weights for testing the torque output of the actuator.

Figure 5.7 Actuator computer model and completed bench-top tester

Testing of the new actuator is carried out using the same methods as with the 1 DOF prosthesis. This allows the determination of actual range of motion, available torque, and control

testing. The effective range of motion is experimentally determined to be 98 degrees, 6 degrees greater than the 1 DOF design. In order to experimentally validate the torque output of this actuator, a large inertial load is applied to the prosthesis. Then the pneumatic valve is fully opened until the prosthesis comes to rest. The angle vs. time data for this test is recorded, and from this we can determine the instantaneous acceleration. For a known inertia, mass, and acceleration, it is possible to determine the instantaneous torque.

Figure 5.8 shows the results of the available torque test, performed with several different loads at the end of the tester ranging from unloaded to 50 kg. It is difficult to exactly reproduce the curve, but testing shows that the torque output is at an appropriate range based on the design. Some sources of error are the compliance of the rope and the limitation of the rate of shortening of the muscle.

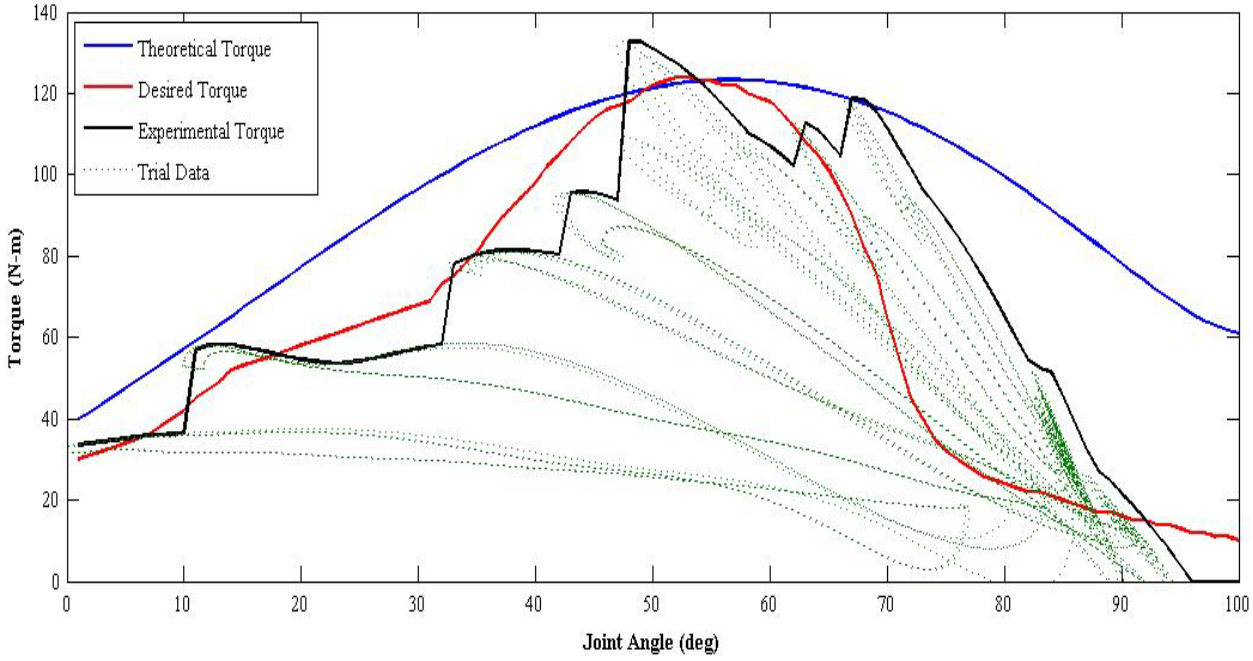

Figure 5.8 Experimental and theoretical actuator torque

The control method used for the initial testing differs from that of the 1 DOF design. The high level of non-linearity added by the variable radius and spring, in addition to the non-linear PAM force, makes impedance control very difficult. Instead, a two stage closed loop proportional controller is utilized. This controller measures the difference between actual and desired joint angle and provides a proportional valve opening. The two stages are used to vary the proportional value during swing and stance phase. A more advanced non-linear sliding mode controller will be developed before a new prosthesis is constructed. Figure 5.9 shows the positional tracking test results.

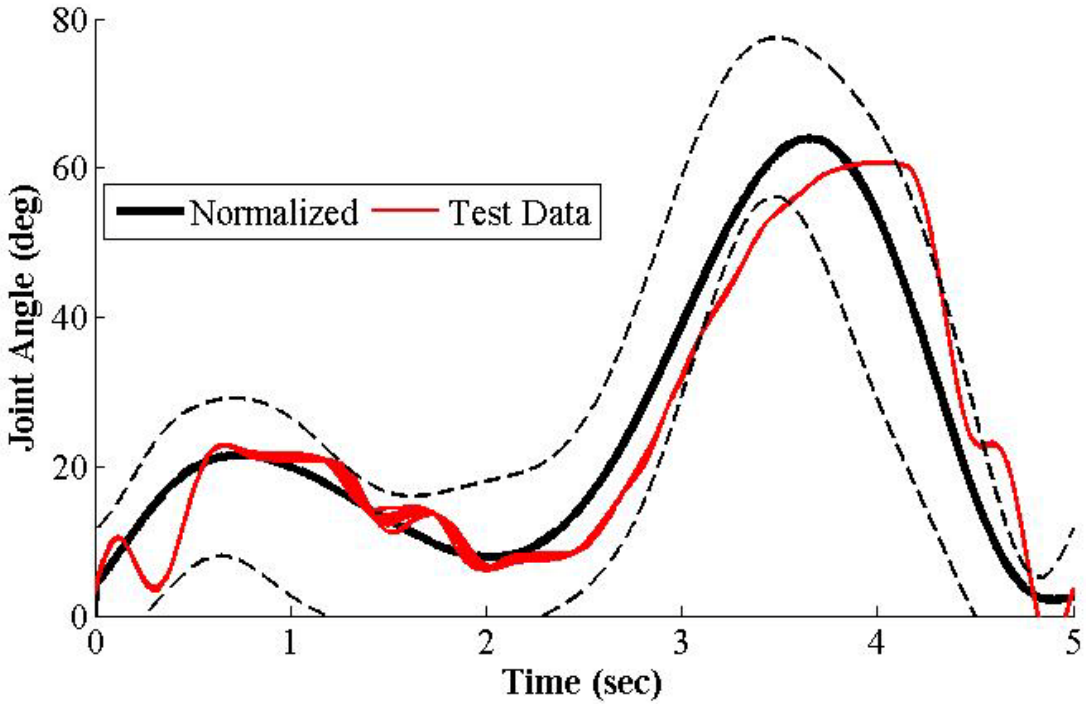

Figure 5.9 Elliptical actuator positional tracking

CHAPTER 6: TWO DOF PROSTHESIS CONCEPTUAL DESIGN

6.1 Introduction to Two DOF Prosthesis

While a powered knee significantly improves the capability of an AK amputee, it is still impossible to fully mimic normal gait and provide an energy cost comparable to a healthy individual. This is due in large part to the lack of a powered ankle, since the ankle provides most of the propulsive force during walking. It is therefore advantageous to incorporate a powered ankle joint into the design of a prosthesis.

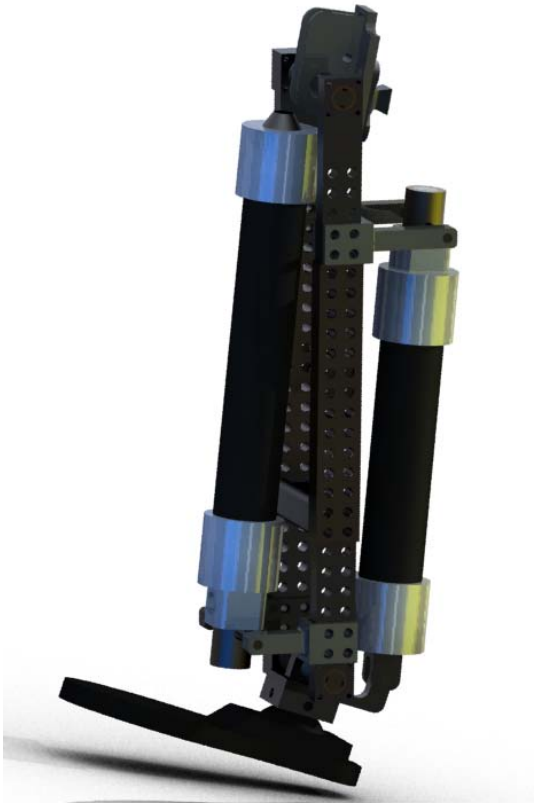

Figure 6.1 Model of 2 DOF conceptual design

6.2 Component Configuration

While using the initial antagonistic actuator on the 1 DOF design, space constraints made it very difficult to consider an actuated ankle. However, since the newly designed pulley actuator only requires one PAM with a spring return, more space is available for a second actuator. The knee actuator design is very similar to the actuator tester design, since the torque curves used in the design are identical. One change to the actuator is the spring implementation, where the linear spring is replaced by a torsional spring. This torsional spring takes up less space and allows for easier adjustability of the leg length. Also, the fixed point of the muscle is moved closer to the axis of the knee to minimize the overall length of the prosthesis.

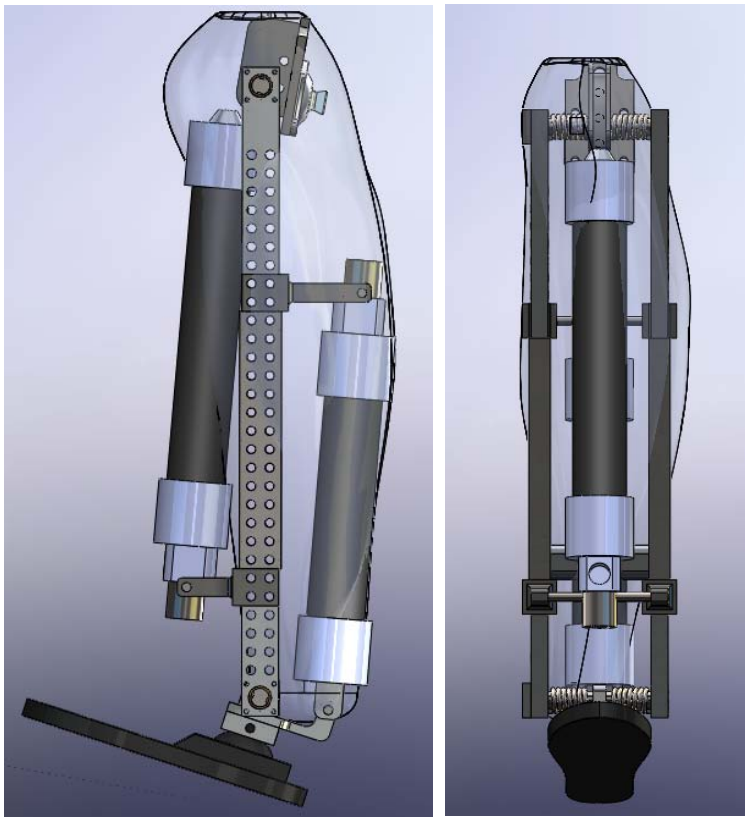

Figure 6.2 Front and side views of design with 50% male anthropometry

Since the ankle has a different range of motion and torque output requirement, it was necessary to repeat the optimization process to determine the most effective actuation method. As shown in the previous chapter, it was determined that the most effective actuator would be a slider-crank type, rather than an elliptical pulley. The smaller range of motion and larger peak torque value makes a slider crank more effective. This actuator is also simpler to manufacture and can be configured shorter than the pulley actuator, allowing space for instrumentation components.

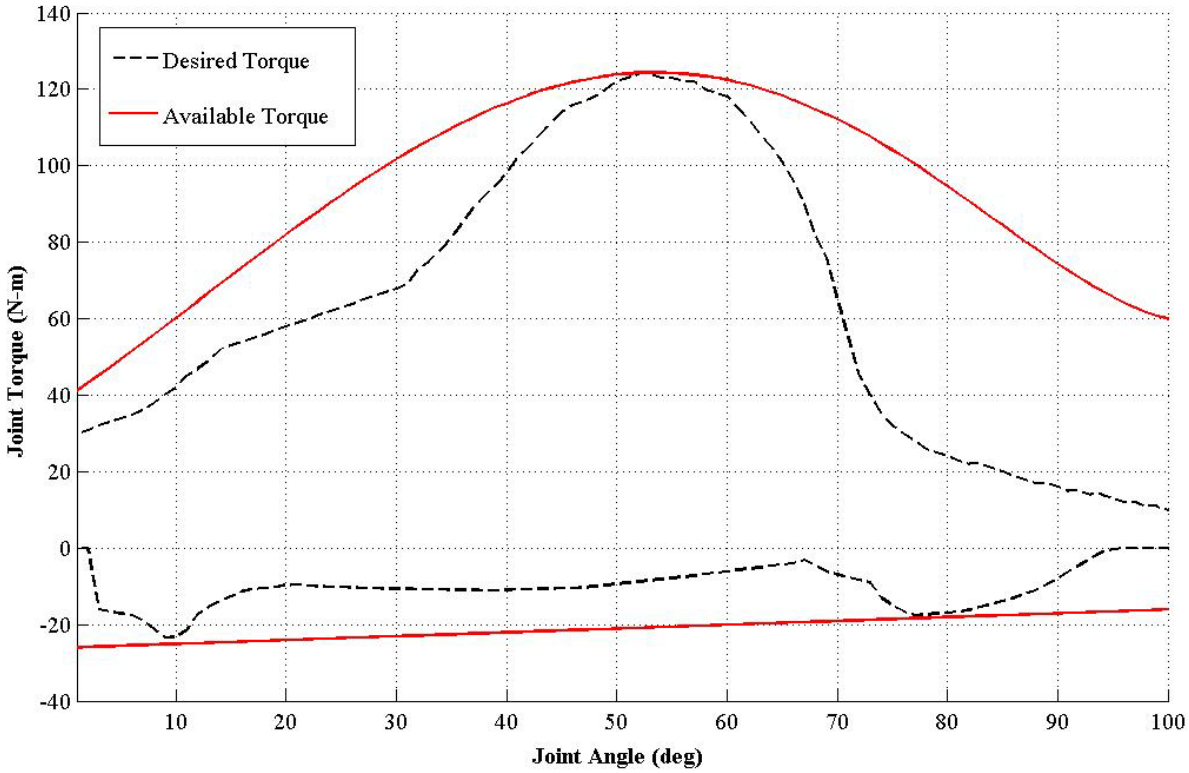

Figure 6.3 Theoretical knee torque for 2 DOF concept

The 2 DOF concept accounts for various users by including adjustable length. The relative position of the actuator and pulley combination must stay constant to ensure correct

output torque, so each one is mounted separately and attached to the center supports, allowing the leg to achieve lengths from 432-533 mm (17”-21”) to suit a 5% female and 95% male, respectively. The prosthesis maintains standard pyramid connections for prosthetic feet and sockets, allowing it to be easily adapted to a user.

The mass of the prosthesis is roughly 4.3 kg and the inertia ranges from .138 kg-m^2 in the shortest configuration to .207 kg-m^2 fully extended, all of which are well within the acceptable region.

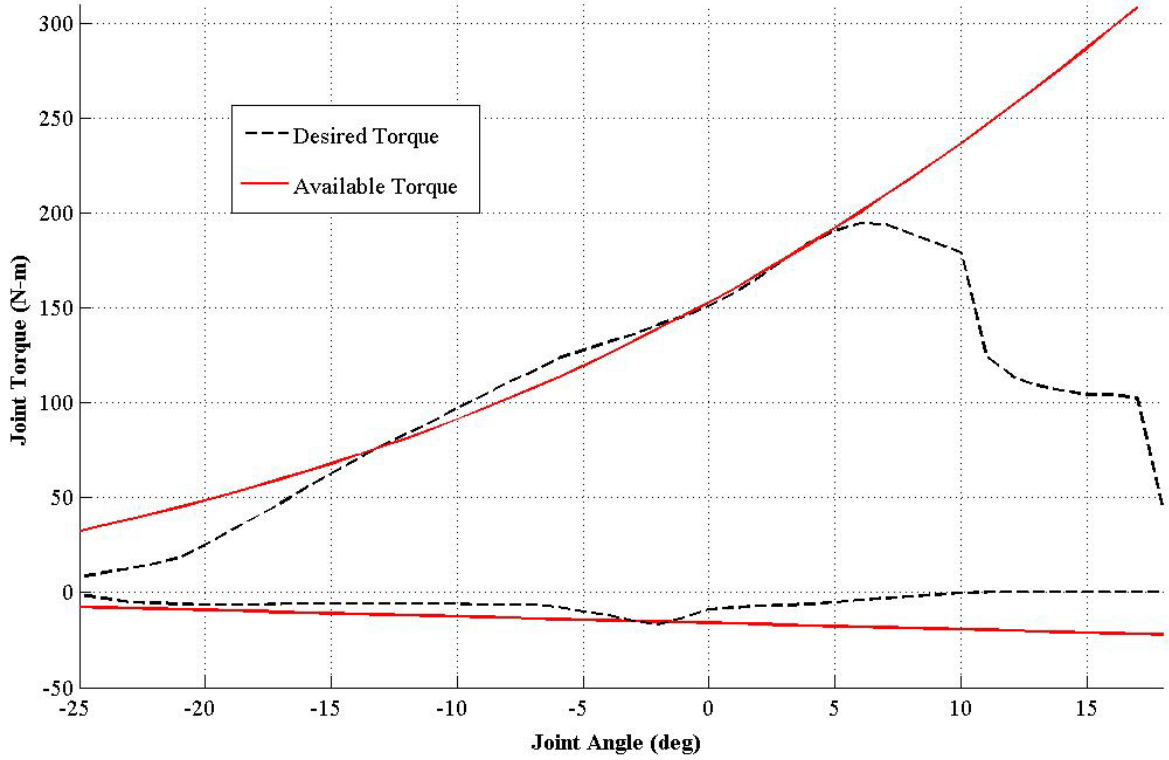

Figure 6.4 Theoretical ankle torque for 2 DOF concept

CHAPTER 7: CONCLUSION AND FUTURE WORK

7.1 Future Work

Upon completion of this research, several future goals have become evident. Firstly, the 2 DOF concept must be constructed and the design validated as with the 1 DOF design. A new non-linear control method will be developed to improve the tracking performance of the prosthesis to improve the functionality of the device

Another future endeavor would be to conduct a study using amputees to determine the energy cost of ambulation with their standard prosthesis as it compares to the new 2 DOF design, and see what factors may need improvement to allow for increased comfort and capability as well as further decreasing energy costs. Some important issues to test would be metabolic rate, oxygen intake, walking speed, and user comfort and balance.

Also, the prosthesis in its current state requires a large amount of instrumentation, electrical power, and a supply of compressed air. In order to facilitate the portability of the design, so-called hot gas actuation techniques are a promising alternative to traditional compressed air. This process uses liquid hydrogen peroxide, which, when combined with a catalyst, can be used to produce an on demand supply of gas hydrogen and oxygen. This provides an on demand supply of gas that is much more energy dense than a tank of compressed air

7.2 Conclusions

This thesis described the design and testing of a basic powered above knee prosthesis using pneumatic muscles, the design of a new actuator, and the conceptual design of a two degree of freedom prosthesis. It was shown that pneumatic artificial muscles can be used as an effective replacement to traditional actuators for powered prosthetics. Using a novel actuator configuration with an elliptical pulley, the effectiveness of PAM can be improved to more closely mimic the biological torque curve and speed requirements. While the PAM present some challenges with their implementation and control, they also provide advantages with power density and compliance. Ultimately, PAM are shown to be an effective option under circumstances for a prosthetic actuator, providing improved capability of a prosthetic device.

Appendix A – Part Drawings

1 DOF Leg Parts:

1. Bar
2. Crossmember
3. Female Belt Clamp
4. Foot Plate
5. Knee Side
6. Knee Support
7. Knee Top
8. Male Belt Clamp
9. Potentiometer Holder
10. Shaft

Pulley Tester Parts:

1. Crossmember
2. Potentiometer Holder
3. Potentiometer Support
4. Pulley Center
5. Pulley Guard
6. Pulley Top
7. Rope Adaptor Base
8. Rope Adaptor Top
9. Shaft
10. Support

2 DOF Leg Parts:

1. Adjustable Support Long
2. Adjustable Support Short
3. Adjustment Sheath
4. Ankle 3 Bar Linkage
5. Crossmember
6. Foot Adaptor
7. Knee Pulley Center
8. Knee Pulley Guard
9. Knee Pulley Top
10. Muscle Mount
11. Potentiometer Holder
12. Shaft
13. Shim
14. Three Bar Adaptor

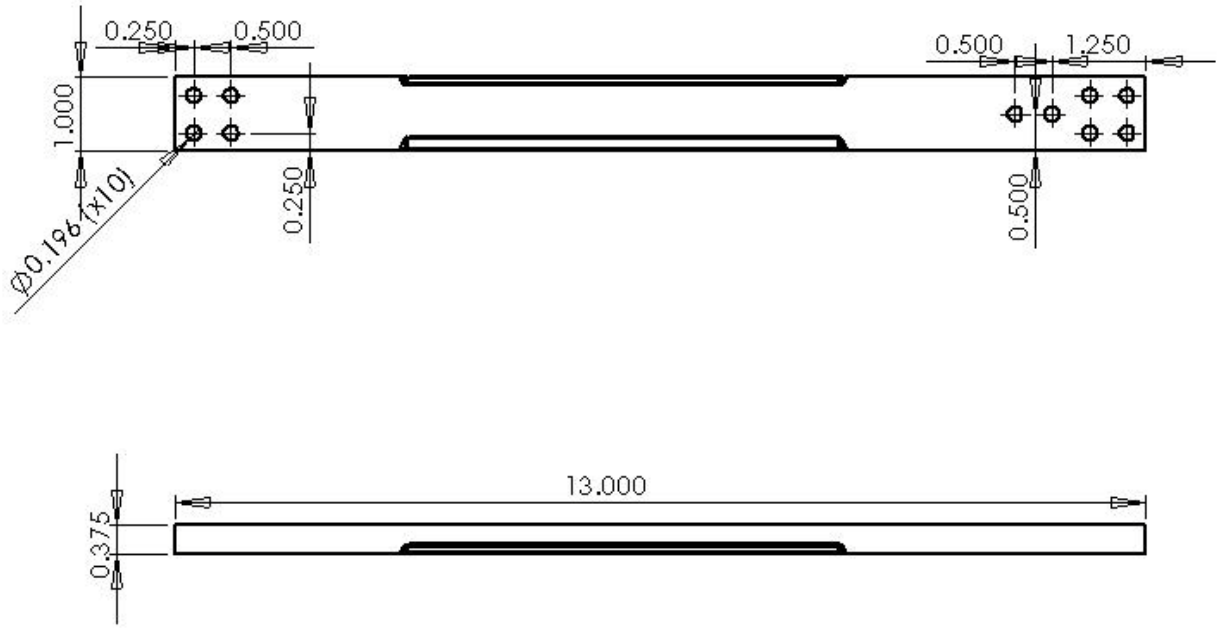

Garrett Waycaster
Project: Pneumatic Prosthesis
Xiangrong Shen
Part: Support Bar
Material: 6061 Aluminum
Quantity: 2

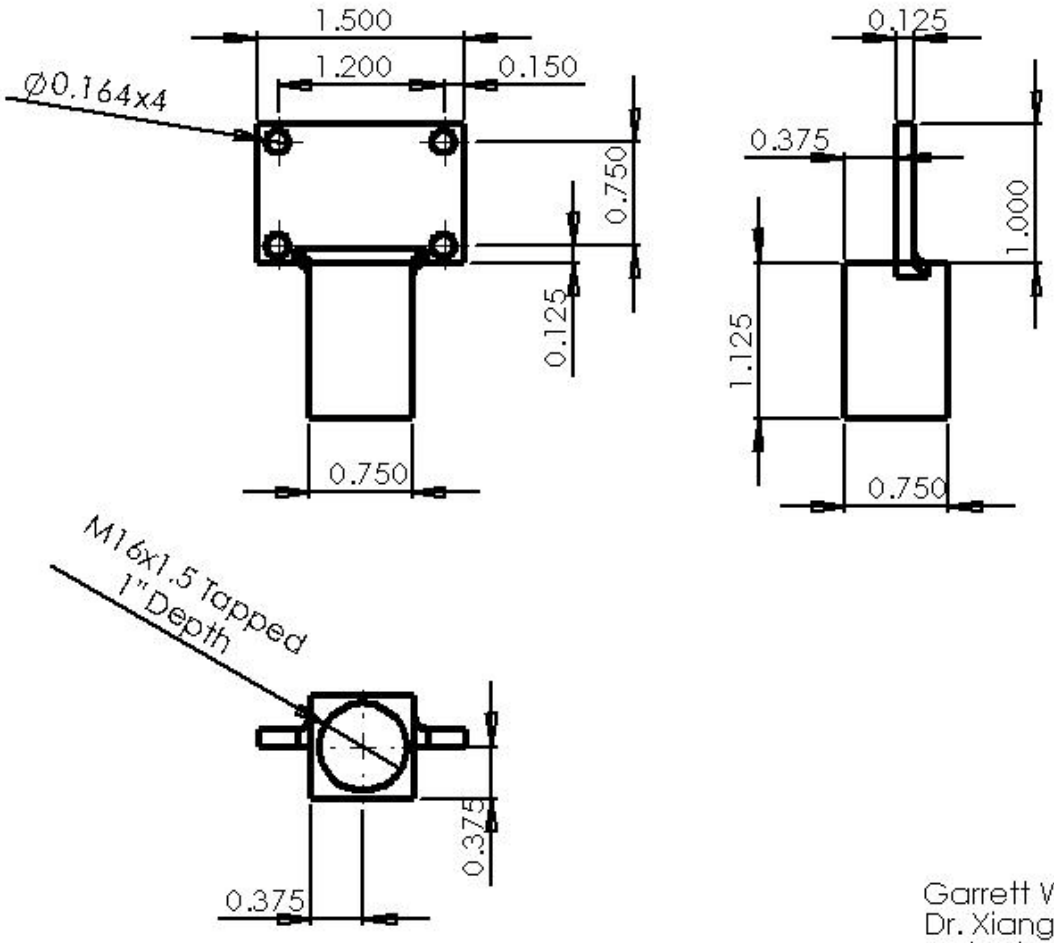

Garrett Waycaster
Dr. Xiangrong Shen
Project: Pneumatic Leg Prosthesis
Part: Flat Belt Clamp
Material: 6061 T6 Aluminum
Quantity: 2

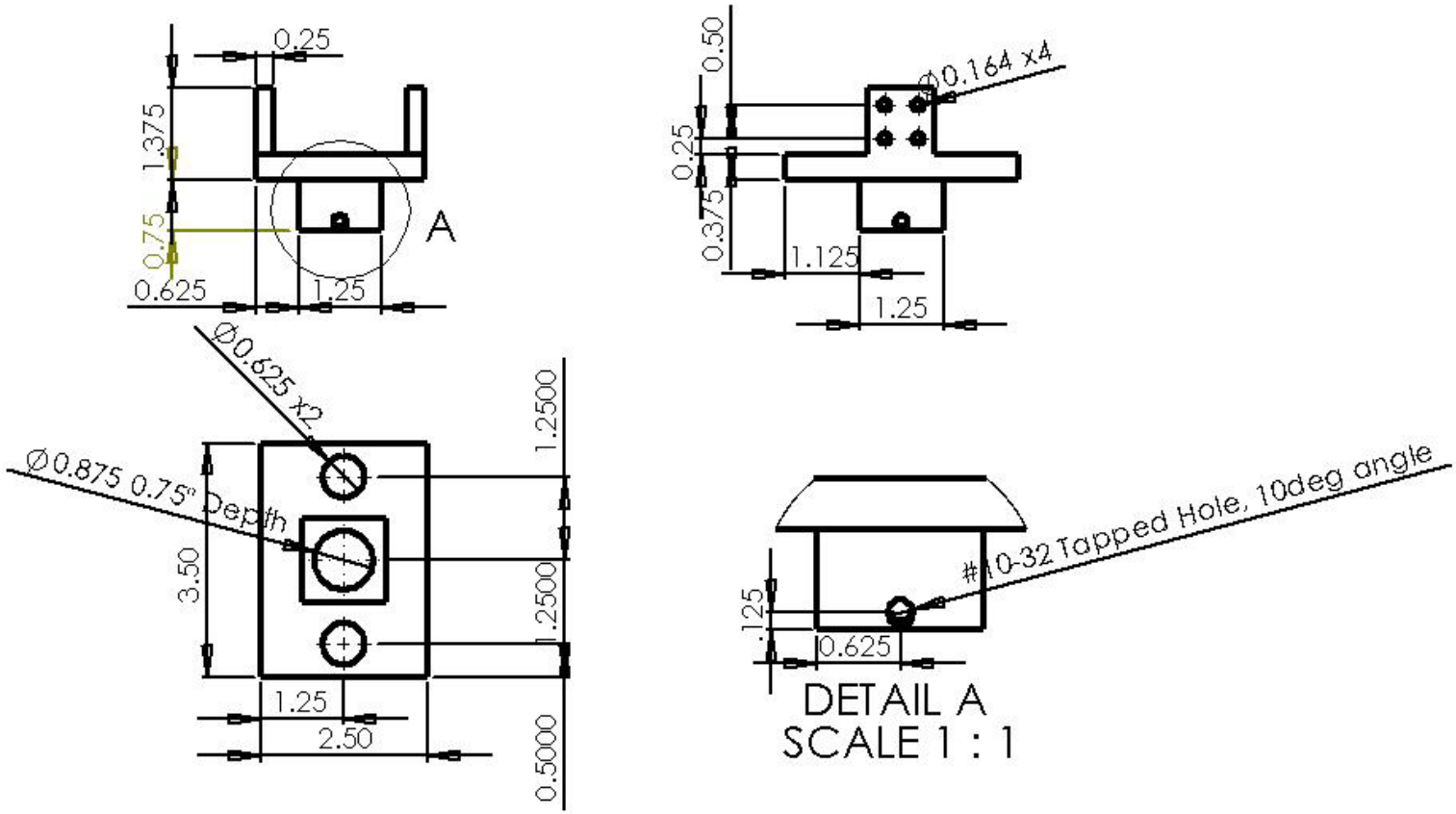

Garrett Waycaster
Dr. Xiangrong Shen
Project: Pneumatic Leg Prosthesis
Part: Foot Plate
Material: 6061 T6 Aluminum
Quantity: 1

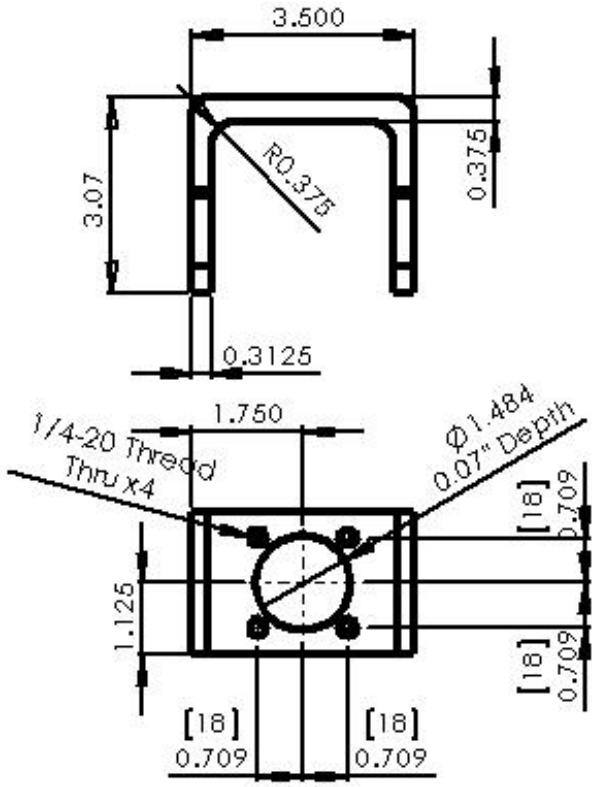

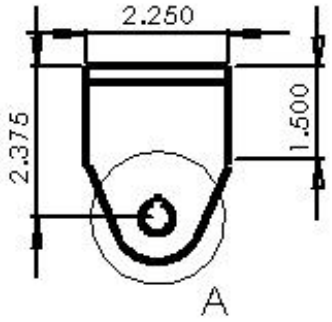

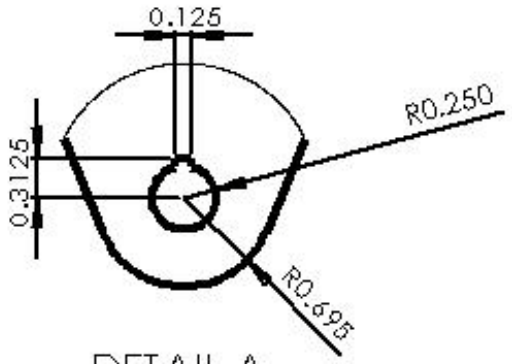

DETAIL A
SCALE 1 : 1

Garrett Waycaster
Dr. Xiangrong Shen
Project: Pneumatic Leg Prosthesis
Part: Knee
Material: 6061 T6 Aluminum
Quantity: 1

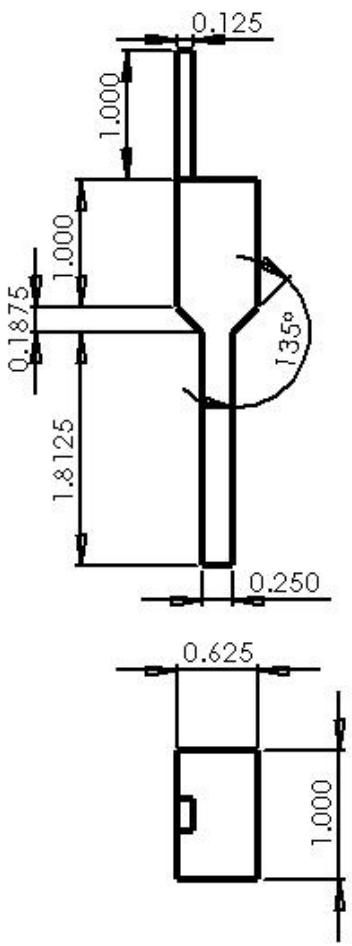

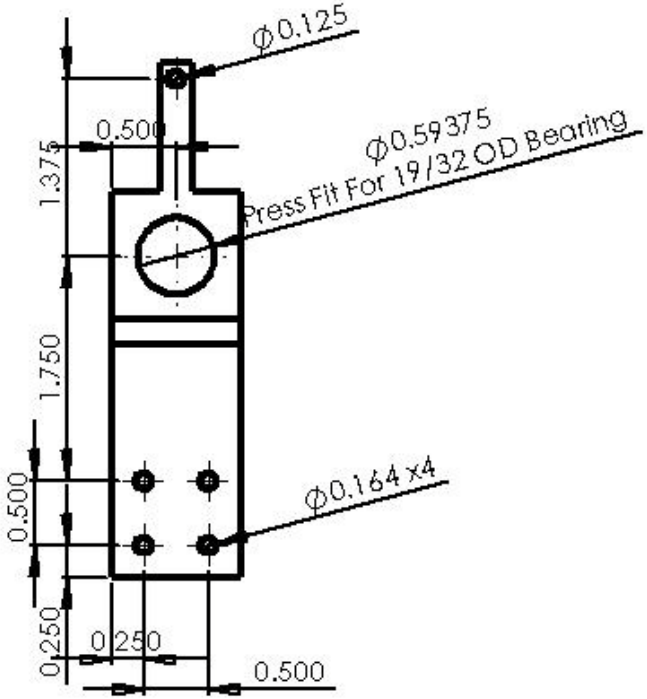

Garrett Waycaster
Dr. Xiangrong Shen
Project: Pneumatic Leg Prosthesis
Part: Knee Support
Material: 6061 T6 Aluminum
Quantity: 2

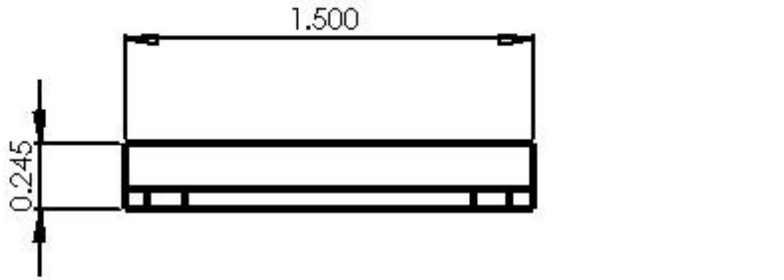

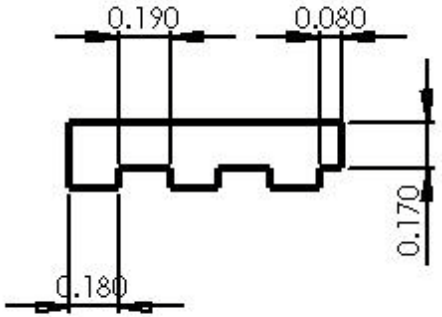

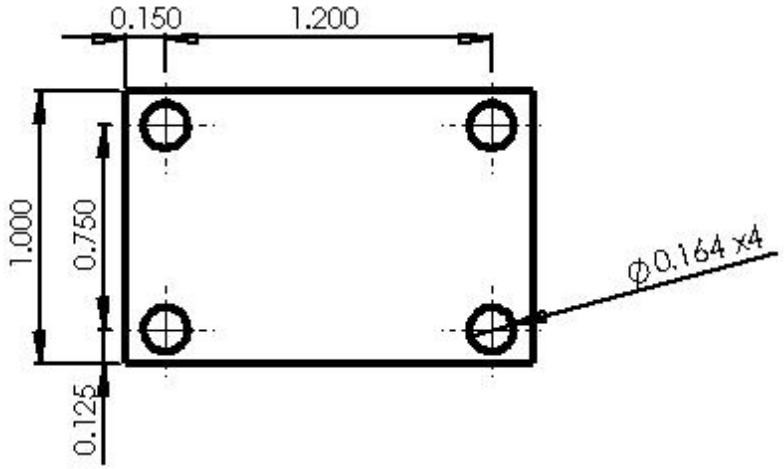

Garrett Waycaster
Dr. Xiangrong Shen
Project: Pneumatic Leg Prosthesis
Part: Male Belt Clamp
Material: 6061 T6 Aluminum
Quantity:

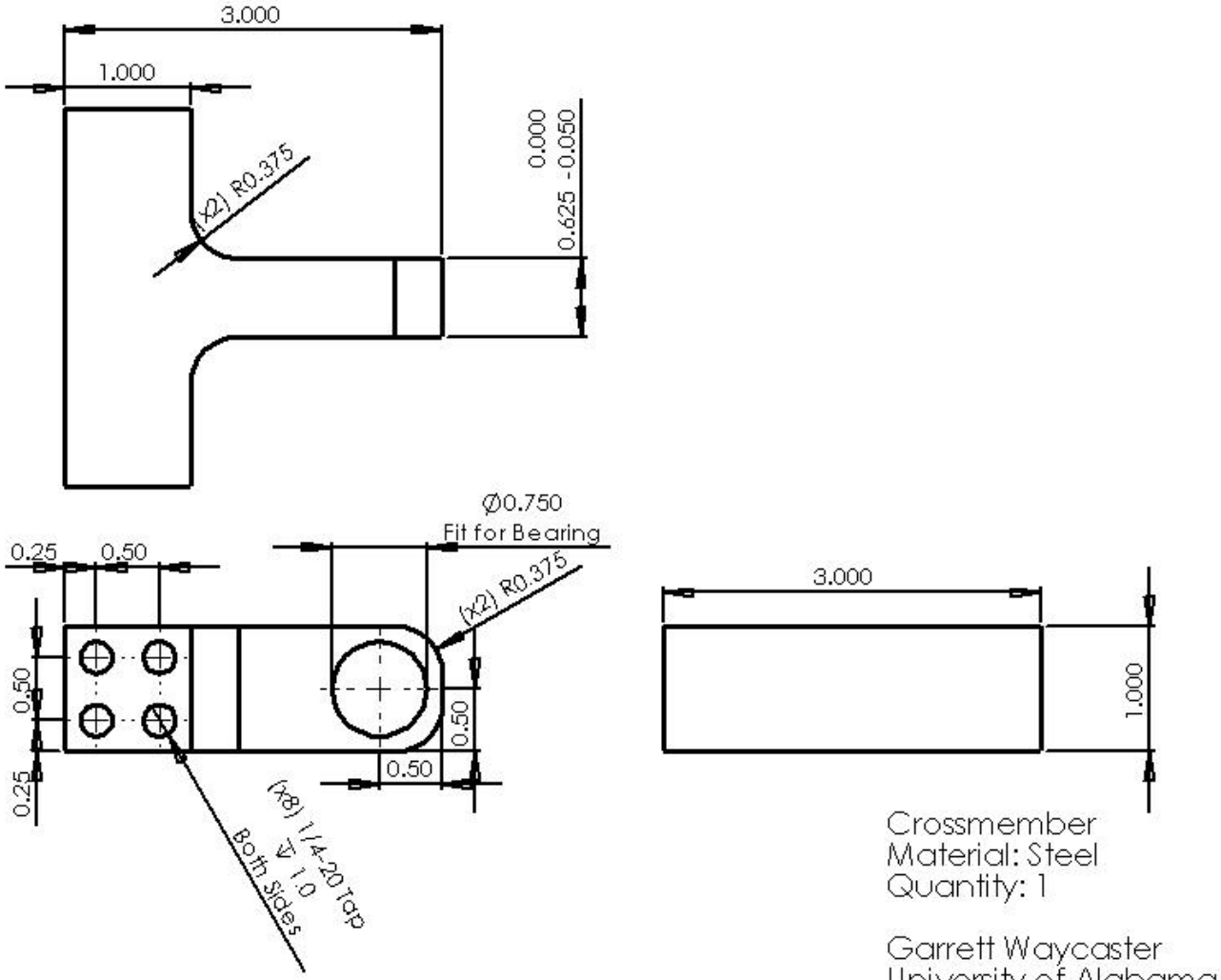

Crossmember
Material: Steel
Quantity: 1

Garrett Waycaster
University of Alabama

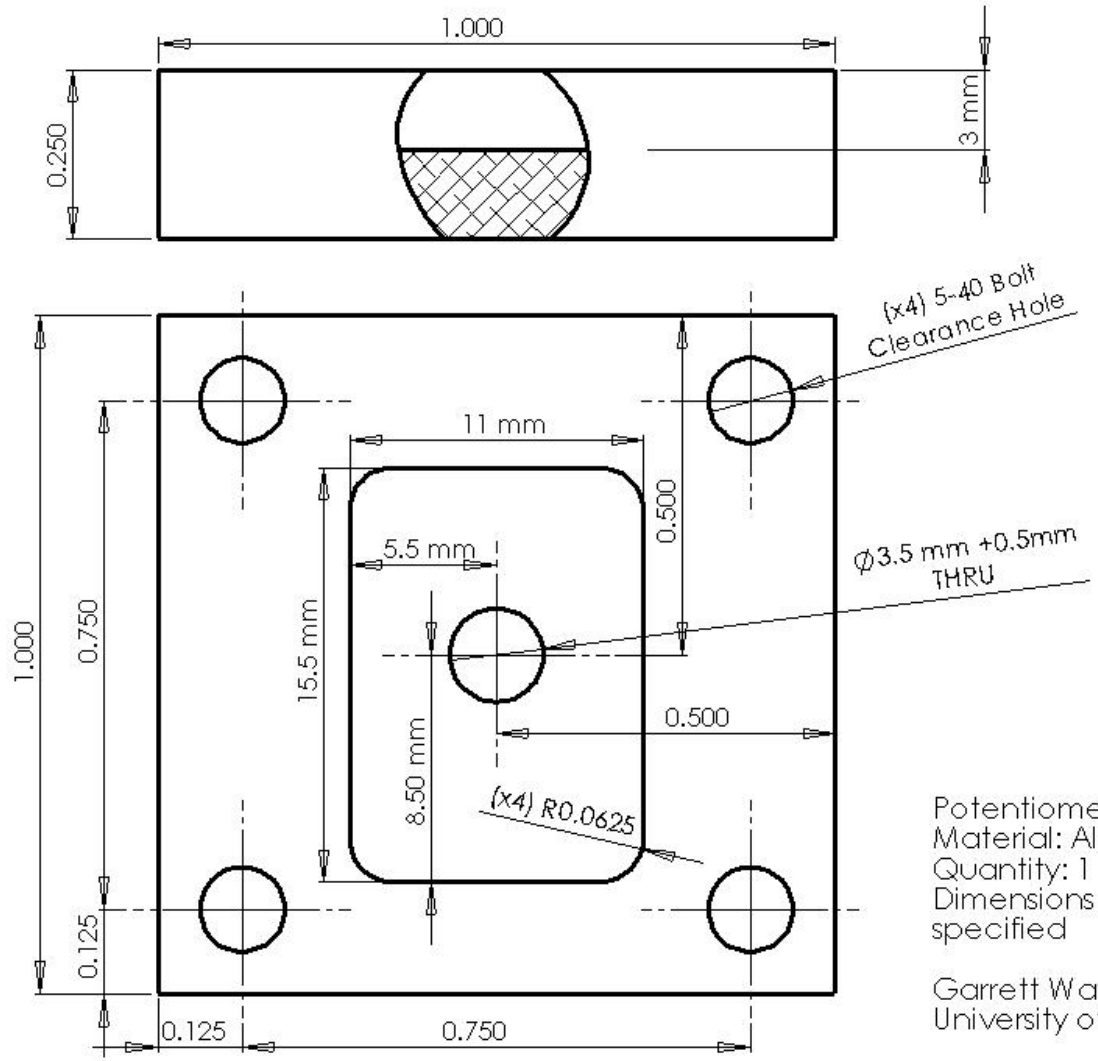

Potentiometer Holder
Material: Aluminum
Quantity: 1
Dimensions in inches unless specified

Garrett Waycaster
University of Alabama

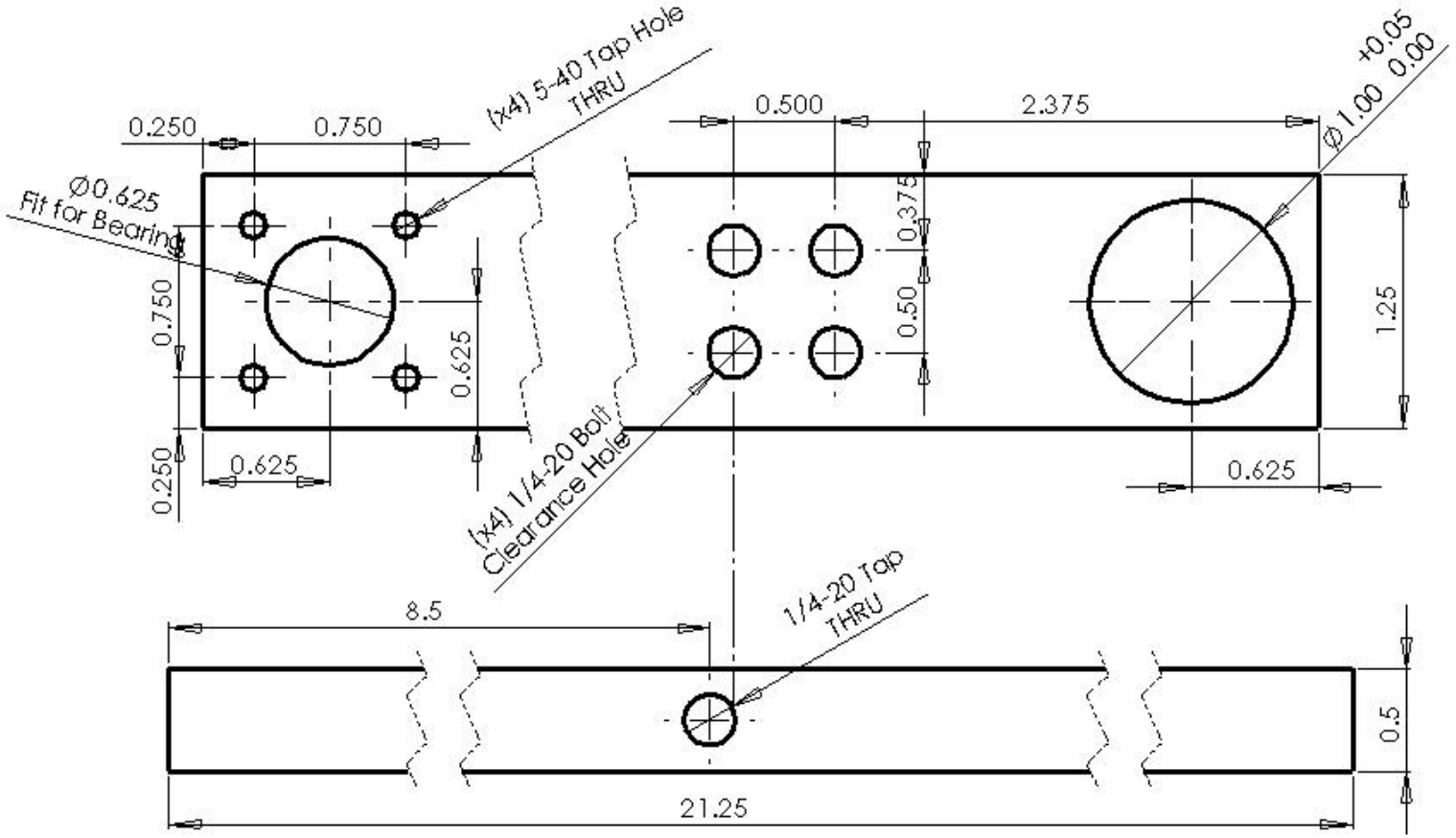

Potentiometer Support
Material: Aluminum
Quantity: 1

Garrett Waycaster
University of Alabama

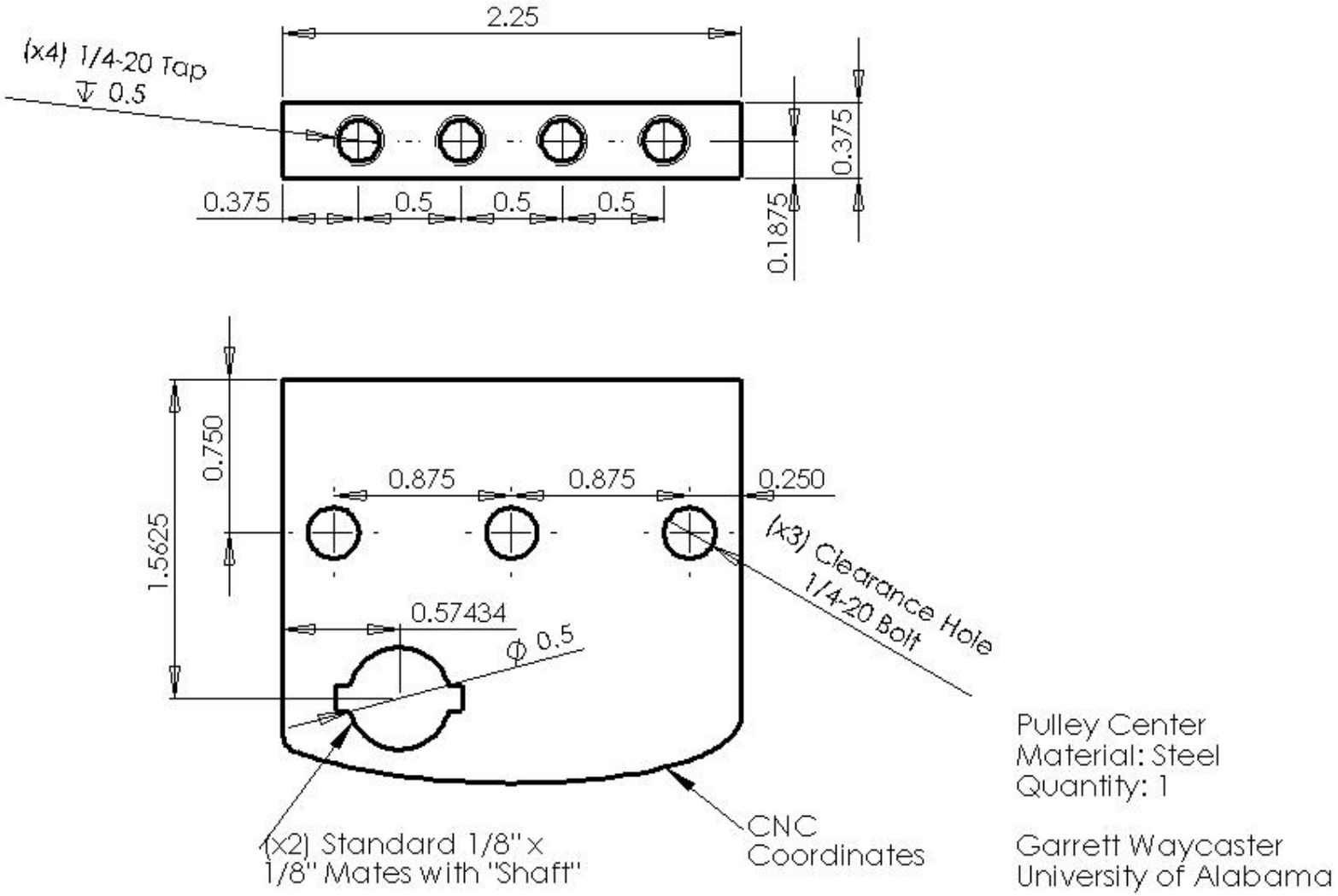

Pulley Center
Material: Steel
Quantity: 1

Garrett Waycaster
University of Alabama

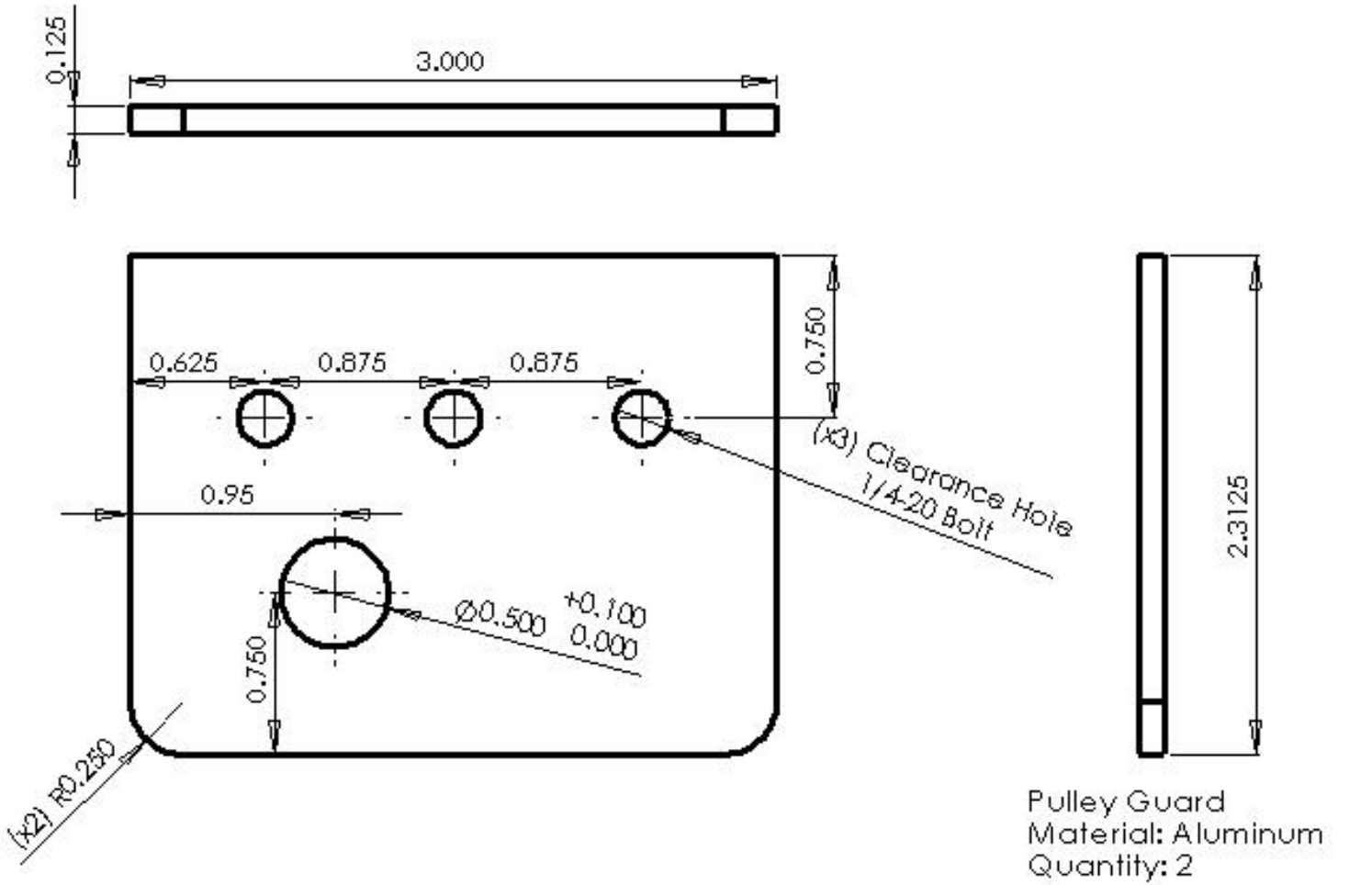

Pulley Guard
Material: Aluminum
Quantity: 2

Garrett Waycaster
University of Alabama

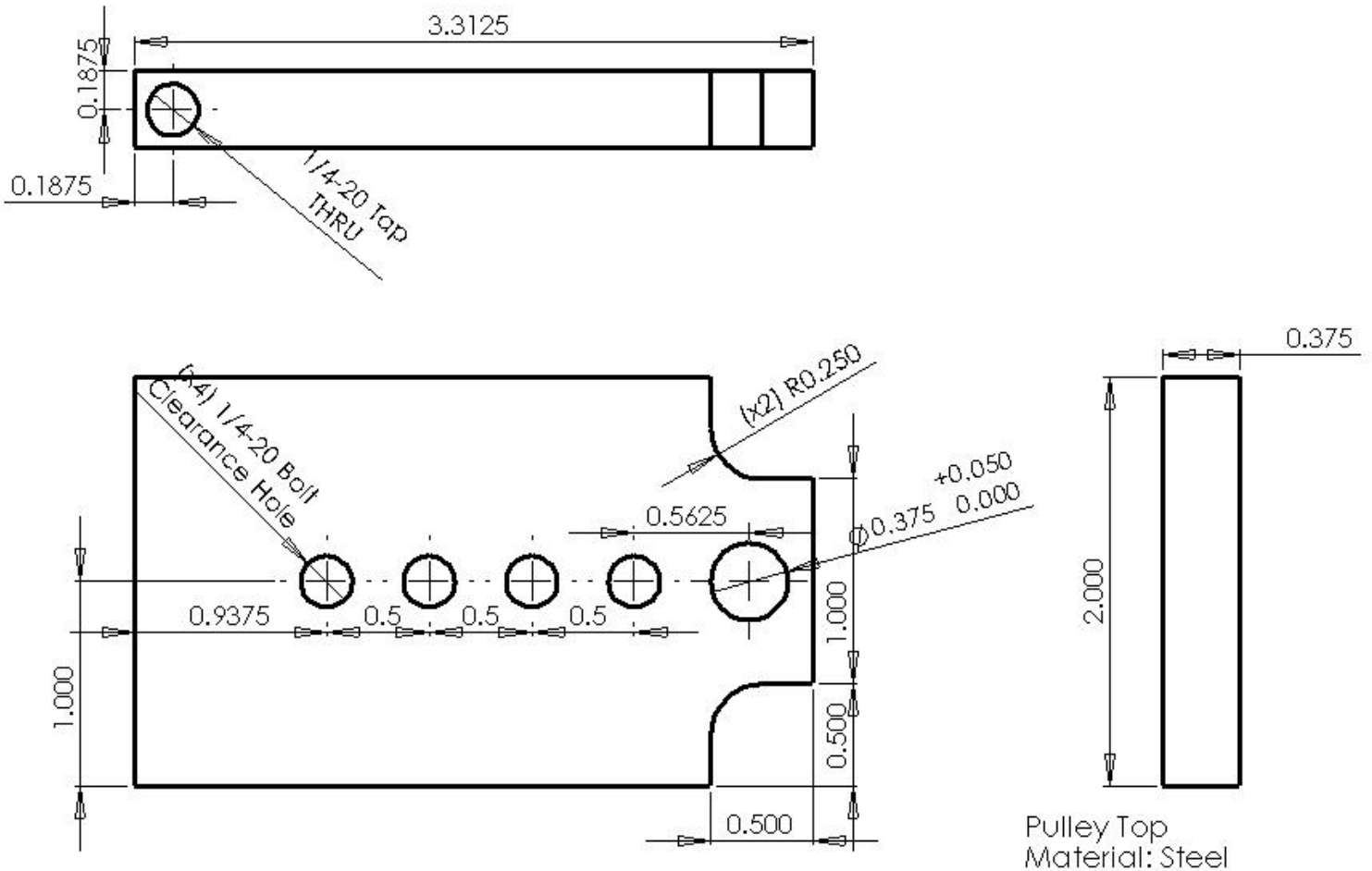

Pulley Top
Material: Steel
Quantity: 1

Garrett Waycaster
University of Alabama

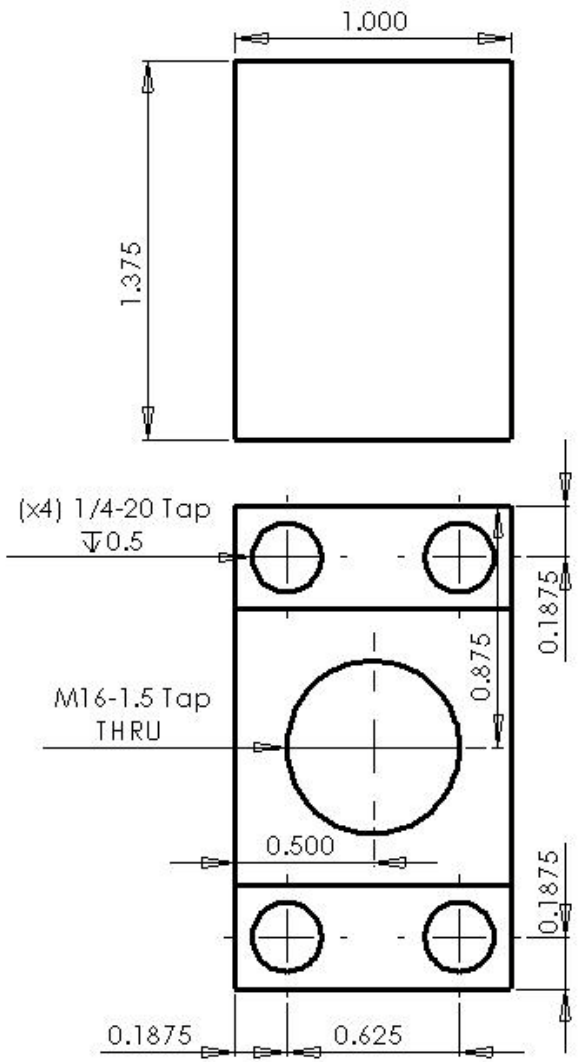

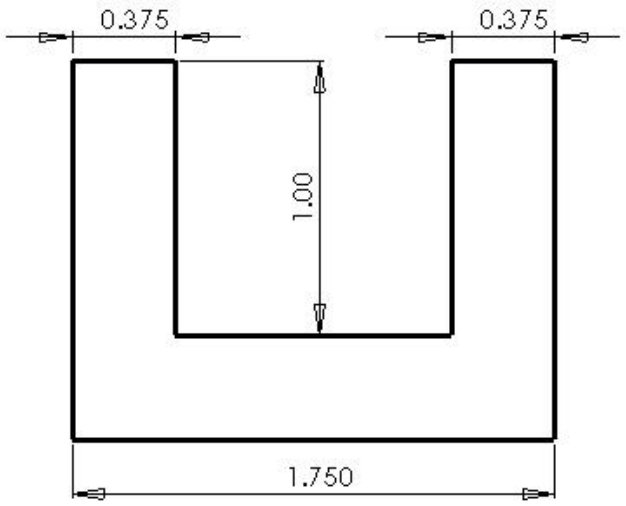

Rope Adaptor Base
Material: Steel
Quantity: 1

Garrett Waycaster
University of Alabama

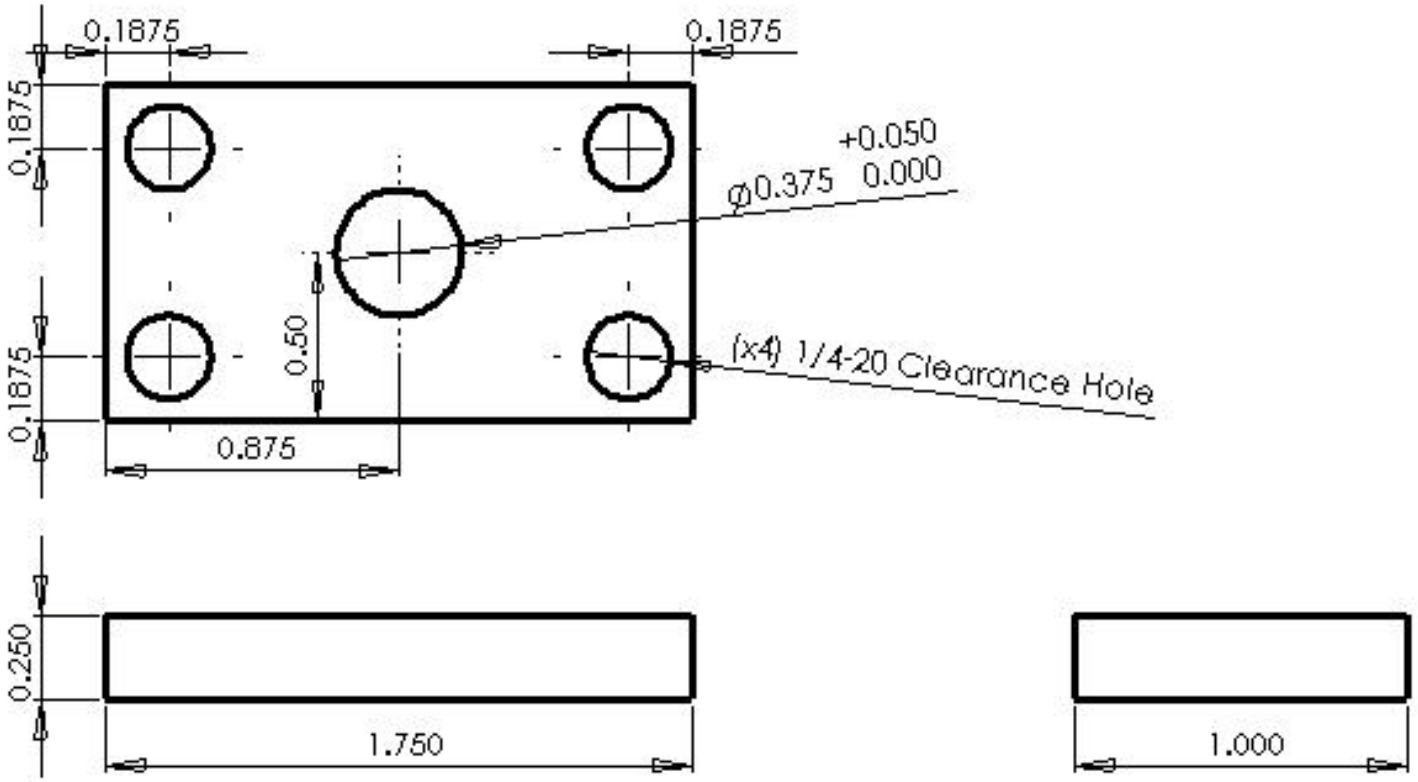

Rope Adaptor Top
Material: Steel
Quantity: 1

Garrett Waycaster
University of Alabama

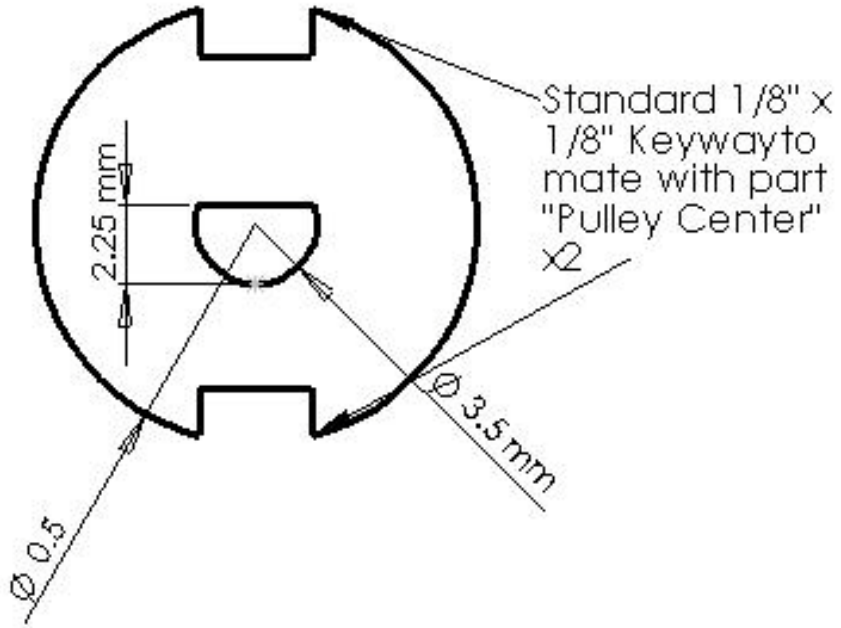

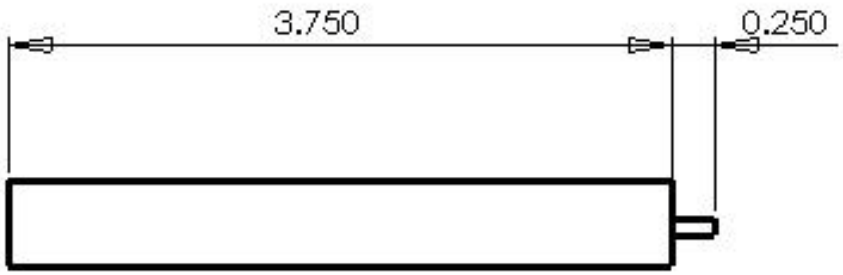

Shaft
Material: Steel
Quantity: 1
All Dimensions in Inches Unless Specified

Garrett Waycaster
University of Alabama

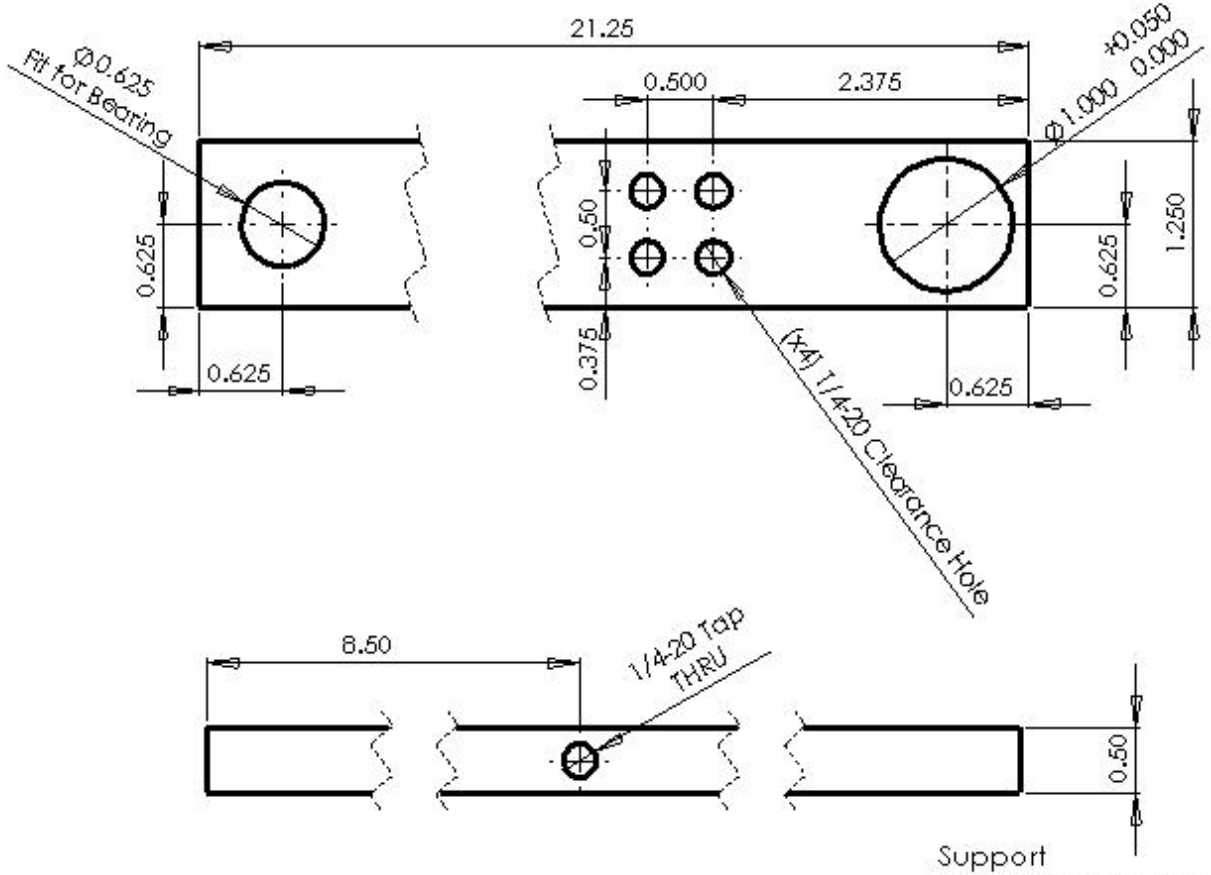

Support
Material: Aluminum
Quantity: 1

Garrett Waycaster
University of Alabama

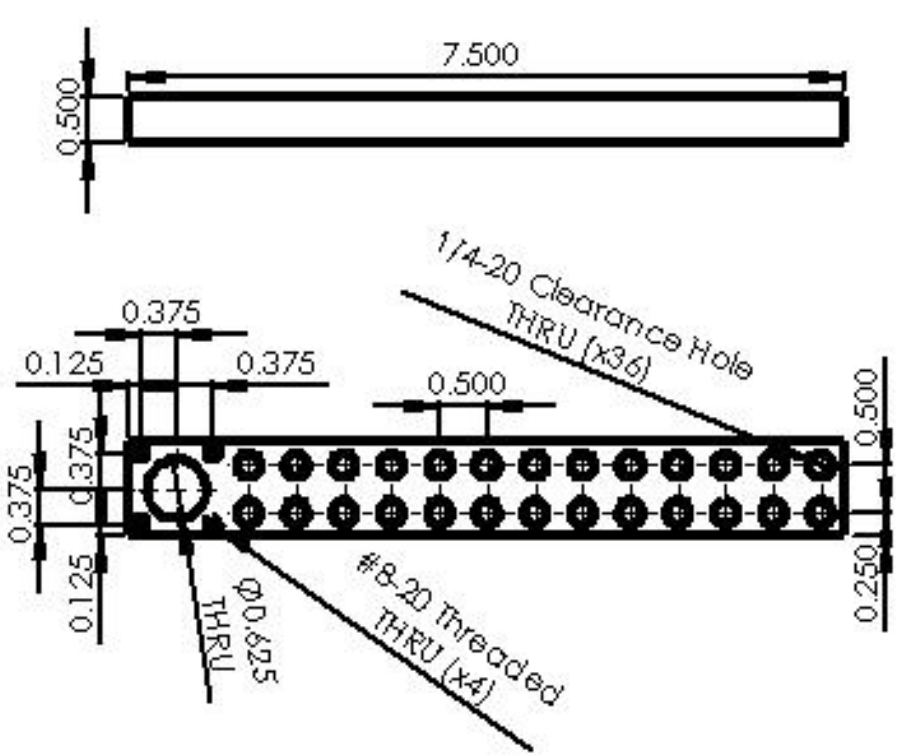

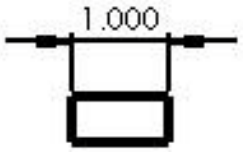

Adjustable Support Long
Material: Aluminum
Quantity: 2

University of Alabama
Garrett Waycaster

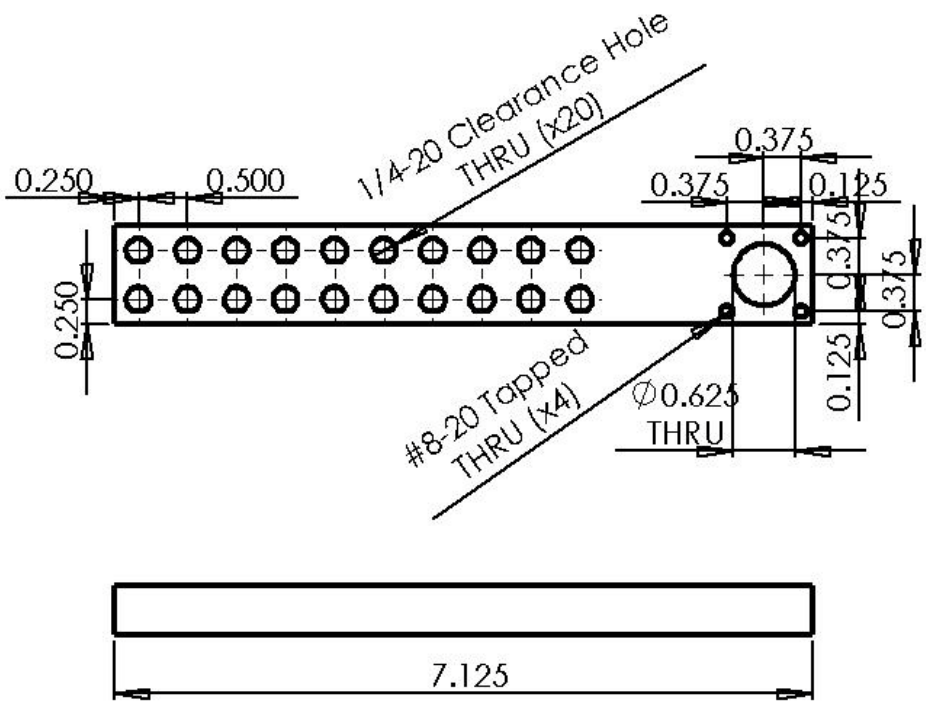

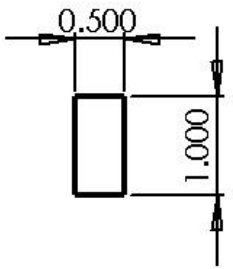

Adjustable Support Short
Material: Aluminum
Quantity: 2

University of Alabama
Garrett Waycaster

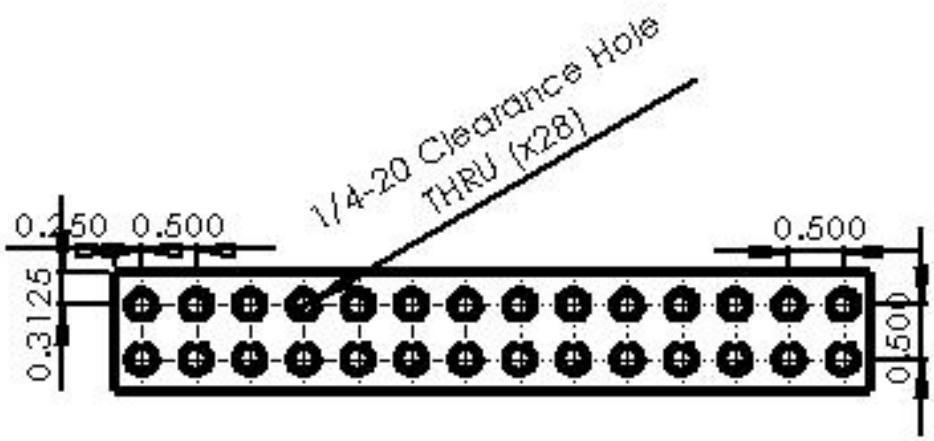

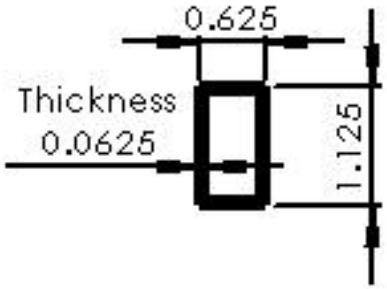

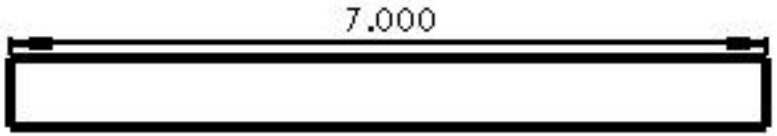

Adjustment Sheath
Material: Steel
Quantity: 2

University of Alabama
Garrett Waycaster

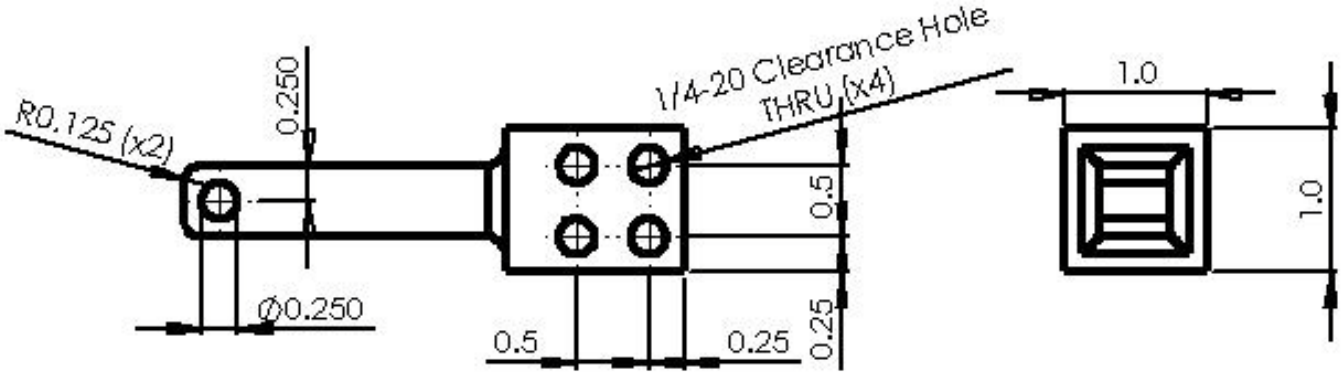

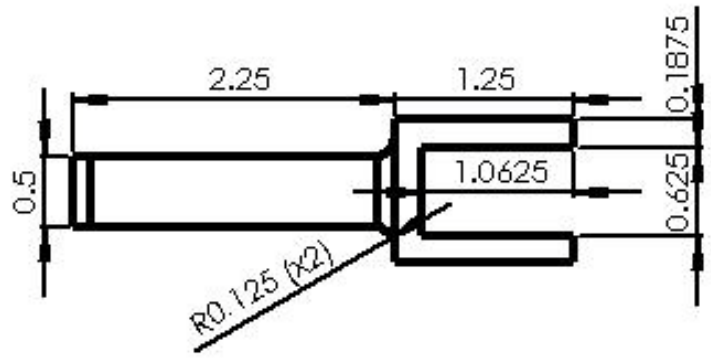

Ankle Muscle Mount
Material: Steel
Quantity: 2

University of Alabama
Garrett Waycaster

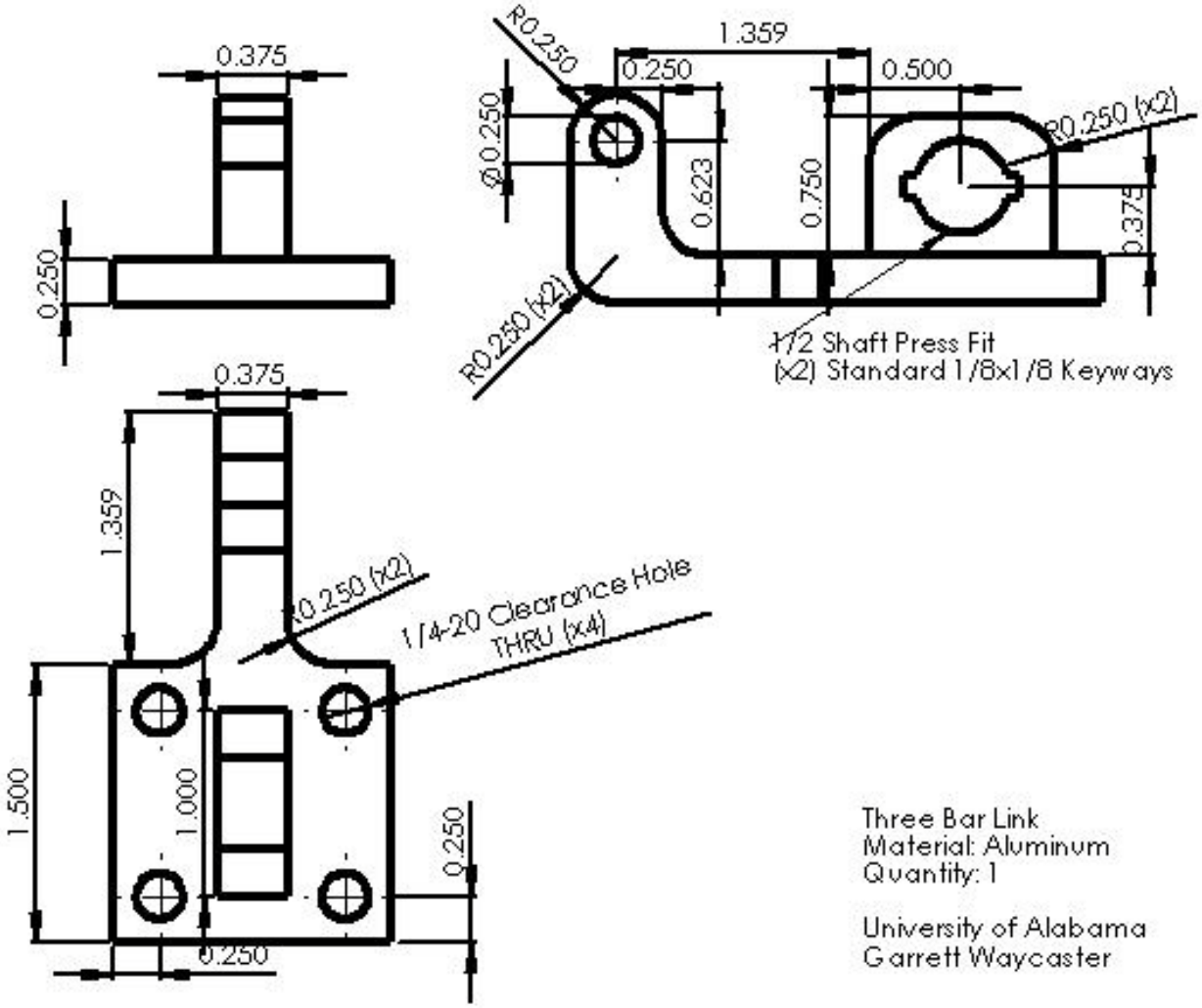
0.375
0.250
R0.250
1.359
0.250
0.500
Ø0.250
0.623
0.750
R0.250 (x2)
0.375
R0.250 (x2)
1/2 Shaft Press Fit
(x2) Standard 1/8x1/8 Keyways
0.375
1.359
R0.250 (x2)
1/4-20 Clearance Hole
THRU (x4)
1.500
1.000
0.250
0.250
Three Bar Link
Material: Aluminum
Quantity: 1
University of Alabama
Garrett Waycaster

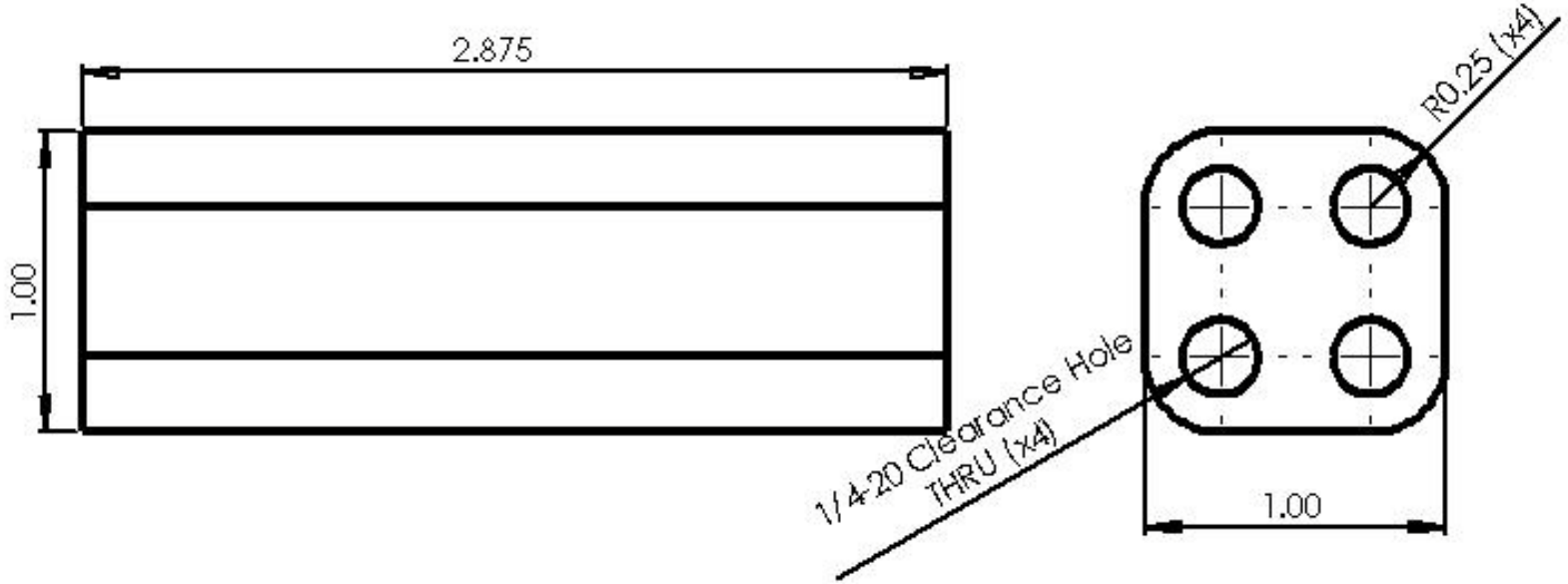

Crossmember
Material: Aluminum
Quantity: 1

University of Alabama
Garrett Waycaster

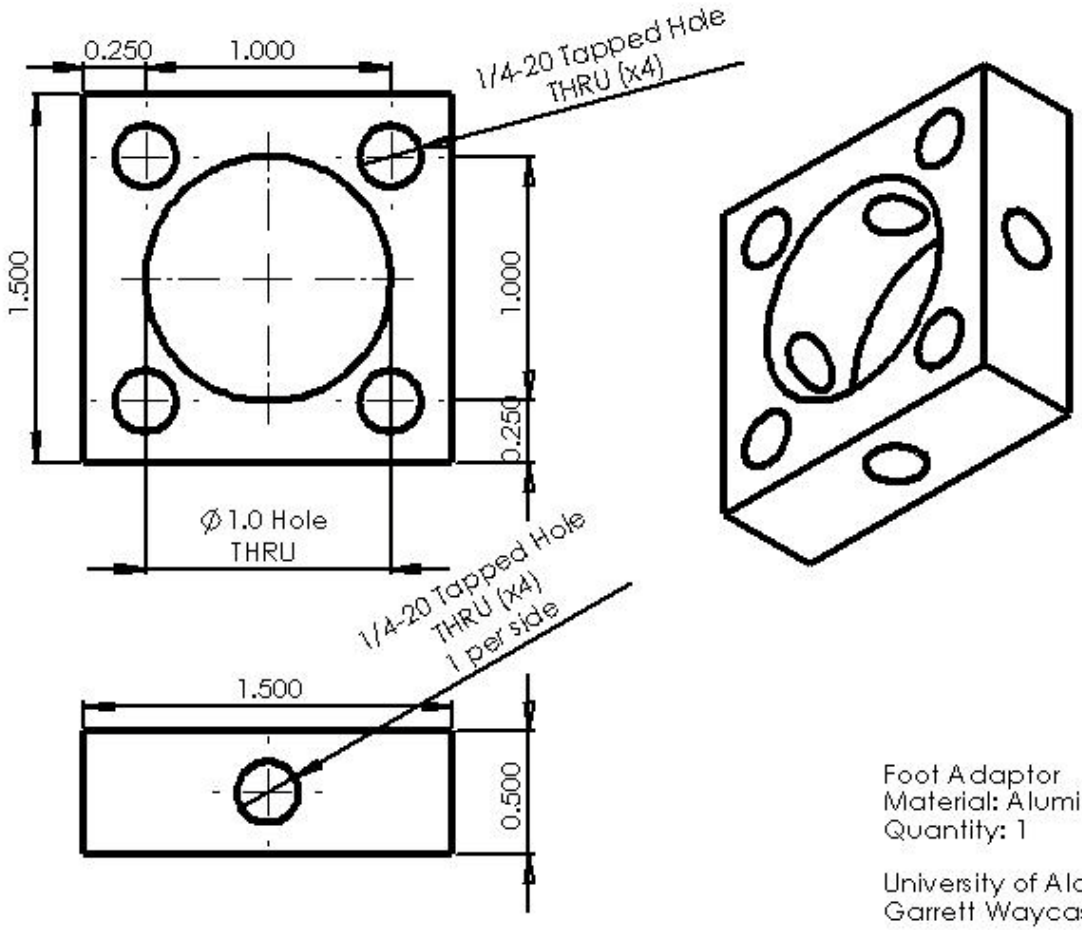

Foot Adaptor
Material: Aluminum
Quantity: 1

University of Alabama
Garrett Waycaster

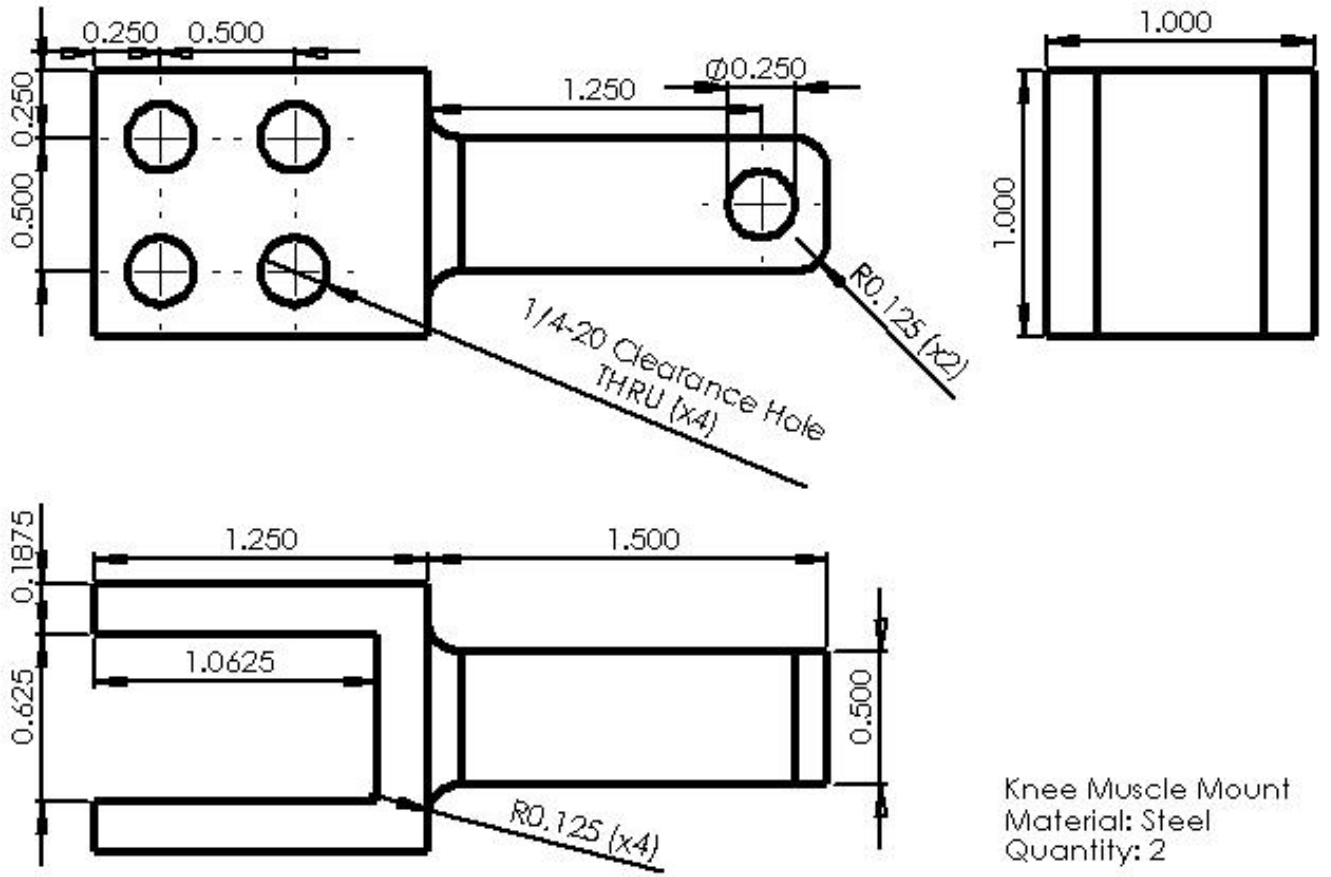

Knee Muscle Mount
Material: Steel
Quantity: 2

University of Alabama
Garrett Waycaster

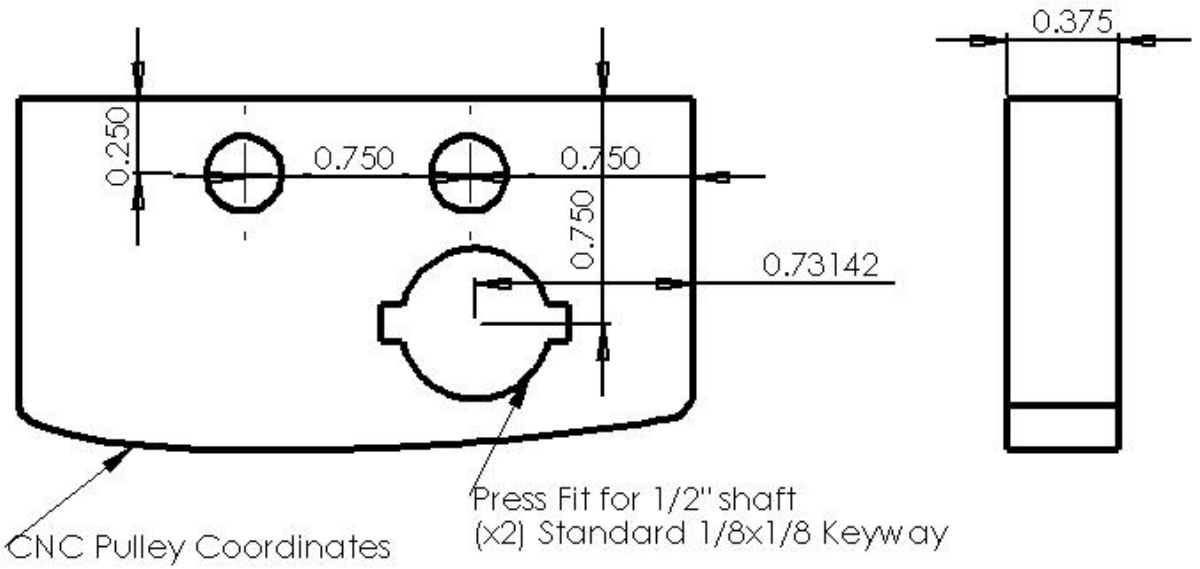

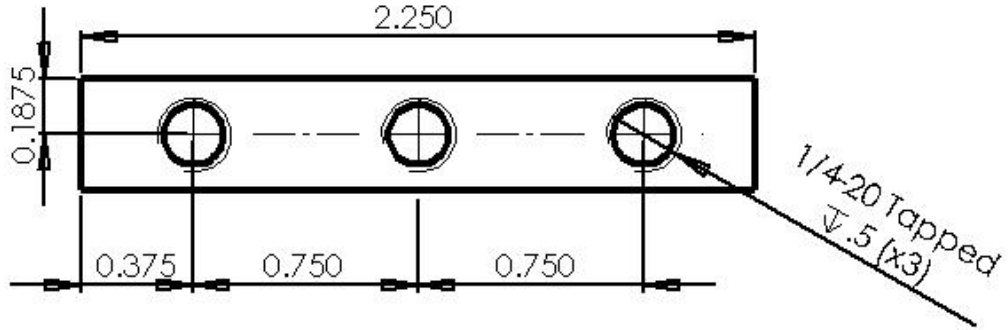

Knee Pulley
Material: Steel
Quantity: 1

University of Alabama
Garrett Waycaster

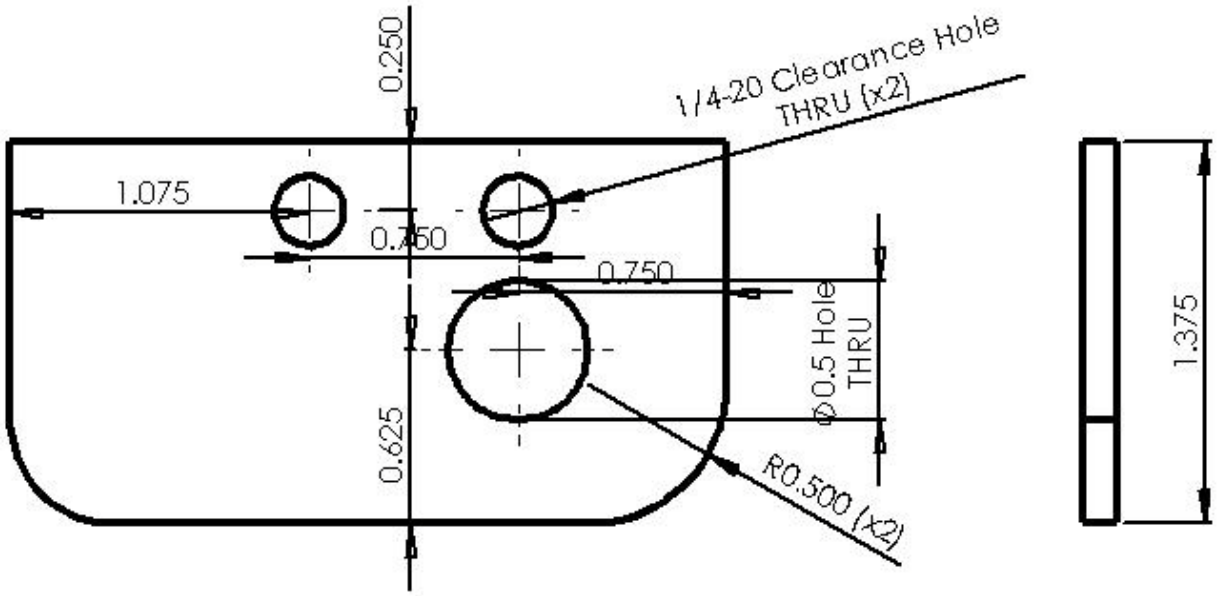

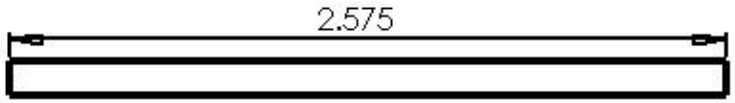

Pulley Guard
Material: Aluminum
Quantity: 2

University of Alabama
Garrett Waycaster

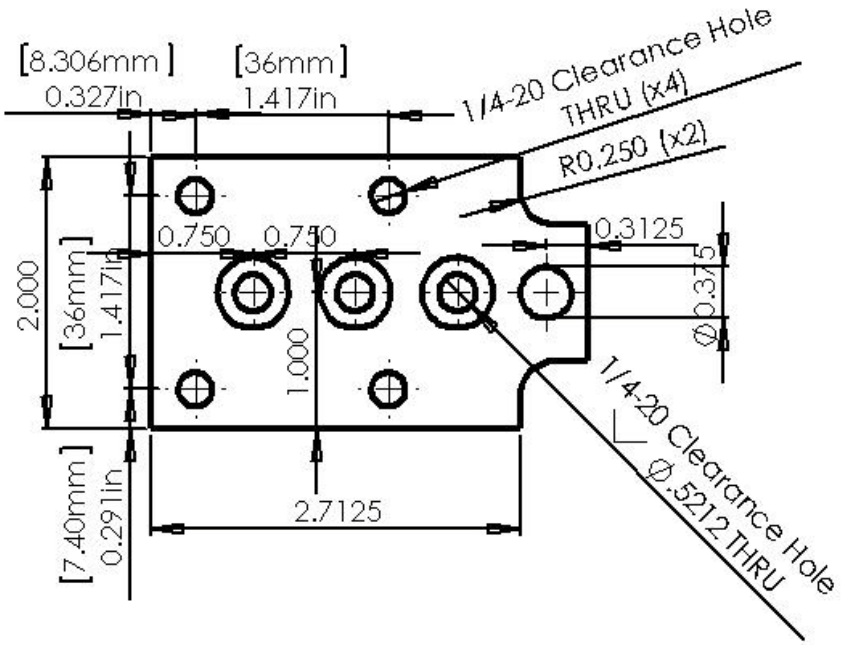

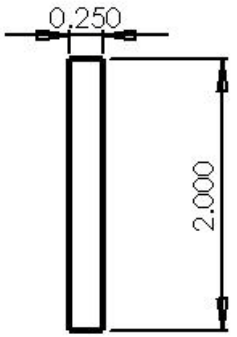

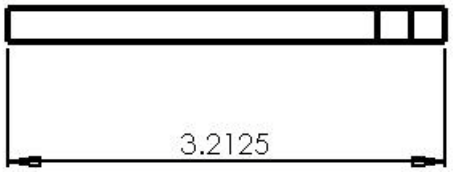

Knee Top
Material: Steel
Quantity: 1

University of Alabama
Garrett Waycaster

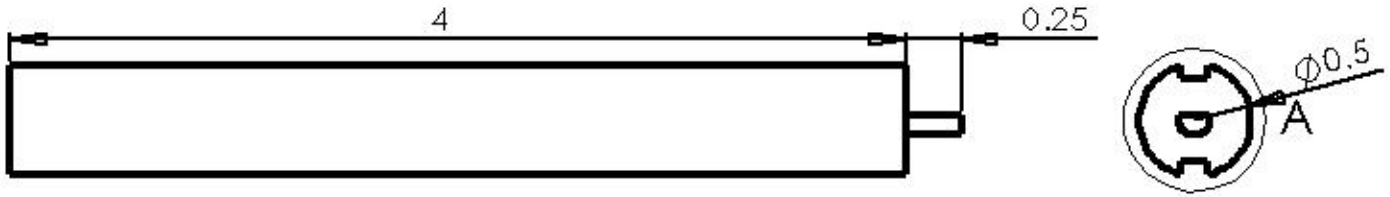

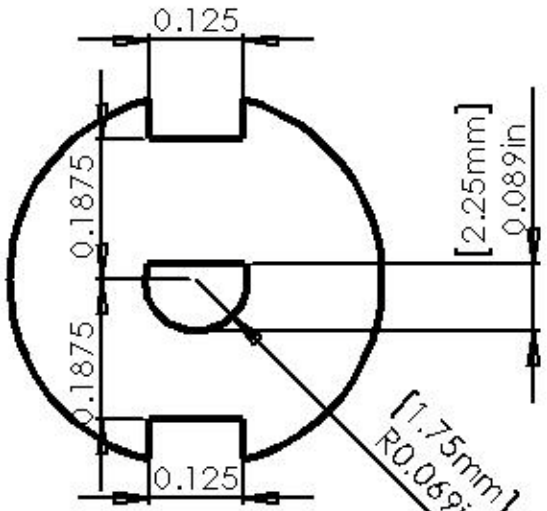

DETAIL A
SCALE 5 : 1

Shaft
Material: Steel
Quantity: 2

University of Alabama
Garrett Waycaster

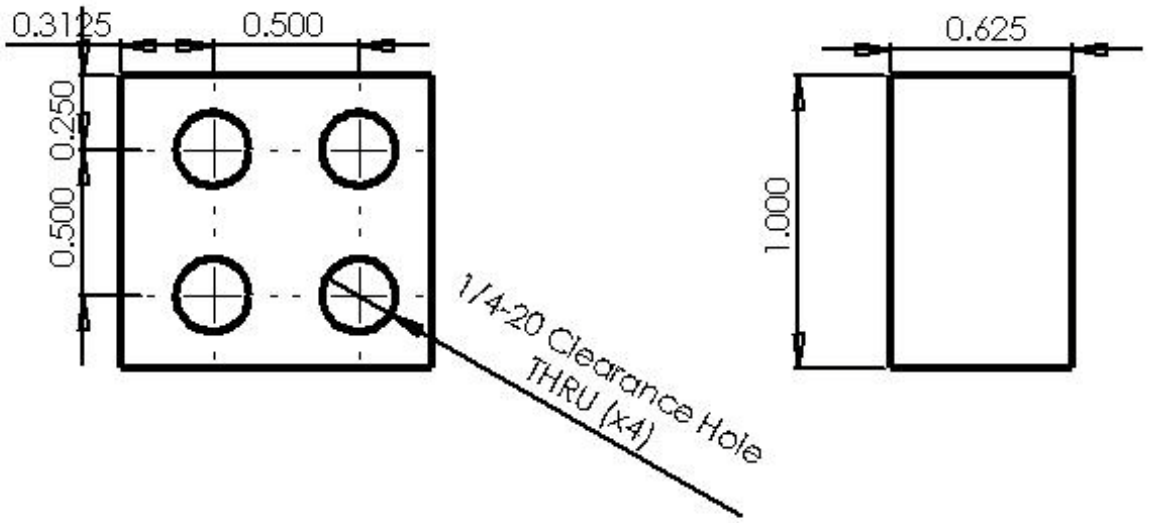

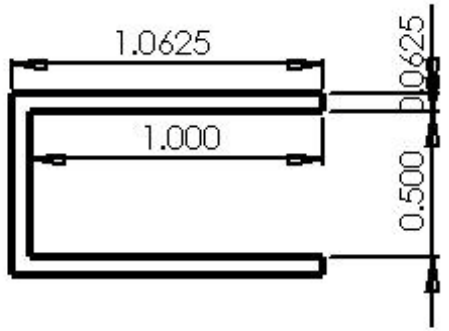

Mount Shim
Material: Aluminum
Quantity: 4

University of Alabama
Garrett Waycaster

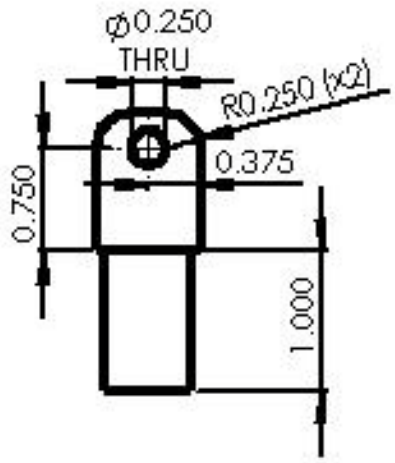

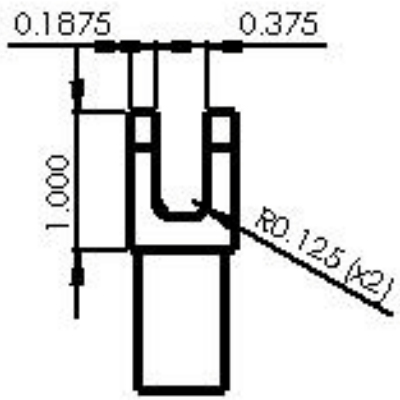

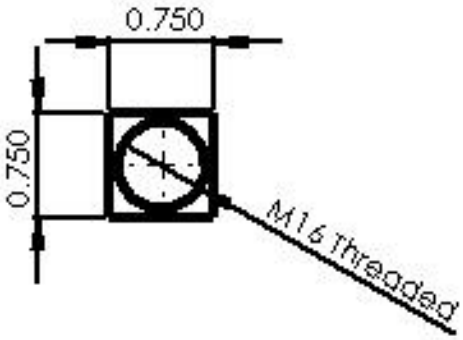

Three Bar Termination
Material: Aluminum
Quantity:1

University of Alabama
Garrett Waycaster

Appendix B – Optimization Code

Matlab M-Files:

1. Linear Spring Error
2. Torsional Spring Error
3. Constant Radius Pulley Error
4. Constant Radius Pulley Constraint
5. Slider-Crank Error
6. Slider-Crank Constraint
7. Elliptical Pulley Error
8. Elliptical Pulley Constraint
9. Linear Spring Torque
10. Torsional Spring Torque
11. Constant Radius Torque
12. Slider-Crank Torque
13. Elliptical Pulley Torque
14. Optimization Script

```
function f=linearspringerror(x)

K=x(1); %spring constant, N/m
r=x(2)/1000; %torque arm, mm
L=x(3)/1000; %equilibrium spring length, mm
theta=x(4); %initial r rotation relative to vertical, deg
L0=x(5)/1000; %x location of spring fixed point, mm
L1=x(6)/1000; %y location of spring fixed point, mm
Tdes=x(7:end); %desired torque, Nm

%presize vectors
Tact=zeros(1,length(Tdes));
error=zeros(1,length(Tdes));
F=zeros(1,length(Tdes));
reff=zeros(1,length(Tdes));

for i=1:length(Tdes)
    phi=i-1;
    x(i)=sqrt(r^2+L0^2+L1^2-2*cosd(theta-phi)*r*sqrt(L0^2+L1^2));
    F(i)=K*(x(i)-L);
    reff(i)=sqrt(L0^2+L1^2)*sin(acos((L1^2+L0^2+r^2-
x(i)^2)/(2*r*sqrt(L0^2+L1^2))));
    Tact(i)=F(i)*reff(i);
    error(i)=Tact(i)-Tdes(i);
    if error(i)<0
        error(i)=abs(error(i)*10);
    end
end

f=sum(error);
```

```
function f=torsionspringerror(x)

K=x(1); %spring constant Nm/deg
P=x(2); %pre-stretched torque Nm
Tdes=x(3:end); %Desired torque data with length = ROM

%presize vectors
Tact=zeros(1,length(Tdes));
error=zeros(1,length(Tdes));

for i=1:length(Tdes)
    phi=i-1;
    Tact(i)=K*phi+P;
    error(i)=Tact(i)-Tdes(i);
    if error(i)<0
        error(i)=abs(error(i)*10);
    end
end

f=sum(error);
```

```
function f=constantpulleyerror(x)

r=x(1)/1000; %joint link length, mm
Lnom=x(2)/1000; %nominal muscle length, mm
Tdes=x(3:end); %desired torque, Nm, with length=ROM deg


%presize vectors
error=zeros(1,length(Tdes));
Tact=zeros(1,length(Tdes));

for i=1:length(Tdes)
    h=100*(r*(length(Tdes)-i)*pi/180)/Lnom;
    Tact(i)=r*(2.8571*r*h^2-271.14*r*h+5992.9);
    error(i)=Tact(i)-Tdes(i);
    if error(i)<0
        error(i)=abs(error(i)*10);
    end
end

f=sum(error);
```

```
function [c, ceq]=constantpulleyconstraint(x)

r=x(1)/1000; %joint link length, mm
Lnom=x(2)/1000; %nominal muscle length, mm
Tdes=x(3:end); %desired torque, Nm, with length=ROM deg

hmax=100*(r*(length(Tdes)-1)*pi/180)/Lnom;

c(1)=hmax*100-2500; %max hysteresis must be less than 25%
ceq=[];
```

```
function f=slidercrankerror(x)

r=x(1)/1000; %joint link length, mm
L0=x(2)/1000; %relative x position of muscle fixed point, mm
L1=x(3)/1000; %relative y fixed position of muscle fixed point, mm
theta=x(4); %inital rotation of r relative to vertical, deg
Lnom=x(5)/1000; %nominal muscle length, mm
Tdes=x(6:end); %desired torque, Nm, with length=ROM

%presize vectors
Tact=zeros(1,length(Tdes));
error=zeros(1,length(Tdes));
F=zeros(1,length(Tdes));
reff=zeros(1,length(Tdes));

%determine actuator length and effective radius at each rotation angle
for i=length(Tdes)
    phi=i-1;
    x(i)=sqrt(r^2+L0^2+L1^2-2*cosd(theta-phi)*r*sqrt(L0^2+L1^2));
    reff(i)=sqrt(L0^2+L1^2)*sin(acos((L1^2+L0^2+r^2-
x(i)^2)/(2*r*sqrt(L0^2+L1^2))));
end

F(length(Tdes))=6000; %initial force, N

%determine force, torque, and error for each angle of rotation
for i=length(Tdes):-1:2
    h=100*(x(length(Tdes))-x(i))/Lnom;
    F(i-1)=2.8571*h^2-271.14*h+5992.9;
    Tact(i)=F(i)*reff(i);
    error(i)=Tact(i)-Tdes(i);
    if error(i)<0
        error(i)=abs(error(i)*10);
    end
end

error(1)=F(1)*reff(1);
if error(1)<0
    error(1)=abs(error(1)*10);
end

f=sum(error);
```

```
function [c, ceq]=slidercrankconstraint(x)

r=x(1)/1000; %joint link length, mm
L0=x(2)/1000; %relative x position of muscle fixed point, mm
L1=x(3)/1000; %relative y fixed position of muscle fixed point, mm
theta=x(4); %inital rotation of r relative to vertical, deg
Lnom=x(5)/1000; %nominal muscle length, mm
Tdes=x(6:end); %desired torque, Nm, with length=ROM


%presize vector
reff=zeros(1,length(Tdes));

for i=length(Tdes)
    phi=i-1;
    x(i)=sqrt(r^2+L0^2+L1^2-2*cosd(theta-phi)*r*sqrt(L0^2+L1^2));
    reff(i)=sqrt(L0^2+L1^2)*sin(acos((L1^2+L0^2+r^2-
x(i)^2)/(2*r*sqrt(L0^2+L1^2))));
end

hmax=100*(x(length(Tdes))-x(1))/Lnom;

c(1)=hmax*100-2500; %max hysteresis can not exceed 25%
c(2)=x(1)-(Lnom*1000+125); % initial "x" must be greater than total actuator
length
ceq=[];
```

```
function f=ellipsepulleyerror(x)

adia=x(1)/1000; %major semi-diameter, m
bdia=x(2)/1000; %minor semi-diameter, m
trot=x(3); %ellipse rotation deg
r0=x(4)/1000; %ellipse center radius relative to rotation center, m
t0=x(5); %ellipse center angle relative to rotation center, deg
L0=x(6)/1000; %relative x position of muscle fixed point, m
L1=x(7)/1000; %relative y fixed position of muscle fixed point, m
Lnom=x(8)/1000; %nominal muscle length, m
Tdes=x(9:end); %desired torque, Nm, with length=ROM deg


%presize vectors
xrot=zeros(181,length(Tdes));
yrot=zeros(181,length(Tdes));
teff=zeros(length(Tdes),1);
P=zeros(181,1);
R=zeros(181,1);
Q=zeros(181,1);
r=zeros(181,1);
reff=zeros(length(Tdes),1);
error=zeros(length(Tdes),1);
H=zeros(length(Tdes),1);

F(length(Tdes))=6000; %initial PAM force, N

for theta=1:181
    theta1=theta-1;
    P(theta)=r0*((bdia^2-adia^2)*cosd(theta1+t0-
2*trot)+(adia^2+bdia^2)*cosd(theta1-t0));
    R(theta)=(bdia^2-adia^2)*cosd(2*theta1-2*trot)+adia^2+bdia^2;
    Q(theta)=sqrt(2)*adia*bdia*sqrt(R(theta)-2*r0^2*sind(theta1-t0)^2);
    r(theta)=(P(theta)+Q(theta))/R(theta);
end

%find radius points in cartesian coordinates
for theta=1:181
    for phi=1:length(Tdes)
        xrot(theta,phi)=r(theta)*cosd(((theta-1)-(phi-1)));
        yrot(theta,phi)=r(theta)*sind(((theta-1)-(phi-1)));
    end
end

%find effective point of pulley
%find tangent line at effective point
%determine effective radius given tangent line
for phi=1:length(Tdes)
    for theta=1:181
        %find the last point, k, that is left of the line from muscle fixed
        %point to center of trottion
        if (0-L1)*(yrot(theta,phi)-L0)-(0-L0)*(xrot(theta,phi)-L1)>=0
```

```
            k=theta;
            %check all points less than k to see if they are left of
            %line from muscle fixed point to k
            for j=k-1:-1:1
                if (xrot(k,phi)-L1)*(yrot(j,phi)-L0)-(yrot(k,phi)-
L0)*(xrot(j,phi)-L1)>=0
                    k=j;
                end
            end
            teff(phi)=k;
            %find rcalc(phi)
            %find the slope, m
            m=(yrot(teff(phi),phi)-L0)/(xrot(teff(phi),phi)-L1);
            reff(phi)=abs(L0-m*L1)/sqrt(m^2+1);
        end
    end
end

%compute force and torque for each degree of rotation, find error
for i=length(Tdes):-1:2
    H(i)=100/Lnom*sqrt((reff(i)*cosd(i-1)-reff(i-1)*cosd(i-
2))^2+(reff(i)*sind(i-1)-reff(i-1)*cosd(i-2))^2);
    h=sum(H);
    F(i-1)=2.8571*h^2-271.14*h+5992.9;
    Tact(i)=F(i)*reff(i);
    error(i)=Tact(i)-Tdes(i);
    if error(i)<0
        error(i)=abs(error(i)*10);
    end
end

error(1)=F(1)*reff(1);
if error(1)<0
    error(1)=abs(error(1)*10);
end

f=sum(error);
```

```
function [c, ceq]=ellipsepulleyconstraint(x)


adia=x(1)/1000; %major semi-diameter, m
bdia=x(2)/1000; %minor semi-diameter, m
trot=x(3); %ellipse rotation deg
r0=x(4)/1000; %ellipse center radius relative to rotation center, m
t0=x(5); %ellipse center angle relative to rotation center, deg
L0=x(6)/1000; %relative x position of muscle fixed point, m
L1=x(7)/1000; %relative y fixed position of muscle fixed point, m
Lnom=x(8)/1000; %nominal muscle length, m
Tdes=x(9:end); %desired torque, Nm, with length=ROM deg



xrot=zeros(181,length(Tdes));
yrot=zeros(181,length(Tdes));
teff=zeros(length(Tdes),1);
P=zeros(181,1);
R=zeros(181,1);
Q=zeros(181,1);
r=zeros(181,1);
reff=zeros(length(Tdes),1);
H=zeros(length(Tdes),1);

for theta=1:181
    theta1=theta-1;
    P(theta)=r0*((bdia^2-adia^2)*cosd(theta1+t0-
2*trot)+(adia^2+bdia^2)*cosd(theta1-t0));
    R(theta)=(bdia^2-adia^2)*cosd(2*theta1-2*trot)+adia^2+bdia^2;
    Q(theta)=sqrt(2)*adia*bdia*sqrt(R(theta)-2*r0^2*sind(theta1-t0)^2);
    r(theta)=(P(theta)+Q(theta))/R(theta);
end



for theta=1:181
    for phi=1:length(Tdes)
        xrot(theta,phi)=r(theta)*cosd(((theta-1)-(phi-1)));
        yrot(theta,phi)=r(theta)*sind(((theta-1)-(phi-1)));
    end
end

for phi=1:length(Tdes)
    for theta=1:181
        %find the last point, k, that is left of the line from muscle fixed
        %point to center of trottion
        if (0-L1)*(yrot(theta,phi)-L0)-(0-L0)*(xrot(theta,phi)-L1)>=0
            k=theta;
            %check all points less than k to see if they are left of
            %line from muscle fixed point to k
            for j=k-1:-1:1
```

```
                if (xrot(k,phi)-L1)*(yrot(j,phi)-L0)-(yrot(k,phi)-
L0)*(xrot(j,phi)-L1)>=0
                    k=j;
                end
            end
            teff(phi)=k;
            %find rcalc(phi)
            %find the slope, m
            m=(yrot(teff(phi),phi)-L0)/(xrot(teff(phi),phi)-L1);
            reff(phi)=abs(L0-m*L1)/sqrt(m^2+1);
        end
    end
end


for i=length(Tdes):-1:2
    H(i)=100/Lnom*sqrt((reff(i)*cosd(i-1)-reff(i-1)*cosd(i-
2))^2+(reff(i)*sind(i-1)-reff(i-1)*sind(i-2))^2);
end


hmax=sum(H);

c(1)=hmax*100-2500; %max hysteresis must be less than 25%
c(2)=10-min(r)*1000; %smallest radius must be larger than 10 mm to ensure
manufacturability
ceq=max(imag(r)); %calculated pulley radius must be real
```

```
function Tact=lineartorque(x)

K=x(1); %spring constant, N/m
r=x(2)/1000; %torque arm, mm
L=x(3)/1000; %equilibrium spring length, mm
theta=x(4); %initial r rotation relative to vertical, deg
L0=x(5)/1000; %x location of spring fixed point, mm
L1=x(6)/1000; %y location of spring fixed point, mm
Tdes=x(7:end); %desired torque, Nm, with length=ROM deg

%presize vectors
Tact=zeros(1,length(Tdes));
F=zeros(1,length(Tdes));
reff=zeros(1,length(Tdes));

for i=1:length(Tdes)
    phi=i-1;
    x(i)=sqrt(r^2+L0^2+L1^2-2*cosd(theta-phi)*r*sqrt(L0^2+L1^2));
    F(i)=K*(x(i)-L);
    reff(i)=sqrt(L0^2+L1^2)*sin(acos((L1^2+L0^2+r^2-
x(i)^2)/(2*r*sqrt(L0^2+L1^2))));
    Tact(i)=F(i)*reff(i);
end
```

```
function Tact=torsiontorque(x)

K=x(1); %spring constant Nm/deg
P=x(2); %pre-stretched torque Nm
Tdes=x(3:end); %desired torque, Nm, with length=ROM deg

%presize vectors
Tact=zeros(1,length(Tdes));

for i=1:length(Tdes)
    phi=i-1;
    Tact(i)=K*phi+P;
end
```

```
function Tact=constanttorque(x)

r=x(1)/1000; %joint link length, mm
Lnom=x(2)/1000; %nominal muscle length, mm
Tdes=x(3:end); %desired torque, Nm, with length=ROM deg


%presize vectors
Tact=zeros(1,length(Tdes));

for i=1:length(Tdes)
    h=100*(r*(length(Tdes)-i)*pi/180)/Lnom;
    Tact(i)=r*(2.8571*r*h^2-271.14*r*h+5992.9);
end
```

```
function Tact=slidercranktorque(x)

r=x(1)/1000; %joint link length, mm
L0=x(2)/1000; %relative x position of muscle fixed point, mm
L1=x(3)/1000; %relative y fixed position of muscle fixed point, mm
theta=x(4); %inital rotation of r relative to vertical, deg
Lnom=x(5)/1000; %nominal muscle length, mm
Tdes=x(6:end); %desired torque, Nm, with length=ROM deg

%presize vectors
Tact=zeros(1,length(Tdes));
F=zeros(1,length(Tdes));
reff=zeros(1,length(Tdes));

%determine actuator length and effective radius at each rotation angle
for i=length(Tdes)
    phi=i-1;
    x(i)=sqrt(r^2+L0^2+L1^2-2*cosd(theta-phi)*r*sqrt(L0^2+L1^2));
    reff(i)=sqrt(L0^2+L1^2)*sin(acos((L1^2+L0^2+r^2-
x(i)^2)/(2*r*sqrt(L0^2+L1^2))));
end

F(length(Tdes))=6000; %initial force, N

%determine force, torque, and error for each angle of rotation
for i=length(Tdes):-1:2
    h=100*(x(length(Tdes))-x(i))/Lnom;
    F(i-1)=2.8571*h^2-271.14*h+5992.9;
    Tact(i)=F(i)*reff(i);
end
```

```
function Tact=ellipsetorque(x)

adia=x(1)/1000; %major semi-diameter, m
bdia=x(2)/1000; %minor semi-diameter, m
trot=x(3); %ellipse rotation deg
r0=x(4)/1000; %ellipse center radius relative to rotation center, m
t0=x(5); %ellipse center angle relative to rotation center, deg
L0=x(6)/1000; %relative x position of muscle fixed point, m
L1=x(7)/1000; %relative y fixed position of muscle fixed point, m
Lnom=x(8)/1000; %nominal muscle length, m
Tdes=x(9:end); %desired torque, Nm, with length=ROM deg


%presize vectors
xrot=zeros(181,length(Tdes));
yrot=zeros(181,length(Tdes));
teff=zeros(length(Tdes),1);
P=zeros(181,1);
R=zeros(181,1);
Q=zeros(181,1);
r=zeros(181,1);
reff=zeros(length(Tdes),1);
H=zeros(length(Tdes),1);

F(length(Tdes))=6000; %initial PAM force, N

for theta=1:181
    theta1=theta-1;
    P(theta)=r0*((bdia^2-adia^2)*cosd(theta1+t0-
2*trot)+(adia^2+bdia^2)*cosd(theta1-t0));
    R(theta)=(bdia^2-adia^2)*cosd(2*theta1-2*trot)+adia^2+bdia^2;
    Q(theta)=sqrt(2)*adia*bdia*sqrt(R(theta)-2*r0^2*sind(theta1-t0)^2);
    r(theta)=(P(theta)+Q(theta))/R(theta);
end

%find radius points in cartesian coordinates
for theta=1:181
    for phi=1:length(Tdes)
        xrot(theta,phi)=r(theta)*cosd(((theta-1)-(phi-1)));
        yrot(theta,phi)=r(theta)*sind(((theta-1)-(phi-1)));
    end
end

%find effective point of pulley
%find tangent line at effective point
%determine effective radius given tangent line
for phi=1:length(Tdes)
    for theta=1:181
        %find the last point, k, that is left of the line from muscle fixed
        %point to center of trottion
        if (0-L1)*(yrot(theta,phi)-L0)-(0-L0)*(xrot(theta,phi)-L1)>=0
            k=theta;
```

```
            %check all points less than k to see if they are left of
            %line from muscle fixed point to k
            for j=k-1:-1:1
                if (xrot(k,phi)-L1)*(yrot(j,phi)-L0)-(yrot(k,phi)-
L0)*(xrot(j,phi)-L1)>=0
                    k=j;
                end
            end
            teff(phi)=k;
            %find rcalc(phi)
            %find the slope, m
            m=(yrot(teff(phi),phi)-L0)/(xrot(teff(phi),phi)-L1);
            reff(phi)=abs(L0-m*L1)/sqrt(m^2+1);
        end
    end
end

%compute force and torque for each degree of rotation, find error
for i=length(Tdes):-1:2
    H(i)=100/Lnom*sqrt((reff(i)*cosd(i-1)-reff(i-1)*cosd(i-
2))^2+(reff(i)*sind(i-1)-reff(i-1)*cosd(i-2))^2);
    h=sum(H);
    F(i-1)=2.8571*h^2-271.14*h+5992.9;
    Tact(i)=F(i)*reff(i);
end
```

```
mass=100; %user mass, kg

%desired spring torque data, normalized Nm/kg
Tdesanklespring=mass*-1*[-0.0100 -0.0300 -0.0500 -0.0550 -0.0600 -0.0650 -
0.0650 -0.0630 -0.0620 -0.0620 -0.0620 -0.0620 -0.0620 -0.0620 -0.0620 -
0.0620 -0.0630 -0.0630 -0.0640 -0.0750 -0.1000 -0.1200 -0.1500 -0.1700 -
0.1300 -0.0900 -0.0800 -0.0700 -0.0680 -0.0600 -0.0500 -0.0400 -0.0300 -
0.0200 -0.0100 -0.0020 0 0 0 0 0 0 0 0];

opts=optimset('Display','iter','TolFun', 1,'TolCon',1e-1);

MS=MultiStart('Display','iter','TolFun',1,'TolX',1e-1);
GS=GlobalSearch('Display','iter','TolFun',1,'TolX',1e-1);



flag=1;
L0springmin=0;
L0springmax=101.6;
L0springguess=(L0springmin+L0springmax)/2;

L1springmin=0;
L1springmax=254;
L1springguess=(L1springmin+L1springmax)/2;

rmin=12.7;
rmax=127;
rguess=(rmin+rmax)/2;

Kmin=0;
Kmax=1000;
Kguess=(Kmin+Kmax)/2;

Lmin=0;
Lmax=254;
Lguess=(Lmin+Lmax)/2;

%find optimal linear spring
x=[Kguess rguess Lguess thetaguess L0springguess L1springguess
Tdesanklespring];
while flag~=0
    if flag==1;
        anklelinear=createOptimProblem('fmincon','objective',
@linearspringerror, 'x0', x, 'lb', [Kmin rmin Lmin thetamin L0springmin
L1springmin Tdesanklespring], 'ub', [Kmax rmax Lmax thetamax L0springmax
L1springmax Tdesanklespring], 'options', opts);

        [x_anklelinear,f_anklelinear]=run(GS,anklelinear);

        if max(abs(x-x_anklelinear))==0
            flag=0;
```

```
        else
            flag=2;
            x=x_anklelinear;
        end
    end
    if flag==2;

        anklelinear=createOptimProblem('fmincon','objective',
@linearspringerror, 'x0', x, 'lb', [Kmin rmin Lmin thetamin L0springmin
L1springmin Tdesanklespring], 'ub', [Kmax rmax Lmax thetamax L0springmax
L1springmax Tdesanklespring], 'options', opts);

        [x_anklelinear,f_anklelinear]=run(MS,anklelinear,100);

        if max(abs(x-x_anklelinear))==0
            flag=0;
        else
            flag=1;
            x=x_anklelinear;
        end
    end
end


flag=1;

Kmin=0;
Kmax=1000;
Kguess=(Kmin+Kmax)/2;

Pmin=0;
Pmax=200;
Pguess=(Pmin+Pmax)/2;

%find optimial torsion spring
x=[Kguess Pguess Tdesanklespring];
while flag~=0
    if flag==1;
        ankletorsion=createOptimProblem('fmincon','objective',
@torsionspringerror, 'x0', x, 'lb', [Kmin Pmin Tdesanklespring], 'ub', [Kmax
Pmax Tdesanklespring], 'options', opts);

        [x_ankletorsion,f_ankletorsion]=run(GS,ankletorsion);

        if max(abs(x-x_ankletorsion))==0
            flag=0;
        else
            flag=2;
            x=x_ankletorsion;
        end
    end
```

```
    if flag==2;

        ankletorsion=createOptimProblem('fmincon','objective',
@torsionspringerror, 'x0', x, 'lb', [Kmin Pmin Tdesanklespring], 'ub', [Kmax
Pmax Tdesanklespring], 'options', opts);

        [x_ankletorsion,f_ankletorsion]=run(MS,ankletorsion,100);

        if max(abs(x-x_ankletorsion))==0
            flag=0;
        else
            flag=1;
            x=x_ankletorsion;
        end
    end
end
%compare spring options and select best
if f_ankletorsion<f_anklelinear
    x_anklespring=x_ankletorsion;
    Tanklespring=torsiontorque(x_ankletorsion);
else
    x_anklespring=x_anklelinear;
    Tanklespring=lineartorque(x_anklelinear);
end


Tdesankle=Tanklespring+mass*[0.0300 0.0500 0.0700 0.0900 0.1200 0.1800 0.2500
0.3200 0.3900 0.4700 0.5400 0.6100 0.6800 0.7400 0.8000 0.8700 0.9300 1.0000
1.0500 1.1200 1.1600 1.2000 1.2400 1.2900 1.3300 1.3800 1.4500 1.5300 1.6200
1.7100 1.7700 1.8100 1.8000 1.7500 1.7000 1.6500 1.1000 1.0000 0.9500 0.9200
0.9000 0.9000 0.8800 0.3000];



flag=1;

Lnomankle=152;

rmin=38.1;
rmax=127;
rguess=(rmin+rmax)/2;


%find optimal constant radius pulley
x=[rguess Lnomankle Tdesankle];
while flag~=0
    if flag==1;
        ankleconstant=createOptimProblem('fmincon','objective',
@constantpulleyerror, 'x0', x, 'lb', [rmin Lnom Tdesankle], 'ub', [rmax Lnom
Tdesankle],'nonlcon', @constantpulleyconstraint, 'options', opts);
```

```
        [x_ankletorsion,f_ankleconstant]=run(GS,ankleconstant);

        if max(abs(x-x_ankleconstant))==0
            flag=0;
        else
            flag=2;
            x=x_ankleconstant;
        end
    end
    if flag==2;

        ankleconstant=createOptimProblem('fmincon','objective',
@constantpulleyerror, 'x0', x, 'lb', [rmin Lnom Tdesankle], 'ub', [rmax Lnom
Tdesankle],'nonlcon', @constantpulleyconstraint, 'options', opts);

        [x_ankleconstant,f_ankleconstant]=run(MS,ankleconstant,100);
        if max(abs(x-x_ankleconstant))==0
            flag=0;
        else
            flag=1;
            x=x_ankleconstant;
        end
    end
end


flag=1;

L0min=38.1;
L0max=76.2;
L0guess=(L0min+L0max)/2;

L1min=203.2;
L1max=279.4;
L1guess=(L1min+L1max)/2;

Lnomankle=152;

rmin=12.7;
rmax=127;
rguess=(rmin+rmax)/2;


%find optimal slider crank configuration
x=[rguess L0guess L1guess thetaguess Lnomankle Tdesankle];
while flag~=0
    if flag==1;
        anklecrank=createOptimProblem('fmincon','objective',
@slidercrankerror, 'x0', x, 'lb', [rmin L0 L1ankle thetamin Lnomankle
Tdesankle], 'ub', [rmaxs L0 L1ankle thetamax Lnomankle Tdesankle], 'nonlcon',
@slidercrankconstraint, 'options', opts);
```

```
        [x_anklecrank,f_anklecrank]=run(GS,ankletorsion);

        if max(abs(x-x_anklecrank))==0
            flag=0;
        else
            flag=2;
            x=x_anklecrank;
        end
    end
    if flag==2;

        anklecrank=createOptimProblem('fmincon','objective',
@slidercrankerror, 'x0', x, 'lb', [rmin L0 L1ankle thetamin Lnomankle
Tdesankle], 'ub', [rmax L0 L1ankle thetamax Lnomankle Tdesankle], 'nonlcon',
@slidercrankconstraint, 'options', opts);

        [x_anklecrank,f_anklecrank]=run(MS,anklecrank,100);

        if max(abs(x-x_anklecrank))==0
            flag=0;
        else
            flag=1;
            x=x_anklecrank;
        end
    end
end


adiamin=6.35;
adiamax=127;
adiaguess=(adiamin+adiamax)/2;

bdiamin=6.35;
bdiamax=127;
bdiaguess=(bdiamin+bdiamax)/2;

trotmin=0;
trotmax=180;
trotguess=(trotmin+trotmax)/2;

r0min=0;
r0max=127;
r0guess=(r0min+r0max)/2;

t0min=0;
t0max=360;
t0guess=(t0min+t0max)/2;

L0=50.8;
L1ankle=279.4;
```

```
%find optimal elliptical pulley
x=[adiaguess bdiaguess trotguess r0guess t0guess L0 L1ankle Tdesankle];
while flag~=0
    if flag==1;
        ankleellipse=createOptimProblem('fmincon','objective',
@ellipsepulleyerror, 'x0', x, 'lb', [adiamin bdiamin trotmin r0min t0min L0
L1ankle Tdesankle], 'ub', [adiamax bdiamax trotmax r0max t0max L0 L1ankle
Tdesankle], 'nonlcon', @ellipsepulleyconstraint, 'options', opts);

        [x_ankleellipse,f_ankleellipse]=run(GS,ankleellipse);

        if max(abs(x-x_ankleellipse))==0
            flag=0;
        else
            flag=2;
            x=x_ankleellipse;
        end
    end
    if flag==2;

        ankleellipse=createOptimProblem('fmincon','objective',
@ellipsepulleyerror, 'x0', x, 'lb', [adiamin bdiamin trotmin r0min t0min L0
L1ankle Tdesankle], 'ub', [adiamax bdiamax trotmax r0max t0max L0 L1ankle
Tdesankle], 'nonlcon', @ellipsepulleyconstraint, 'options', opts);

        [x_ankleellipse,f_ankleellipse]=run(MS,ankleellipse,100);

        if max(abs(x-x_ankleellipse))==0
            flag=0;
        else
            flag=1;
            x=x_ankleellipse;
        end
    end
end

if f_ankleellipse<f_ankleconstant && f_ankleellipse<f_anklecrank
    x_ankle=x_ankleellipse;
    Tankle=ellipsetorque(x_ankleellipse);
elseif f_anklecrank<f_ankleconstant && f_anklecrank<f_ankleellipse
    x_ankle=x_anklecrank;
    Tankle=slidercranktorque(x_anklecrank);
else
    x_ankle=x_ankleconstant;
    Tankle=constanttorque(x_ankleconstant);
end



%desired spring torque data, normalized Nm/kg
```

```
Tdeskneespring=mass*-1*[-0.2500 -0.3500 -0.4000 -0.4000 -0.4000 -0.3750 -
0.3625 -0.3750 -0.4000 -0.4000 -0.4000 -0.3750 -0.3250 -0.3000 -0.2875 -
0.2750 -0.2625 -0.2500 -0.2400 -0.2300 -0.2200 -0.2100 -0.2000 -0.2000 -
0.1900 -0.1800 -0.1700 -0.1600 -0.1600 -0.1500 -0.1500 -0.1400 -0.1400 -
0.1400 -0.1300 -0.1300 -0.1300 -0.1300 -0.1300 -0.1300 -0.1300 -0.1300 -
0.1300 -0.1300 -0.1300 -0.1300 -0.1300 -0.1250 -0.1250 -0.1200 -0.1200 -
0.1100 -0.1100 -0.1100 -0.1000 -0.1000 -0.1000 -0.1000 -0.1000 -0.0900 -
0.0900 -0.0900 -0.0900 -0.0900 -0.0900 -0.0900 -0.0900 -0.0900 -0.0900 -
0.0900 -0.0900 -0.0900 -0.1000 -0.1500 -0.1750 -0.2000 -0.2000 -0.2000 -
0.2000 -0.2000 -0.2000 -0.1875 -0.1750 -0.1750 -0.1750 -0.1500 -0.1500 -
0.1375 -0.1250 -0.1000 -0.0900 -0.0800 -0.0600 -0.0400 -0.0200 -0.0100 -
0.0100 -0.0100 -0.0100 -0.0100 -0.0100];

opts=optimset('Display','iter','TolFun', 1,'TolCon',1e-1);

MS=MultiStart('Display','iter','TolFun',1,'TolX',1e-1);
GS=GlobalSearch('Display','iter','TolFun',1,'TolX',1e-1);



flag=1;
L0springmin=0;
L0springmax=101.6;
L0springguess=(L0springmin+L0springmax)/2;

L1springmin=0;
L1springmax=254;
L1springguess=(L1springmin+L1springmax)/2;

rmin=12.7;
rmax=127;
rguess=(rmin+rmax)/2;

Kmin=0;
Kmax=1000;
Kguess=(Kmin+Kmax)/2;

Lmin=0;
Lmax=254;
Lguess=(Lmin+Lmax)/2;

%find optimal linear spring
x=[Kguess rguess Lguess thetaguess L0springguess L1springguess
Tdeskneespring];
while flag~=0
    if flag==1;
        kneelinear=createOptimProblem('fmincon','objective',
@linearspringerror, 'x0', x, 'lb', [Kmin rmin Lmin thetamin L0springmin
L1springmin Tdeskneespring], 'ub', [Kmax rmax Lmax thetamax L0springmax
L1springmax Tdeskneespring], 'options', opts);
```

```
        [x_kneelinear,f_kneelinear]=run(GS,kneelinear);

        if max(abs(x-x_kneelinear))==0
            flag=0;
        else
            flag=2;
            x=x_kneelinear;
        end
    end
    if flag==2;

        kneelinear=createOptimProblem('fmincon','objective',
@linearspringerror, 'x0', x, 'lb', [Kmin rmin Lmin thetamin L0springmin
L1springmin Tdeskneespring], 'ub', [Kmax rmax Lmax thetamax L0springmax
L1springmax Tdeskneespring], 'options', opts);

        [x_kneelinear,f_kneelinear]=run(MS,kneelinear,100);

        if max(abs(x-x_kneelinear))==0
            flag=0;
        else
            flag=1;
            x=x_kneelinear;
        end
    end
end



flag=1;

Kmin=0;
Kmax=1000;
Kguess=(Kmin+Kmax)/2;

Pmin=0;
Pmax=200;
Pguess=(Pmin+Pmax)/2;

%find optimial torsion spring
x=[Kguess Pguess Tdeskneespring];
while flag~=0
    if flag==1;
        kneetorsion=createOptimProblem('fmincon','objective',
@torsionspringerror, 'x0', x, 'lb', [Kmin Pmin Tdeskneespring], 'ub', [Kmax
Pmax Tdeskneespring], 'options', opts);

        [x_kneetorsion,f_kneetorsion]=run(GS,kneetorsion);

        if max(abs(x-x_kneetorsion))==0
            flag=0;
        else
```

```
            flag=2;
            x=x_kneetorsion;
        end
    end
    if flag==2;

        kneetorsion=createOptimProblem('fmincon','objective',
@torsionspringerror, 'x0', x, 'lb', [Kmin Pmin Tdeskneespring], 'ub', [Kmax
Pmax Tdeskneespring], 'options', opts);

        [x_kneetorsion,f_kneetorsion]=run(MS,kneetorsion,100);

        if max(abs(x-x_kneetorsion))==0
            flag=0;
        else
            flag=1;
            x=x_kneetorsion;
        end
    end
end
%compare spring options and select best
if f_kneetorsion<f_kneelinear
    x_kneespring=x_kneetorsion;
    Tkneespring=torsiontorque(x_kneetorsion);
else
    x_kneespring=x_kneelinear;
    Tkneespring=lineartorque(x_kneelinear);
end


Tdesknee=Tkneespring+mass*[0 0 0 0 0 0 0 0.0500 0.1000 0.1500 0.2000 0.2500
0.3000 0.3500 0.4000 0.4500 0.5000 0.6000 0.6750 0.7500 0.8500 0.9500 1.0500
1.1500 1.1750 1.1750 1.1500 1.1250 1.0000 1.0000 1.0000 1.0000 0.7500 0.7750
0.8000 0.8250 0.8500 0.9000 0.9500 1.0000 1.0500 1.1000 1.1250 1.1500 1.1750
1.2000 1.2250 1.2500 1.2750 1.3000 1.3250 1.3300 1.3400 1.3500 1.3600 1.3700
1.3800 1.3800 1.3800 1.3800 1.3800 1.3700 1.3600 1.3500 1.3400 1.3000 1.2800
1.2500 1.2300 1.2100 1.1800 1.1500 1.1200 1.0900 1.0500 1.0100 0.9700 0.9200
0.8700 0.8200 0.7700 0.7100 0.6500 0.5900 0.5300 0.4700 0.4100 0.3500 0.2900
0.2300 0.1700 0.1100 0.0600 0.0600 0.0600 0.0600 0.0200 0.0200 0.0200 0.0200
0.0200];


flag=1;

Lnomknee=152;

rmin=38.1;
rmax=127;
rguess=(rmin+rmax)/2;
```

```
%find optimal constant radius pulley
x=[rguess Lnomknee Tdesknee];
while flag~=0
    if flag==1;
        kneeconstant=createOptimProblem('fmincon','objective',
@constantpulleyerror, 'x0', x, 'lb', [rmin Lnom Tdesknee], 'ub', [rmax Lnom
Tdesknee],'nonlcon', @constantpulleyconstraint, 'options', opts);

        [x_kneetorsion,f_kneeconstant]=run(GS,kneeconstant);

        if max(abs(x-x_kneeconstant))==0
            flag=0;
        else
            flag=2;
            x=x_kneeconstant;
        end
    end
    if flag==2;

        kneeconstant=createOptimProblem('fmincon','objective',
@constantpulleyerror, 'x0', x, 'lb', [rmin Lnom Tdesknee], 'ub', [rmax Lnom
Tdesknee],'nonlcon', @constantpulleyconstraint, 'options', opts);

        [x_kneeconstant,f_kneeconstant]=run(MS,kneeconstant,100);
        if max(abs(x-x_kneeconstant))==0
            flag=0;
        else
            flag=1;
            x=x_kneeconstant;
        end
    end
end


flag=1;

L0min=38.1;
L0max=76.2;
L0guess=(L0min+L0max)/2;

L1min=203.2;
L1max=279.4;
L1guess=(L1min+L1max)/2;

Lnomknee=203;

rmin=12.7;
rmax=127;
rguess=(rmin+rmax)/2;
```

```
%find optimal slider crank configuration
x=[rguess L0guess L1guess thetaguess Lnomknee Tdesknee];
while flag~=0
    if flag==1;
        kneecrank=createOptimProblem('fmincon','objective',
@slidercrankerror, 'x0', x, 'lb', [rmin L0 L1knee thetamin Lnomknee
Tdesknee], 'ub', [rmaxs L0 L1knee thetamax Lnomknee Tdesknee], 'nonlcon',
@slidercrankconstraint, 'options', opts);

        [x_kneecrank,f_kneecrank]=run(GS,kneetorsion);

        if max(abs(x-x_kneecrank))==0
            flag=0;
        else
            flag=2;
            x=x_kneecrank;
        end
    end
    if flag==2;

        kneecrank=createOptimProblem('fmincon','objective',
@slidercrankerror, 'x0', x, 'lb', [rmin L0 L1knee thetamin Lnomknee
Tdesknee], 'ub', [rmax L0 L1knee thetamax Lnomknee Tdesknee], 'nonlcon',
@slidercrankconstraint, 'options', opts);

        [x_kneecrank,f_kneecrank]=run(MS,kneecrank,100);

        if max(abs(x-x_kneecrank))==0
            flag=0;
        else
            flag=1;
            x=x_kneecrank;
        end
    end
end


adiamin=6.35;
adiamax=127;
adiaguess=(adiamin+adiamax)/2;

bdiamin=6.35;
bdiamax=127;
bdiaguess=(bdiamin+bdiamax)/2;

trotmin=0;
trotmax=180;
trotguess=(trotmin+trotmax)/2;

r0min=0;
r0max=127;
```

```
r0guess=(r0min+r0max)/2;

t0min=0;
t0max=360;
t0guess=(t0min+t0max)/2;

L0=50.8;
L1knee=279.4;

%find optimal elliptical pulley
x=[adiaguess bdiaguess trotguess r0guess t0guess L0 L1knee Tdesknee];
while flag~=0
    if flag==1;
        kneeellipse=createOptimProblem('fmincon','objective',
@ellipsepulleyerror, 'x0', x, 'lb', [adiamin bdiamin trotmin r0min t0min L0
L1knee Tdesknee], 'ub', [adiamax bdiamax trotmax r0max t0max L0 L1knee
Tdesknee], 'nonlcon', @ellipsepulleyconstraint, 'options', opts);

        [x_kneeellipse,f_kneeellipse]=run(GS,kneeellipse);

        if max(abs(x-x_kneeellipse))==0
            flag=0;
        else
            flag=2;
            x=x_kneeellipse;
        end
    end
    if flag==2;

        kneeellipse=createOptimProblem('fmincon','objective',
@ellipsepulleyerror, 'x0', x, 'lb', [adiamin bdiamin trotmin r0min t0min L0
L1knee Tdesknee], 'ub', [adiamax bdiamax trotmax r0max t0max L0 L1knee
Tdesknee], 'nonlcon', @ellipsepulleyconstraint, 'options', opts);

        [x_kneeellipse,f_kneeellipse]=run(MS,kneeellipse,100);

        if max(abs(x-x_kneeellipse))==0
            flag=0;
        else
            flag=1;
            x=x_kneeellipse;
        end
    end
end

if f_kneeellipse<f_kneeconstant && f_kneeellipse<f_kneecrank
    x_knee=x_kneeellipse;
    Tknee=ellipsetorque(x_kneeellipse);
elseif f_kneecrank<f_kneeconstant && f_kneecrank<f_kneeellipse
    x_knee=x_kneecrank;
    Tknee=slidercranktorque(x_kneecrank);
else
```

```
    x_knee=x_kneeconstant;
    Tknee=constanttorque(x_kneeconstant);
end
```

Bibliography

Bodyworks Human Engineering Models. (2008). Retrieved from http://www.human2go.com/component/option,com_frontpage/Itemid,1/

Caldwell, D.G., Razak, A., Goodwin, M.J. (1993). Braided pneumatic muscle actuators. *IFAC Conference on Intelligent Autonomous Vehicles*, 507-512.

Daerden, F., Lefeber, D. (2002). Pneumatic Artificial Muscles: actuators for robotics and automation. *European Journal of Mechanical and Environmental Engineering, 47*(1), 11-21.

Dillingham, R.T., Pezzin, L.E., MacKenzie, E.J. (2002). Limb Amputation and Limb Deficiency: Epidemiology and Recent Trends in the United States. *Southern Medical Journal, 95(3)*, 875-883.

Enderle, J., Blanchard, S., Bronzino, J., (2005). *Introduction to Biomedical Engineering*. Burlington, MA: Elsevier.

FESTO. (2010). Retrieved from http://www.festo.com/cms/en-us_us/index.htm

Fite, K., Mitchell, J., Sup, F., Goldfarb, M. (2007). Design and Control of an Electrically Powered Knee Prosthesis. *Proceedings of the IEEE Intl. Conf. on Rehabilitation Robotics*, 902-905.

Freedom Innovations. (2010). Retrieved from http://www.freedom-innovations.com/

Hannaford, B., Winters, J.M. (1990). Actuator properties and movement control: biological and technological models. *Multiple Muscle Systems: Biomechanics and Movement Organization*, 101-120, New York, NY: Springer-Verlag.

Hata, N., Hori, Y., (2002). Basic research on power limb using gait information of able-side leg. *Proceedings of the 7th Intl. Workshop on Advanced Motion Control*, 540-545.

Hata, N., Hori, Y., (2002). Basic research on power limb using variable stiffness mechanism. *Proceedings of the Power Conversion Conference*, *2*, 917-920.

Hosoda, K., Takuma, T., and Nakamoto, A. (2006). Design and Control of 2D Biped that can Walk and Run with Pneumatic Artificial Muscles. *Proceedings of 2006 IEEE-RAS Intl. Conf. on Humanoid Robots*. 284-289.

Isermann, R. and Raab, U. (1993) "Intelligent actuators – Ways to autonomous systems." *Automatica*, *29*(5), 1315-1331.

Lambrecht, B.G.A., Kazerooni, H. (2009). "Design of a Semi-Active Knee Prosthesis." *Proceedings of 2009 IEEE International Conference on Robotics and Automation*, 639-645.

Martinez-Villalpando, E.C., Herr, H. (2009). "Agonist-Antagonist Active Knee Prosthesis: A Preliminary Study in Level-Ground Walking." *Journal of Rehabilitation Research & Development*, *46*(3), 361-374.

McDowell, M.A., Fryar, C.D., Ogden, C.L., Flegal, K.M. (2008). Anthropometric Reference Data for Children and Adults: United States, 2003–2006. *National Health Statistics Reports No. 10*. Hyattsville, MD: National Center for Health Statistics.

OttoBock. (2010). Retrieved from http://www.ottobockus.com/

Riener, R., Rabuffetti, M., Frigo, C. (2002). Stair ascent and descent at different inclinations. *Gait and Posture, 15*, 32-44.

Robinson DW, Pratt JE, Paluska DJ, Pratt GA. (1999). Series elastic actuator development for a biomimetic walking robot. *Proceedings of the IEEE/ASME Intl. Conf. on Advanced Intelligent Mechatronics,* 561–68.

Sup, F., Bohara, A., Goldfarb, M. (2008). Design and Control of a Powered Transfemoral Prosthesis. *The Intl. Journal of Robotics Research*, *27*(2), 263-273.

Sup, F., Varol, H.A., Mitchell, J. Withrow, T.J., Goldfarb, M. (2009). Self-Contained Powered Knee and Ankle Prosthesis: Initial Evaluation on a Transfemoral Amputee. *Proceedings of the 11th IEEE Intl. Conf. on Rehabilitation Robotics.* 263-273.

Tang, P.C., Ravji, K., Key, J.J., Mahler, D.B., Blume, P.A., Sumpio, B. (2008). Let Them Walk! Current Prosthesis Options for Leg and Foot Amputees. *Journal of the American College of Surgeons*, *206*(3), 548-560.

Ugray, Z., Ladson, L., Plummer, J., Glover, F., Kelly, J., Marti, F. (2007). Scatter Search and Local NLP Solvers: A Multistart Framework for Global Optimization. *INFORMS Journal on Computing, 19*(3), 328-340.

Versluys, R., Desomer, A., Lenaerts, G., Van Damme, M., Beyl, P., Van der Perre, G., Peeraer, L., Lefeber, D. (2008). A Pneumatically Powered Below-Knee Prosthesis: Design Specifications and First Experiments with an Amputee. *Proceedings of the IEEE/RAS-EMBS Intl. Conf. on Biomedical Robotics and Biomechatronics*. 372-377.

Waters, R.L., Mulroy, S. (1999). The energy expenditure of normal and pathologic gait. *Gait and Posture, 9*, 207-231.

Winter, D.A. (1991). *The Biomechanics and Motor Control of Human Gait: Normal, Elderly and Pathological*. 2nd ed. Hoboken, NJ: Wiley and Sons.

Winter, D.A. (2005). *The Biomechanics and Motor Control of Human Movement.* 3rd ed. Hoboken, NJ: Wiley and Sons.

Ziegler-Graham, K., MacKenzie, E.J., Ephriam, P.L., Travison, T.G., Brookmeyer, R. (2008). Estimating the Prevalence of Limb Loss in the United States: 2005 to 2050. *Archives of Physical Medicine and Rehabilitation*, *89*(3), 422-429.